Groundwater Modeling for Sustainable Groundwater Utilization in Mekong Delta

2017.9

Agricultural and Environmental Engineering
United Graduate School of Agricultural Sciences
Tokyo University of Agriculture and Technology

NGUYEN DINH GIANG NAM

Groundwater Modeling for Sustainable Groundwater Utilization in Mekong Delta

2017.9

Agricultural and Environmental Engineering
United Graduate School of Agricultural Sciences
Tokyo University of Agriculture and Technology

NGUYEN DINH GIANG NAM

Advisors:

Professor GOTO Akira
Associate Professor OSAWA Kazutoshi
Department of Environmental Engineering
Faculty of Agriculture
Utsunomiya University
Associate Professor KATO Tasuku
Department of International Environmental and Agricultural Science
Tokyo University of Agriculture and Technology

SUMMARY

The study for this dissertation was implemented to support and achieve the sustainable groundwater (GW) utilization in the Mekong Delta (MD) mainly based on modeling approaches with the following four topics: (i) Construction of the numerical GW model for the entire MD; (ii) GW modeling in the urban area for analyzing impacts of GW pumping; (iii) GW modeling in the coastal area for GW management under the climate change; and (iv) Land subsidence modeling.

The thesis consists of 7 chapters, of which main chapters are as follow:

Chapter 2 presents reviews of previous studies on GW modeling and GW issues in the MD. For many GW models, their basic concepts and frameworks were examined. Also from the understanding on the GW problems in the MD, the requirements for the GW modeling were identified.

Chapter 3 describes establishment of a regional 3D GW flow model for the whole MD using iMOD. The GW head distribution calculated by the entire Delta model with different grid sizes and 8 layers showed fairly good agreement with the observed values. The results revealed that the small grid requires huge computational time, though it can represent the exact locations better than the coarse grid. In the meantime, as iMOD can easily generate higher resolution grids everywhere inside, the GW head distribution calculated by the model can be utilized as the boundary condition and the initial condition for higher resolution modeling of certain areas. Thus, the model was established as a startup model for more detailed analyses in the following chapters.

In Chapter 4, the steady state GW model in Can Tho city was developed. The model boundaries were set up by the results of the entire Delta model. The necessary data such as aquifer properties, hydraulic parameters, locations and amounts of pumping wells, and meteorological data were compiled and initially assigned to grid cells. The calibrated model showed good agreement between calculated GW heads and the observed ones at 14 monitoring wells. From the calculated spatial distribution of GW heads, the serious GW drawdown zones were identified as depression cones, and it was clarified that they are deeply affected by dense distribution of pumping stations for domestic and industry. As more increased GW demand for water supply is expected in the city until 2035, the model was used to predict the future GW decline. As the result, the formation process of depression cones with the increase in pumping was depicted in 3D graphics, and the serious impacts of increase in pumping were clearly shown.

In Chapter 5, an iMOD model for a coastal area of the Mekong Delta was established, and the model was applied for simulation of the future GW heads. The model was calibrated using historical data of GW level and model input requirements. It was confirmed that the calibrated model could work properly to reproduce the distribution of the GW table and its response. For scenario setting, several cases of future rainfall conditions for the period from 2015 to 2035 were set up based on the downscaled output from the global climate model with bias correction. For each of the combinations of climatic conditions and different pumping rates, model simulation was carried out to estimate GW tables. The results showed: (1) If the GW pumping stays at the same level as present, GW heads can maintain the present level under increased recharge from the future rainfall, whereas slight decline in GW heads would continue under the

current rainfall; (2) If the GW pumping increases along with increasing water demand, significant consecutive drawdown of GW tables will happen; (3) Reduction in pumping rate was found to contribute much for recovery of GW.

In Chapter 6, the three-factor rheology model was applied to simulation of land subsidence associating the GW decline in two areas of the Mekong Delta, the urban area of Can Tho City and the coastal area of Soc Trang. The models were calibrated to get good matching with observed values, though the observation was very limited.. As the results, land subsidence rate in Can Tho was around 2.6 cm/year. For the coastal area, the cumulated subsidence for the period of 1994-2014 was estimated 65 cm. With the current rate of water level decline, another 60 cm of land subsidence was expected over the next 21 years in this area.

Chapter 7 presents all the conclusions drawn from this study and some proposals for the future research. For overall conclusion, basic GW models for the MD were established as useful tools for assessing the current and future statuses of GW, and the approaches for sustainable GW utilization were also presented in this study. Also from the results of the analyses based on the model simulation, it was made clear that the GW use in the MD is in over-exploitation and regulation or conservation measures for GW are required for continuing increase in water demand in the future.

TABLE OF CONTENTS

LIST OF FIGURES

LIST OF TABLES

CHAPTER 1. INTRODUCTION

1.1 Background

The Mekong Delta is the region in southwestern Vietnam where the Mekong River approaches and empties into the sea through a network of distributaries (Fig. 1.1). The Mekong Delta region encompasses a large portion of southwestern Vietnam of 39,000 square kilometers (15,000 sq mi) (IUCN, 2011). The size of the area covered by water depends on the season. The region is one of the most vulnerable regions in the worlds especially under impacts of climate change and sea – level – rise (Syvitski, Kettner et al. 2009; IPPC 2012). Given an intensive surface water network, surface water is allocated for different activities in the region like households, industry, agri-aquaculture and transportation. Nevertheless, due to the high variation (in quantity and quality) of surface water distribution in time and space, the use of other sources including rain water and groundwater (GW) is common in the region (Tuan et al, 20 07).

Under high stresses of water use development due to the increasing population and agriculture demand for more water, GW is an important hidden resource for water use, particularly in the areas of low rainfall and low lying coastal alluvial plains. As in some of developing areas, GW is also a major source of fresh water available for agriculture and other domestic activities apart from human consumption in the Mekong Delta (Danh, 2008).

GW exists in five Cenozoic aquifers underlying the Mekong Delta (Boehmer, 2000). The pervasive and seemingly abundant supply of GW has led its use to indiscriminate and sometimes excessive ones. Monitoring of GW levels for the last several years showed that GW levels are declining year by year (DWRPIS, 2012). As a result, its negative effects such as aquifer depletion, drying of wetlands, degradation of water quality and land subsidence have frequently been reported (IUCN, 2011; Fujihara et al, 2015). The decline of GW tables may be caused not only by GW abstraction but also by recharge areas reduction due to land use change during the last decade (USGS, 1997). These interdisciplinary aspects of GW utilization have brought the concept of

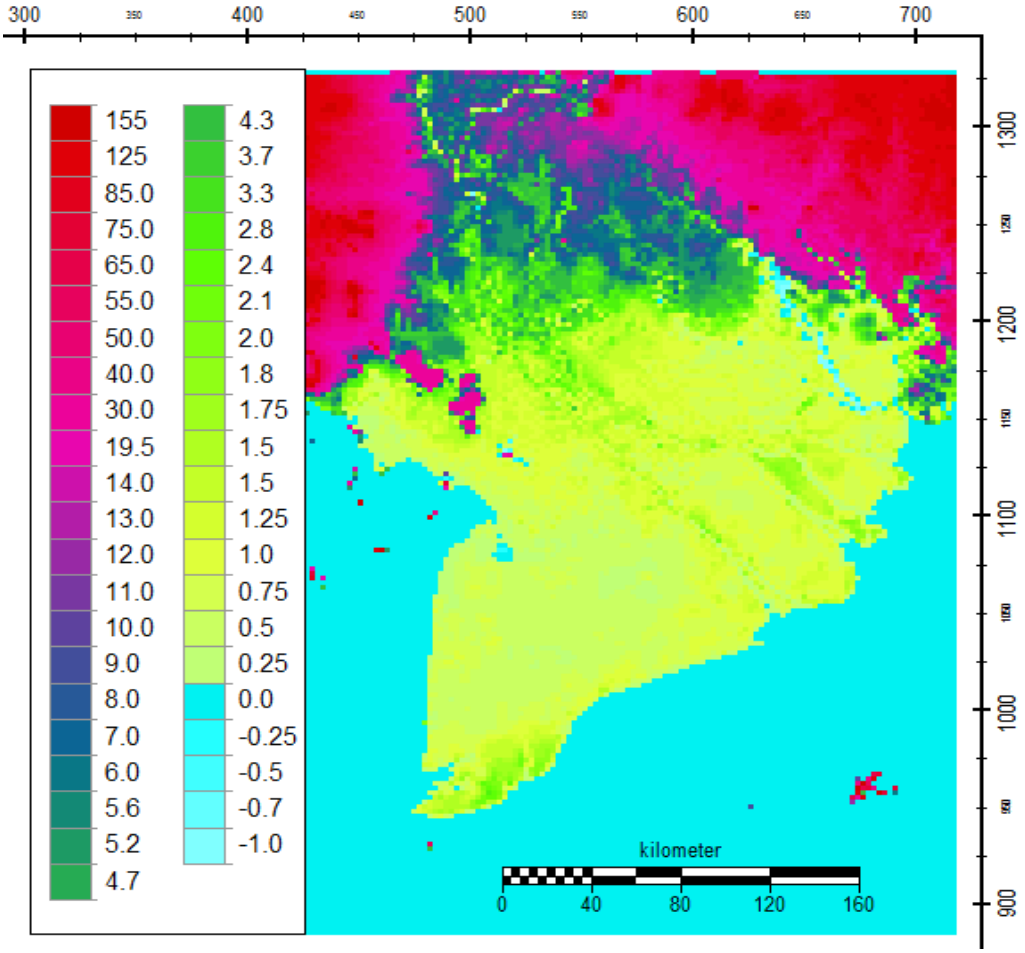

Fig. 1-1 The elevation map of Mekong Delta (Data sources from DWRPIS)

safe yield, which is defined as the maintenance of a long-term balance between the amount of withdrawal and the amount of recharge, into question (Sophocleous, 2000). Thus, the issue of GW sustainability has arisen (Alley and Leake, 2004). To what extent can region's GW resources be exploited without unduly compromising the principle of sustainable development, which is defined as development that meets the needs of the present without compromising the ability of future generations to meet their own needs (WCED, 1987)?

Currently in the Mekong Delta, the concept of sustainable GW resources utilization is taken into consideration particularly in the urban area and the coastal area (DONREs, 2012). Therefore, the decision-makers there have to be provided with adequate information on what is happening in the area's GW in order to formulate sustainable water resources development strategies.

GW models play an important role in development and management of GW resources, and in prediction of effects of management measures (Yangxiao et at, 2011). GW flow models have been used: (1) as interpretative tools for investigating GW system dynamics and understanding the flow patterns; (2) as simulation tools for analyzing responses of the GW system to stresses; (3) as assessment tools for evaluating recharge, discharge and aquifer storage processes, and for quantifying sustainable yield; (4) as predictive tools for predicting future conditions or impacts of human activities; (5) as supporting tools for planning field data collection and designing practical solutions; (6) as screening tools for evaluating GW development scenarios; (7) as management tools for assessing alternative policies; and (8) as visualization tools for communicating key messages to public and decision-makers (Yangxiao et at, 2011)

For preparing the information mentioned above, it is necessary to develop GW models for the Mekong Delta. Hence, by using modeling approaches, this study was implemented to cope with several of the problems that GW utilization in the Mekong Delta is facing. By developing GW models and applying them to future scenarios, the varying impacts of current and future GW management and development decisions should be quantified and evaluated. Based on the results of the model simulations, conservation strategies and alternative GW management options should be considered for sustainable GW utilization in the Mekong Delta.

1.2 Statement of Problem

From reviewing the previous studies related to GW in the Mekong Delta, including investigation and monitoring data of the aquifers over the last nearly 30 years, three major issues of the GW system in the Mekong Delta were identified:

(i) Decline in GW levels in some urban and coastal areas of Mekong Delta caused by a reduction in the volume of water in the aquifer system probably due to extensive drainage, exploitation, and the interception of recharge waters.

(ii) Degradation in GW quality caused by urban, industrial and rural pollutants, and concentration of natural contaminants and salt water intrusion caused by excessive pumping of GW reserve, especially in the coastal zones.

(iii) Land subsidence caused by the decline of GW levels.

1.3 General Objectives

This study was aimed at supporting the decision makers to achieve the policies for sustainable GW utilization in the Mekong Delta region. For this goal, the study was designed with five goals as follows:

1. To construct the numerical GW model for the entire Mekong Delta.
2. To construct a detailed GW model for the Can Tho City area, the middle of the Mekong Delta, in order to analyze the impacts of GW pumping in the urban area.
3. To construct a detailed GW model for the Soc Trang Province area, the coastal area of Mekong Delta, in order to assess different GW management measures under the possible climate changes.
4. To construct a land subsidence model for each of two urban areas of the Mekong Delta, which can estimate subsidence rate from the changes in GW tables.
5. To test GW quality and to assess its sustainability in the coastal area of the Mekong Delta.

CHAPTER 2. LITERATURE REVIEW

2.1 Theoretical Framework

A typical modeling process starts with data integration and description of the hydrogeological setup, then the definition of the conceptual framework for analysis, and finally comes the numerical approximation. The conceptual framework represents an important phase in defining the quantitative framework within which a numerical scheme works. It identifies and specifies the different steps, which can be taken in the process of formulating, analysis, evaluating and presenting alternative models (Koudstall, 1992). According to Sun (1994) application of sound hydrologic reasoning during the development of an appropriate conceptual model of flow represents a full 90% of the solution to most hydro-geologic problems. The hydrogeological framework includes the outline of model geometry, and the different hydrogeologic units

2.2 Previous GIS/MODFLOW Model Connection

As discussed in the previous section, various concepts have been developed within the GIS framework to assist in traditional water modeling. Of more concern for this research, though, is the establishment of a connection between an existing environmental model and the GIS software. Many research endeavors have investigated the feasibility of linking various models to GIS to assist in data management, manipulation, and output processing. Of particular interest for this project were those previous studies which concentrated on water quality and quantity model links. These projects have ranged from incorporating an entire model into the GIS software, to concentrating on a subprogram of the model to connect to the interface.

In the area of GW, literature reviewed included links to the USGS model, MODFLOW, and a European simulation program entitles MICRO-FEM (Biesheuvel and Hemker, 1993). Two studies included investigations with MODFLOW. Rindahl (1996) established an "easy to use interface" through GIS to display drawdowns, stream flow, and aquifer elevations simulated from the GW modeling program. The

research, which developed the link primarily for ease in output presentation, utilized the GIS software, ArcView 2.1 and Arc-View's programming language, Avenue. The study established polygon coverage of the modeled grid, attributed with the information resulting from a typical MODFLOW model run. The attributes were in tabular format and joined to the polygon coverage through a model "identification number" termed a "Loc-Tag". Once joined to the corresponding coverage, the model results could be spatially displayed through Arc-View. Avenue scripts were also compiled which assisted the user in output display. Another study investigating a GIS link to MODFLOW centered on the use of Arc/Info to provide an efficient means of data preparation and visualization of simulation results (Brown, et al., 1996). ModelGIS, an interface using FORTRAN 77 and Arc Macro Language, generated model grids, model layer elevations, aquifer properties, surface water data, and model output. The options in ModelGIS were executed from a customized menu developed in Arc/Info's subprogram, ArcTools. The different choices converted coverages to model based data, assembled the data into MODFLOW input, executed the MODFLOW program, and assisted in the evaluation of the modeling results. Throughout these processes, the user interacted with the interface in the creation of the model grid and data inputs. This link also hasthe capability of establishing a three dimensional modeling surface (Brown, et al., 1996).

2.3 Groundwater Modeling Process

GW modeling can be defined as the quantification and simulation of the natural movement of GW through any porous media. This can be achieved by physical or mathematical means. Modeling plays an extremely important role in the management of water resources. GW models, which replicate the GW flow process at the site of interest, can be used to complement monitoring studies in evaluating and forecasting GW flow and transport. However, every reliable GW model is based on accurate field data and decent prior knowledge of the site. The GW modeling process is summarized in Fig. 2.1.

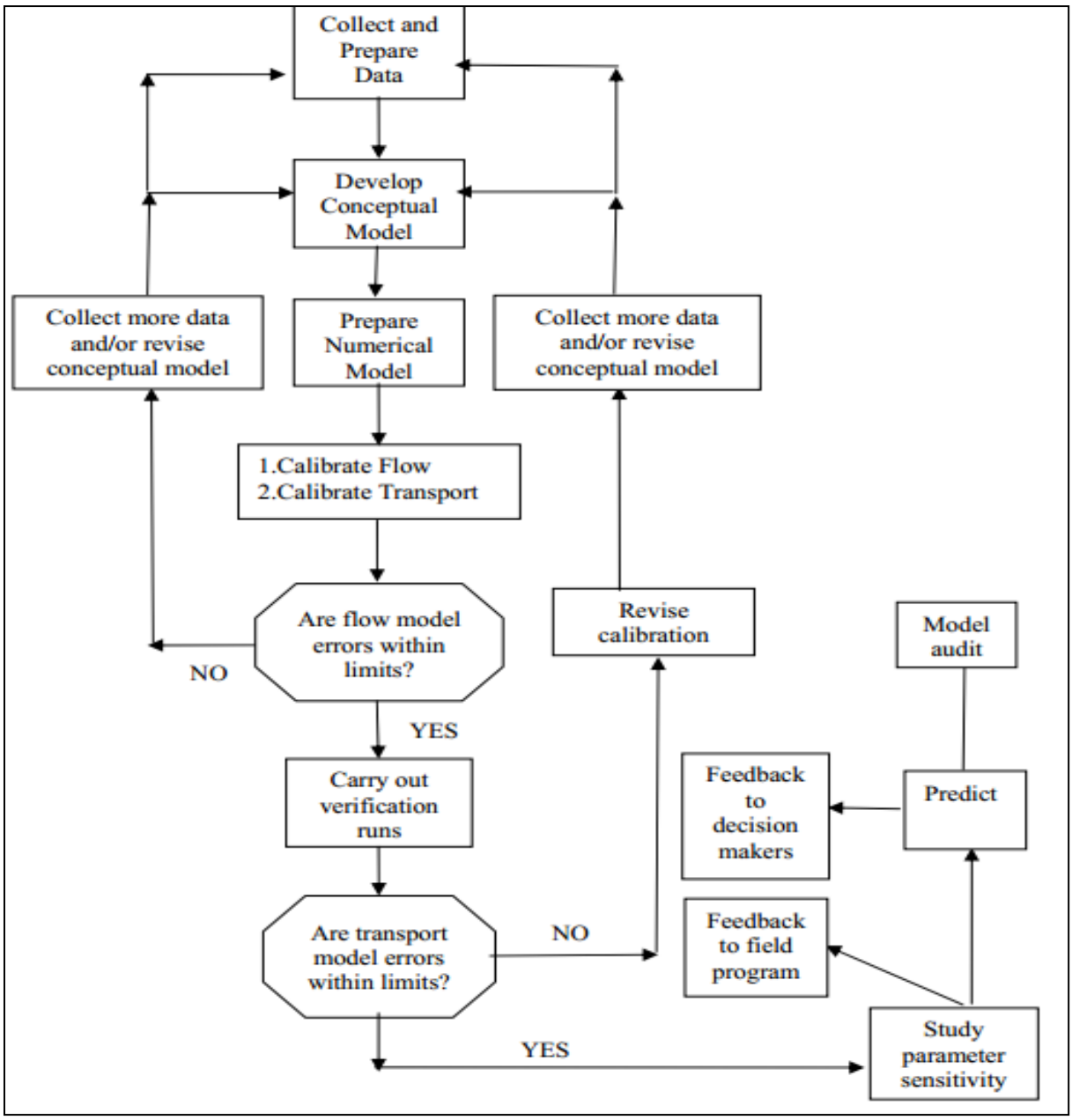

Fig. 2-1 Groundwater modelling process (McKinney, 1994)

2.4 Types of Groundwater Models

There are several ways to classify GW flow models. Models can be either transient or steady-state, confined or unconfined, and consider one, two or three spatial dimensions. In setting up the grid of a numerical model, the classification that is most relevant is one based on spatial dimension (Anderson, 1992). In general, there are three types of models to be used for modeling as physical, mathematical, empirical methods. A mathematical model was used in the study presented here.

A mathematical model is an exact or approximate solution to the governing equations of the process. Mathematical models of GW flow, which are also called white box model, have been in use since the late 1800s. Fundamental theories, principles and some simplifying assumptions are used to derive equations. Simplifying assumptions must always be made in order to construct a model because the field situations are too complicated to be simulated exactly. Usually the assumptions necessary to solve a mathematical model analytically are fairly restrictive. For example, many analytical solutions require the subsurface medium to be homogenous and isotropic. To deal with more realistic situations, it is usually necessary to solve mathematical model approximately using numerical techniques.

The general governing equation for three-dimensional, transient GW flow in a heterogeneous and anisotropic aquifer is given as:

$$\frac{\partial}{\partial x}(K_x \frac{\partial h}{\partial x}) + \frac{\partial}{\partial y}(K_y \frac{\partial h}{\partial y}) + \frac{\partial}{\partial z}(K_z \frac{\partial h}{\partial z}) = S_s \frac{\partial h}{\partial t} - W$$

Here h represent the hydraulic head; x, y, z and trepresent the spatial dimensions and time, respectively; Kx, Ky, Kz are the hydraulic conductivities in the x, y and z directions and Ss is the specific storage of the aquifer. The derivation of this equation is based on the application of the mass balance principle on a finite element representing the saturated porous medium and the substitution of GW flux terms with Darcy's law

2.5 Numerical Models

Numerical models allow analysis of flow or transport solutions, if the complexity of the mathematical model prevents an analytical solution. Numerical modeling techniques are used to solve large set of equations, which describe the physical flow processes in an aquifer. There are two numerical techniques of numerical models which are called finite differences and finite elements methods. These two approximate methods provide a rationale for operating on the differential equations that make up a model and for transforming them into a set of algebraic equations.

Numerical modeling provides a discrete solution over the model domain used by algebraic equations. It uses iterative methods or direct methods for the approximate solution. For many problems numerical solution is more realistic than the analytical solution. In this case, generally numerical models are preferred to use in mathematical model. Values are calculated at only a few points by the numerical models.

2.6 Data Requirements

Compiling the field data relevant to the assembly of the GW flow model is a significant step in modeling. Data requirements for GW modeling can be classified in two sections; the physical and hydrologic framework. The first step of a model study consists of collection and evaluating relevant data on flow system under investigation. Input data for the model are used for (Spitz & Moreno, 1996):

1. Problem definition (material properties and geometry of hydraulic units).
2. Numerical requirements (initial conditions, boundary conditions and transient conditions)
3. Modeling requirements (calibration, validation, and definition of alternate scenarios)

Data in the physical framework define the geometry of the system including thickness and real extent of each hydro-stratigraphic unit. Data within the hydrologic framework include information on heads and fluxes, which are needed to formulate the conceptual model and check model calibration. Hydrogeologic data also define aquifer properties and hydrologic stresses. They include pumping, recharge and evapotranspiration. Recharge is the one of the most difficult parameters to estimate. (Anderson & Woessner, 1992)

The physical framework consists of all geological information about the natural system such as a geological map showing cross-sections, vertical profiles, fault lines and formations, a topographic map showing surface water bodies, residential and industrial areas, surface elevation contours, etc., contour maps showing the elevation of the base of aquifers and confining beds, isopach maps showing the thickness of

streams and lake sediments. The physical framework basically defines the geometry of the system including the thickness of the hydro-stratigraphic units.

Data on hydraulic heads, fluxes, precipitation, and evapotranspiration are included within the hydrological framework. Hydrological data also define hydrologic stresses such as pumping, recharge and evapotranspiration. Hydrological data can come in the form of water table and potentiometric maps for the aquifers of interest, hydrographs of GW head and surface water levels and discharge rates, maps showing hydraulic conductivity and transmissivity distribution, spatial and temporal distribution of rates of GW recharge, GW pumping, natural GW discharge and evapotranspiration.

2.7. Previous Regional Groundwater Modeling Studies

Application of GW flow models to large scale aquifer system simulation started in 1978, with the Regional Aquifer System Analysis (RASA) program of U.S. Geological Survey (Sun and Johnson, 1994). During the 18 years of the program (1978 to 1995), 25 regional aquifer systems were intensively studied. The major contributions of the program were: (1) creation of regional hydrogeological databases; (2) construction of hydrogeological frameworks (conceptual models); (3) understanding of responses of regional aquifer systems to natural stresses (predevelopment) and human interferences (abstraction and land use changes); and (4) the compilation of a national GW atlas. Computer-based numerical GW flow models were constructed and used to characterize flow systems and to simulate the effects of GW development and land use changes. Computer models used in most cases were the USGS 3D finite difference model and the USGS MODLFOW (McDonald and Harbaugh, 1992). Typical regional aquifer system models covered an area of tens of thousands square kilometers. The models simulated 2e10 aquifer layers with a grid spacing ranging from 6 to 25 km. A steady state model was usually calibrated with data from predevelopment time and a transient model was constructed using the calculated heads from the steady state model as initial conditions. More than 900 reports were published from RASA program in USGS Professional Paper numbered

from 1400 to 1428. Finally, a bibliography of the RASA program was compiled listing 1105 reports of various publications (Sun et al., 1994)

Atilla (1998) developed a transient GW flow model for the confined aquifer under the Afyon Plain in Turkey. The spatial and temporal extent of hydraulic head over the plain was simulated using MODFLOW. According to the piezometric level decline and water quality degradation conditions, the prediction of the consequences of the overexploitation requires the identification of the current head distribution. The hydraulic head distribution declines from NW to SE over the plain. The model shows that there is an increase in the decline of the piezometric levels after the year 1976 when intensive GW exploitation is started, and after 1990 when the exploitation is considerably increased. It is simulated that the hydraulic head is decreased 5 to 10 m in some parts of the plain front the year 1965 to 1998. Under these conditions, GW usage In the Plain should he regulated to establish the natural hydraulic balance and, the termination of uncontrolled ground water exploitation.

In the Mekong Delta, the first attempt of HASKONING B.V and Division of investigation for water resources of the South of Vietnam is to develop numerical GW model in 2000. The construction of a stationary and non-stationary model for such a large area has proved to be complex, demanding and time consuming. Important requirements for building and calibrating this model were: (i) staff with a thorough knowledge in hydrogeology and the regional hydrogeology; (ii) a high quality and modern modeling program and (iii) information on GW abstraction through wells. In addition, the models were considered finished for that moment. The GW flow model regime under Nambo Plain including Mekong Delta could be simulated by 10-layer MODFLOW GW model developed by the project in GMS. The GW situation in the two upper layers of the aquifer system could be calibrated better than in the deeper aquifers largely due to lack sufficient data about the deeper aquifers and the difficult tuning of the vertical permeability of the succession of the four separating aquicludes. Some improvement in the calibration of the model may still be achieved by careful changing of some of the input parameters at the required locations. A reduction of specific yield of the Holocene aquiclude and the specific storage values of the aquifers

of the selected polygons after a careful analysis may improve the performance of the model. Changing parameters deliberately deteriorates the quality of model.

2.8 Groundwater Abstraction

2.8.1 Groundwater use in Mekong Delta

In the Mekong Delta, surface water, such as that found in rivers, lakes and canals, is the main source of water for irrigation. However, because of many activities in the upstream part combining with climate change, the Delta is now facing the negative issues, and two of them are the fresh water shortage and the salt intrusion in the dry season. Therefore, GW resource is considered for water supply in some urban cities, especially in coastal area and its use is strongly increasing in the Delta.

The domestic and irrigation using GW is expected to increase in Viet Nam (Eastham et al., 2008; Phuc, 2008). GW is accessed via dug wells, small-scale household tube-wells, or medium and large-scale central supply wells that were dug as part of the Rural Clean Water Supply Program (UNICEF, 1996).

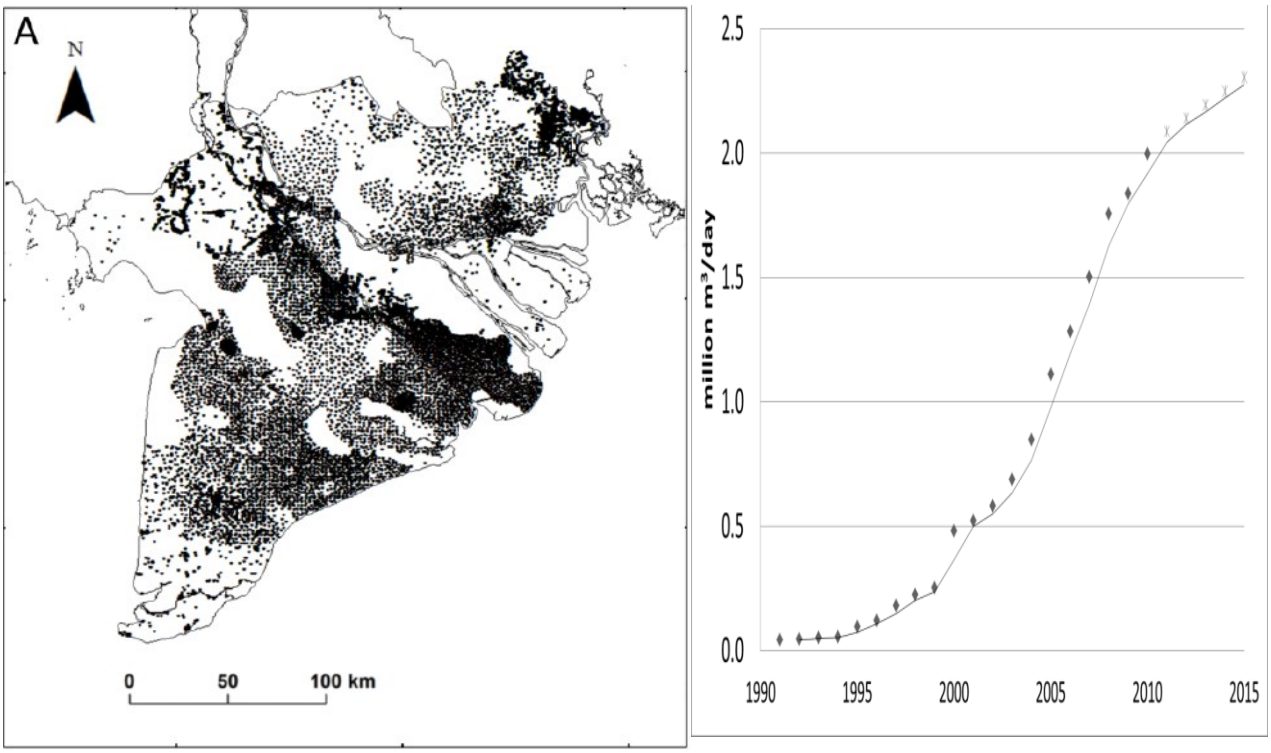

Fig. 2-2 ***(Right)*****- Extraction wells distribution; (*****left)*****- the estimated groundwater extraction in the Mekong Delta** (Minderhoud, 2016)

GW in the Mekong Delta supplies water for domestic use, urban water supply, irrigation, aquaculture, and industrial sites. About 4.5 million people depend upon GW for drinking (Ghassemi, 2000). In 2007, it was estimated there was 465,000 GW wells in the delta that removed a total of 1,229,000 m3/day (DWRPIS, 2009). In 2011, the Fig. 2.3 shows a million extraction wells with depth of 10 m to 300 m is distributed in whole Mekong region (MONREs, 2011). Recently, the total amount of GW pumping of more than 2 m3/day was estimated (Minderhoud, 2016) (Fig. 2.3).

The Division for Water Resources Planning and Investigation (DWRPIS, 2013) found that 60 per cent of wells access the Pleistocene aquifers of the delta (qp2-3and qp1) and that most water supply projects for domestic and industrial water supply use this aquifer.

In the urban city of Mekong Delta, a survey conducted in 2002 by the Can Tho Department of Agricultural and Rural Development found 24 per cent of the population of Can Tho, the largest city in the delta, used GW for domestic use. This proportion is much higher in rural and coastal areas where residents have great difficulty accessing fresh water during the dry season due to saline and/or polluted canal water (Danh, 2008). Therefore, GW has been strongly extracted in the coastal zones of the Delta which mainly used for aqua/agriculture and domestic water supply (DWRPIS, 2013; DONREs, 2012)

2.8.2 Impacts of Groundwater Pumping

The corresponding impacts of intensive GW pumping are recognized, which results the decline in GW levels in some urban and coastal areas of Mekong Delta (Fig. 2.4). GW depletion is primarily caused by sustained GW pumping. Some of the negative effects of GW depletion: (i) drying up of wells; (ii) reduction of water in streams and lakes; (iii) deterioration of water quality; (iv) increased pumping costs; and (v) land subsidence (USGS, 1997)

Environment Agency regulatory staff makes the decision whether to issue a GW abstraction license. They are supported by hydro-geologists from the Environment Agency Area team, who will consider the potential impacts of the new abstraction a) on surface water features, for example rivers, springs, wetlands, lakes and pools, and

b) on other abstractors. The impacts considered include the following: (i) depletion on rivers; (ii) drawdown beneath wetlands; (iii) estimating change in GW flow to & from wetlands as a result of GW abstraction; (iv) effect on water features other boreholes, springs, pools.

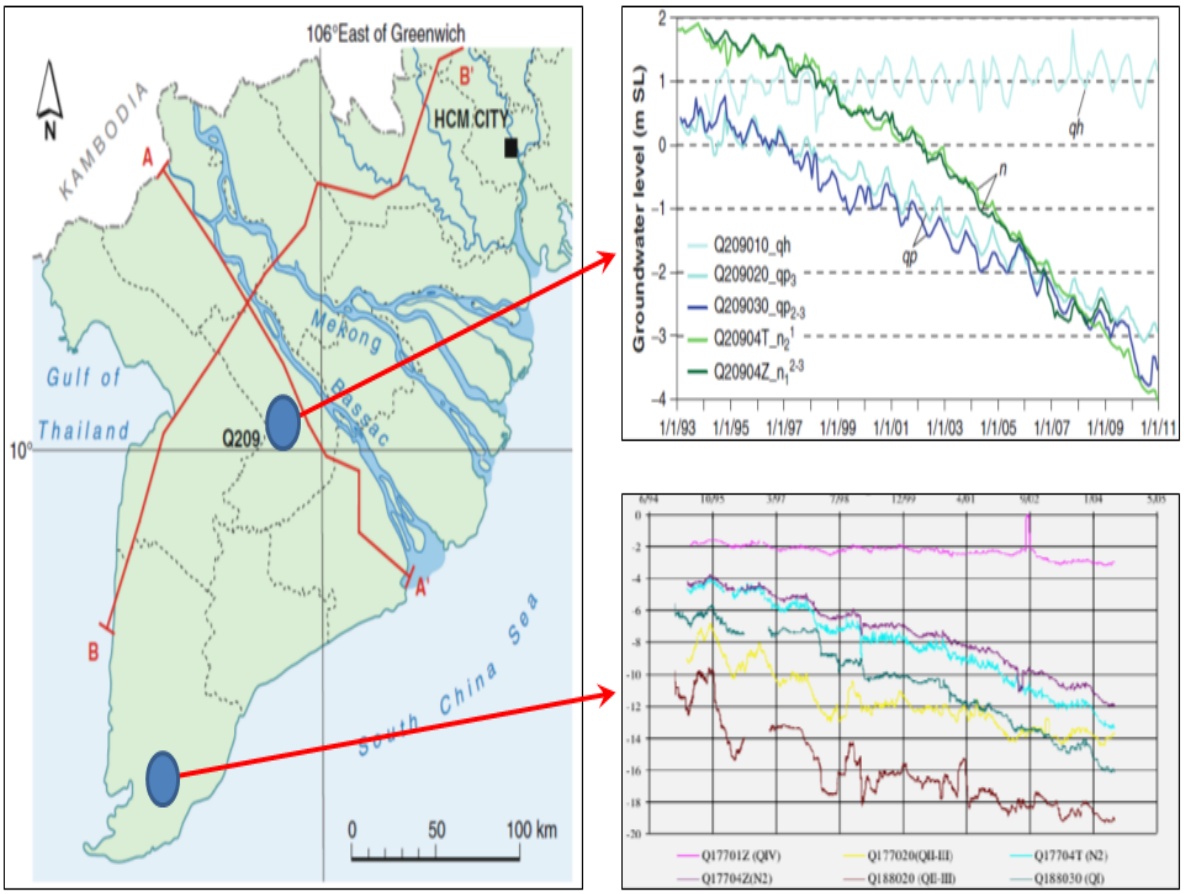

Fig. 2-3 Decline in GW level in urban and coastal areas (DWRPIS, 2013)

CHAPTER 3. GROUNDWATER MODELING OF ENTIRE MEKONG DELTA USING IMOD

3.1 Background

GW in the Mekong Delta is essential and is extensively used in the last decades (Eugene, 1971; IUCN, 2011). A compiled paper by IUCN (2011) showed that GW in the Mekong Delta supplies water for domestic use, urban water supply, irrigation, aquaculture, and industrial sites.

A mathematical model is very essential in water resources management in general and in GW management in particular (Anderson and Woessner, 1992). The appropriate model settings will help in developing suitable management scenarios to prevent GW depletion, management that is the key for sustainable GW use. However, model applications in the Mekong Delta to investigate on GW variability as well as how natural and anthropogenic factors impact on this system is still rather limited. The first attempt was done by Haskoning B.V., DWRPIS (Boehmer, 2000) to set up a regional GW model for the Nam Bo region including the Vietnamese Mekong Delta. The model was used to study the GW flow in the aquifers, to determine the recharge mechanism as well as to determine the GW potential for drinking water supply. Since the model setup, a number of activities were been done to update the model. For example, the new regional hydrological maps DGMS (2004), the rapid increase of GW extraction rate in the last decade, are typical reasons requiring a new model set-up. In this chapter, the model is used for studying the potential GW distribution in time and space of the Mekong Delta.

3.2 Purposes and Scope of Modeling

High resolution Mekong Delta GW flow modeling, necessary to evaluate effects on a local scale, has traditionally been restricted to small regions given the computational limitations of the CPU memory to handle large numerical MODFLOW-grids. This restriction has traditionally forced a model builder to always choose between (1) building a model for a large area with a coarse grid resolution or (2) building a model for a small area with a fine grid resolution. For some time it appeared that finite

element models could fill the gap by refining the grid only where hydrological gradients were anticipated. However, unanticipated stress may also occur in parts of the model area where the grid is not yet refined resulting in a possible undesired underestimation of these effects. Theoretically the modeler could choose to design a finite element network with a high resolution everywhere, but then it becomes more economical to use finite differences. This is why Mekong Delta model has based its innovative modeling techniques on iMOD considering the local scale model of the cities in chapter 4 and chapter 5 below. The GW modeling of entire Mekong Delta was developed to advance the methods and approach used for: (1) flexibility to generate high resolution model grids everywhere when needed, (2) flexibility to use or start with a coarser model grid, (3) reasonable runtimes / high performance computing and (4) conceptual consistency over time for any part of the area within their administrative boundary.

3.3 Modeling Approach

The development of the iMOD approach took off in The Netherlands in 2005 when Deltares and a group of 17 stakeholders decided to jointly build a numerical GW model for their common area of interest (Berendrecht, Snepvangers et al, 2007; Vermeulen, 2013). The GW model encompasses the entire north of the Netherlands at a resolution of 25 x 25 m2 and was constructed together via an internet accessible user-interface. This makes it possible for the modelers to easily access the model data, intermediate results and participate in the model construction. The iMOD approach allows gathering the available input data to be stored at its finest available resolution; these data don't have to be clipped to any pre-defined area of interest or pre-processed to any model grid resolution (Fig. 3.1).

The computer model iMOD is a modular three-dimensional finite difference GW flow model. It has been used for dynamic GW flow simulation in the transient/steady state. The iMOD is constructed commonly with available input parameters for large scale GW flow modeling instead of focusing on small areas. Otherwise, the small scale model with a smaller grid size should be integrated with a large scale model by GIS processing (Vermeulen et al., 2013).

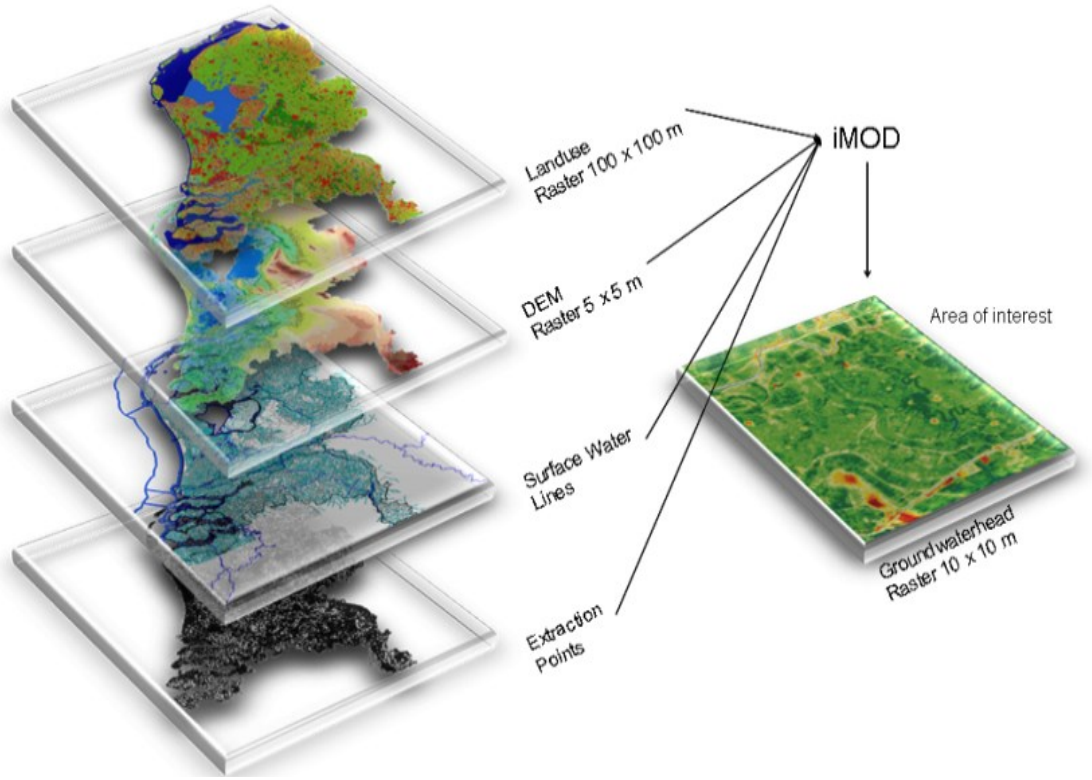

Fig. 3-1 The iMOD-approach: one input data set without clipping to any areas of interest.

It can be also used for full three-dimensional modeling in a complicated hydrogeological property with various natural hydrological processes and artificial activities. In addition to calculation of GW head distribution in space and time, iMOD can simulate the response of aquifer systems to different scenarios on GW resources. The strength of iMOD lies in its powerful GIS pre-processing and possibility of extensive combination of various sub-models. There are a wide range of useful packages such as river, abstraction wells and drainage. The user can also control the solution method and procedures through a wide range of options. For iMOD modeling, there are two different approaches such as the grid approach and the conceptual model approach (Vermeulen et al., 2014). In the grid approach, the 3D model grid is first created and then the sources/sinks and other model parameters are applied on a cell-by-cell basis. The conceptual model approach involves usage of the GIS tools to create the model of the site being modeled. The data are then assigned to the grid. The conceptual model approach is more efficient than the grid approach which is only suitable for simple problems. The software accepts various input formats of raster

images, ArcGIS geo-database, and shape files. There are several import options for borehole data and text formatted files. The iMOD requires the value of horizontal grid spacing to be determined, whereas vertical grid spacing is estimated from supplied values of the bottom by hydrological structure of each layer.

Resolutions of parameters can differ and the distribution of the resolution of one parameter can also be heterogeneous. In addition, the spatial extents of the input parameters don't have to be the same. iMOD will perform up- and down scaling (Vermeulen, 2006) whenever the resolution of the simulation is lower or higher than that of the available data. This approach allows the modeler to interactively generate models of any sub-domain within the area covered by the data set. When priorities change in time (e.g. due to changing political agenda's) the modeler can simply move to that new area of interest and apply any desired grid resolution. In addition the modeler can edit the existing data set and / or add new data types to the data set. Utilizing the internal up- and down-scaling techniques ensures that sub-domain models remain consistent with the bigger regional model or that the regional model can locally be updated with the details added in the sub-domain model (Minnema, Vermeulen et al, 2013).

3.4 Mekong Delta Model

3.4.1 Model Equation

To develop a numerical model of an aquifer, the concepts and laws that control the physical process of the system should be translated into mathematical equations with partial differential equations. Model equation is derived by mathematically combining the water balance equation with Darcy's Law in three dimensions as following:

$$\frac{\partial}{\partial x}(K_x \frac{\partial h}{\partial x}) + \frac{\partial}{\partial y}(K_y \frac{\partial h}{\partial y}) + \frac{\partial}{\partial z}(K_z \frac{\partial h}{\partial z}) = S_s \frac{\partial h}{\partial t} - W$$

where, x is the Cartesian spatial coordinate x, y, z; h = h(x,t) is hydraulic conductivity as a function of x, y, z; Ss is Specific storage; W is source (negative for sink).

The model domain is discretized in space by subdividing the area into blocks/cells. The size of cells in x and y-direction are uniform over a row and over column and are defined a varying spatial resolution for model area. If the fluid density is constant, the

water balance of a block/cell, expressed by sum of all flows into or out of a block and its changes in storage, represents the equation (Essink, 2000):

$$\sum Q_i = S_s \frac{\Delta \phi}{\Delta t} \Delta V$$

where, Ss is Specific storage of the porous material; Qi is Total flow rate in the block/cell; ΔV is Volume of the block/cell; Δϕ is Change in head over a time interval of length Δt.

Applying equation above to block [i,j,k] taking into account the flows from the six adjacent blocks, see Fig. 4.2, as well as an external flow rate Qext (pumpage) yields:

$$Q_{i,j-1/2,k} + Q_{i,j+1/2,k} + Q_{i-1/2,j,k} + Q_{i+1/2,j,k} + Q_{i,j,k-1/2} + Q_{i,j,k+1/2} + Q_{ext_{i,j,k}}$$
$$= SS_{i,j,k} \frac{\phi^t_{i,j,k} - \phi^{t-\Delta t}_{i,j,k}}{\Delta t} \Delta V$$

where, ϕti,j,k – ϕi,j,kt-Δt is a backward difference approach, which mean that Δϕ/Δt is approximated over a time interval which extends backward in time from t.

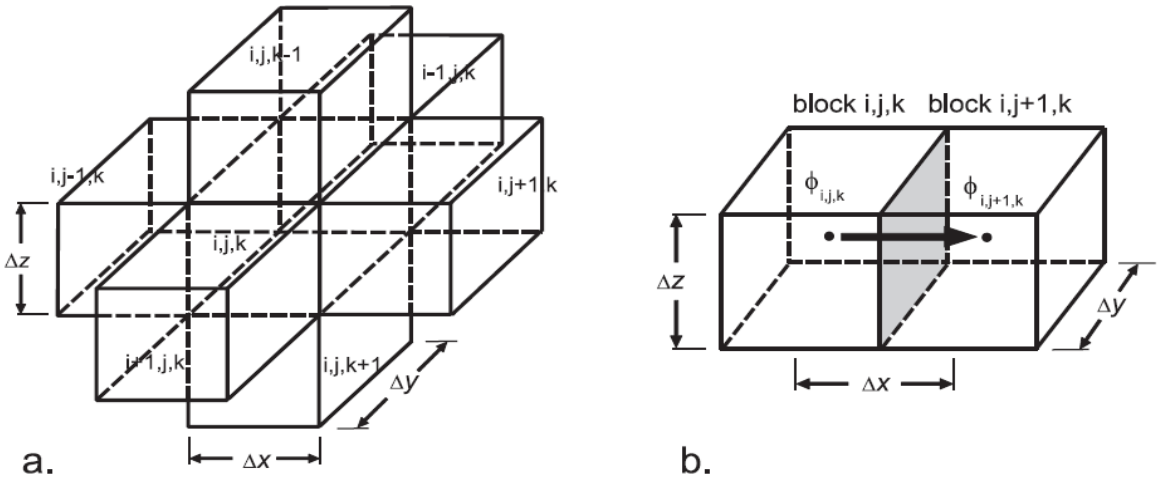

Fig. 3-2 a: block [i,j,k] with the surrounding blocks. b: flow between block [i,j,k] and [i,j+1,k] (Essink, 2000).

3.4.2 Groundwater Balance

A GW balance, also known as a water budget, quantifies the major inflows, outflows and changes in storage of GW system. A water balance can be spatially and/or temporally distributed or it can be reported as a lumped parameters.

The sustainability of GW resources can be accessed by comparing recharge and discharge rates. Discharge exceeding recharge can forewarn of falling GW levels, reduced rainfall as base-flow diminishes, or ground subsidence as previously water-

filled pore spaces collapse. Comparing individual water balance components can provide insight to the hydraulic system and guidance for water management. Based on the conceptual GW balance in the study (Fig. 3.3), the GW balance equation as flowing:

$$(GWI + P + RR + DP) - (GWO + Q + D + SPD + ET) = \Delta GWS$$

Where,

- Positive: GWI is the groundwater inflow; LR is the recharge from local rainfall; RR is the recharge from the Rivers; DP is the deep percolation from the upper system.

- Negative: GWO is the groundwater outflow; Q is the actual groundwater pumpage (exploitation); D is surface drainage; ET is the evapotranspiration losses.

- Δ GWS is the change in groundwater storage

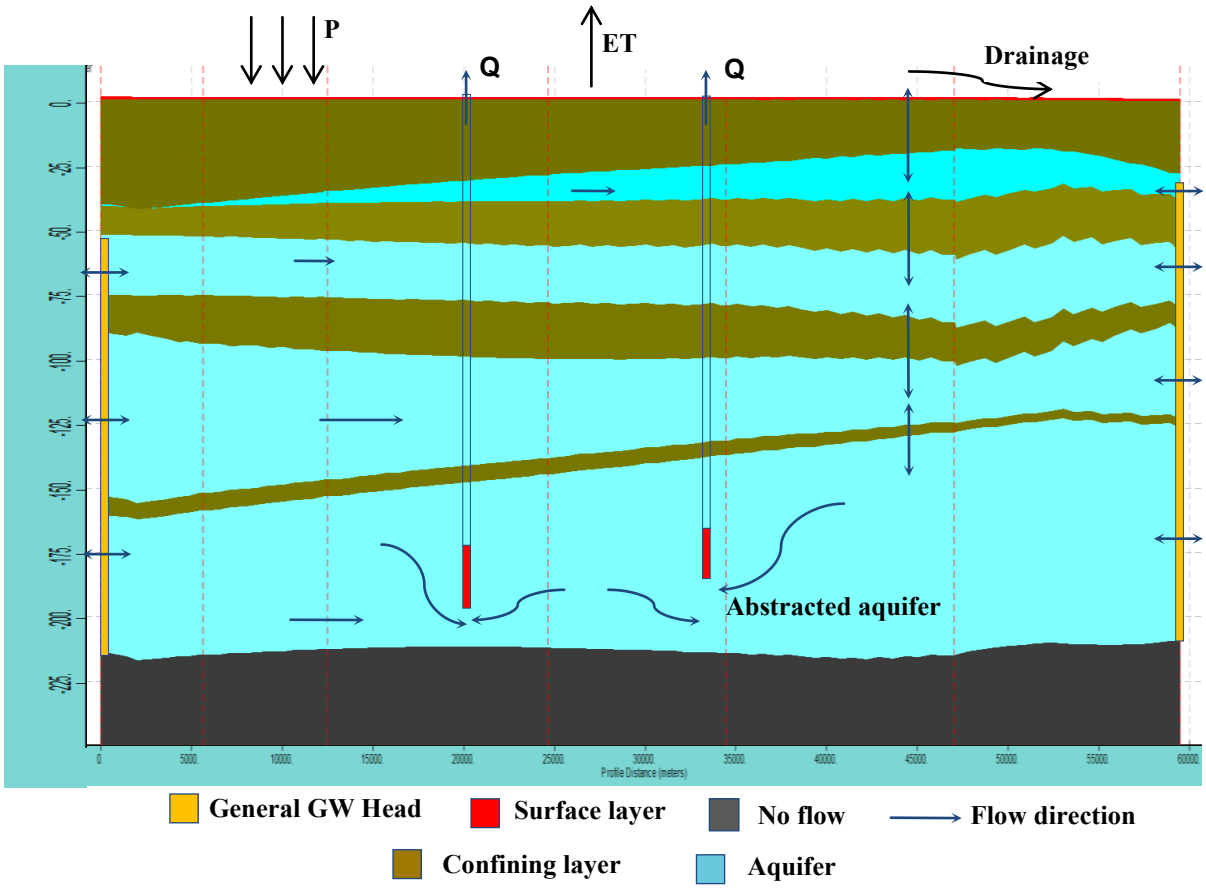

Fig. 3-3 Conceptual GW balance

3.4.3 Model Structure

In 2011 the ambiguous plan arose to build a sustainable model for the Mekong Delta. Therefore, corresponding authors came together for a month to make a first start with

this model. The focus at that time was mainly to get familiar in building a GW flow model similar to other large scale modeling studies recently carried out by Deltares. Most of the time, however, was occupied by collecting the necessary data (private and public accessible sources) and transfer them into the iMOD format. It yielded a preliminary model for the entire Mekong Delta. This section describes the concepts of the Mekong Delta model at that stage and as well as the improvements made recently. This short description illustrates how easy and transparent it can be to improve a model made in iMOD whenever renewed data comes available.

DEM: In 2011, a surface elevation (DEM) on a resolution of 1,000 x 1,000 m was provided by DWRPIS (Division for Water Resources Planning and Investigation for the South of Vietnam). The model needed to be able to compute at least the low-lying area in the Mekong Delta solely. We defined the area of interest as those areas where the DEM was less than 15 m+ MSL assuming that the bedrock was outcropping above this elevation. Currently, we achieved a geological map for the Mekong Delta (Anderson, 1978) and we were able to define the model boundaries better. Moreover, we downloaded a DEM on a resolution of 90 x 90m worldwide (ftp:// e0srp01u.ecs.nasa.gov/srtm/version2/SRTM3). This data file has been used to update the top of the hydrological system, as well as the drainage levels throughout the Mekong Delta (Fig. 3.4).

Boreholes: The subsoil of the GW flow model was built from boreholes provided by DWRPIS (DGMS, 2004), see Fig 3.5–left. In totally 95 boreholes were available for which each borehole was categorized by aquifer number. With this data input, we could use the iMOD SolidTool to create a solid of the subsoil by connecting corresponding interfaces between the boreholes, see Fig 3.5-right. Moreover, scanned geological sections were included (Fig 3.5-middle) to incorporate more detail; such as out wigging of aquitards as well as local modification of interfaces in between boreholes. For the Ho-Chi-Minh-City area we achieved several extra boreholes to improve the solid of the subsoil locally.

Permeability: In 2011 we were using a single assumption for the permeability for each model layer. Recently, more detailed information on the distribution of layer

permeabilities became available which were used to update the permeability field for several aquifers/aquitards.

Surface water systems: Lacking any detailed information about the large river systems in 2011, we generalized those in the Mekong Delta (Mekong and Saigon River) by a simple line representation. The renewed DEM however, shows a very accurate spatial distribution of those rivers and gives a fairly good estimate of its level. In 2013 we received a SOBEK model for Ho Chi Minh City and surrounding including the Saigon River (Deltares, 2013) that was used to improve the interaction between the river systems a GW. For all other areas we assumed that those areas are drained by drains with an offset of 0.25 meter-surface level.

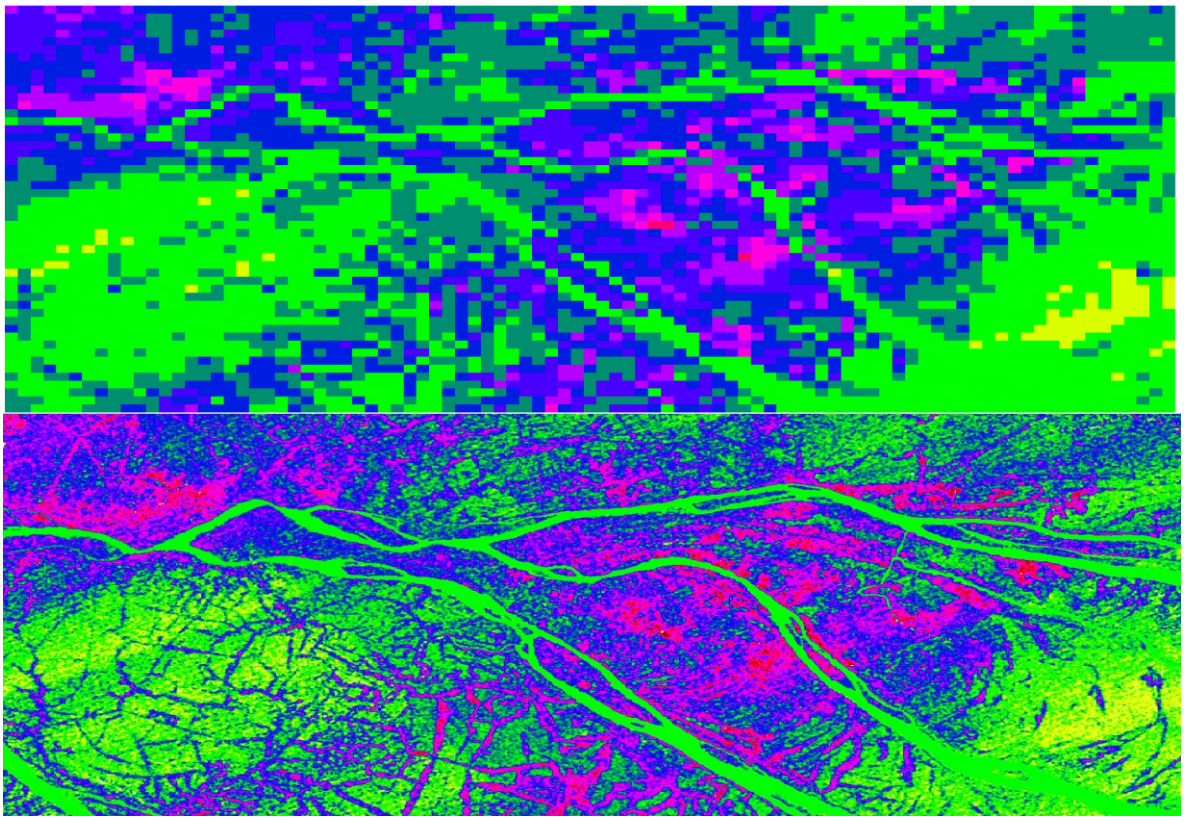

Fig. 3-4 (top) DEM at a scale of 1,000x1,000m^2 and (bottom) the DEM at a scale of 90x90 m^2.

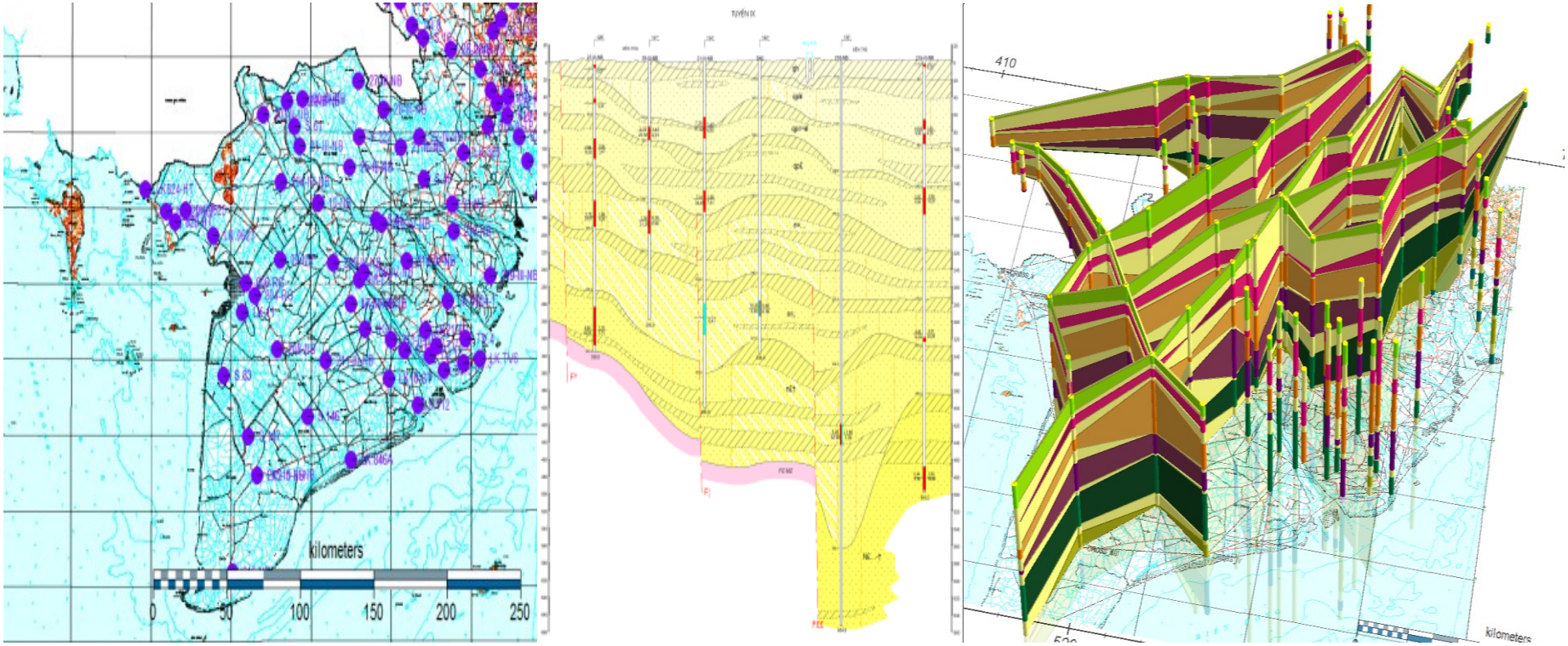

Fig. 3-5 (left) The location of boreholes; (middle) an example of the geological interpretation used in the solid building; (right) the solid of the subsoil for the Mekong Delta.

3.4.4. Groundwater Modeling for Mekong Delta

The entire Mekong Delta model has been simulated on a coarse scale of 1,000 x 1,000 meter, by a simulation network of 308 columns and 410 rows and 8 model layers. It should be noticed that there was no need to scale all input data beforehand to this 1,000 meter scale since iMOD scales internally during the simulation. In the configuration file for iMOD (i.e. a runfile) the scale size is specified as well as the simulation window. In this way it is easy to configure quickly a large variety of models for different scales and simulation windows, interactively. In Fig. 3.7-left we presented the results for this 1,000 x 1,000 m2 model and in Fig. 3.7-middle the layout of the 33 sub-models that we used to create a final model result for the entire Mekong Delta at a scale of 100 x 100 m2. The extent of each sub-model overlaps the adjacent sub-models by 15,000 meter. This size in overlap yielded an optimal trade-off between accuracy and efficiency.

Each sub-model (600 x 600 x 8 rows, columns and layers on average) took approximately 1.5 minute to complete and was run in parallel. Afterwards all results (heads and budget terms) were merged by iMOD to construct images of the entire computed hydraulic heads for the Mekong Delta on a scale of 100 x 100 m as shown in Fig. 3.7-middle. Fig. 3.7-right shows these for model layer 4 that contains most of the extraction wells. The total number of rows and columns in this result grid became eventually 3,080 and 3,660. Taken the 8 model layers into account we were able to simulate this GW flow model within several minutes for 90 million computational nodes. This would take 992 million floating reals to compute that would take 3.6 Gigabytes of RAM, which is hardly available on a regular PC and requires a 64-bits computer.

An important part of this GW modeling is the model calibration. In order for the model to be used in any type of boundary conditions for specific cases in the Mekong region, calibration target is the observed GW levels at 168 monitoring wells whole Mekong Delta in December, 2011. It demonstrated that the model showed fairly good agreement between simulated values and the observed values (Fig. 3.6).

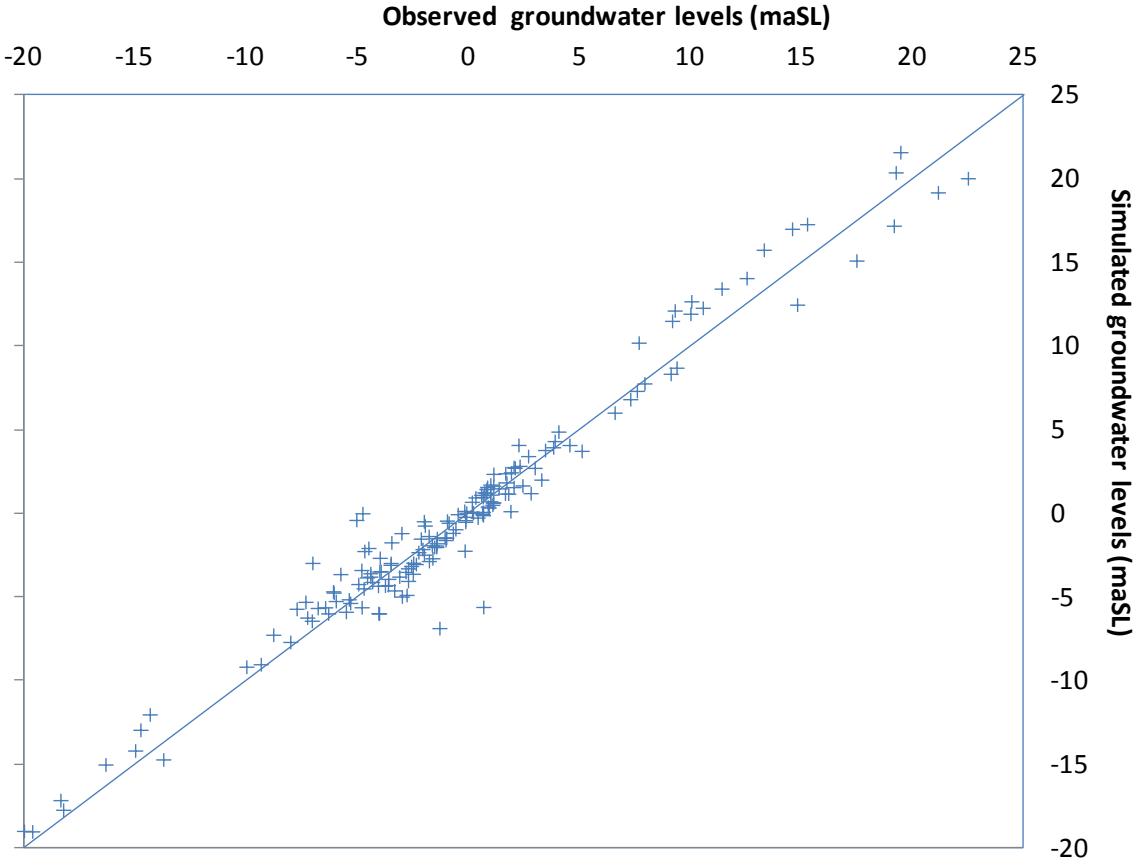

Fig. 3-6 Comparison of simulated vs. Observed at December, 2011

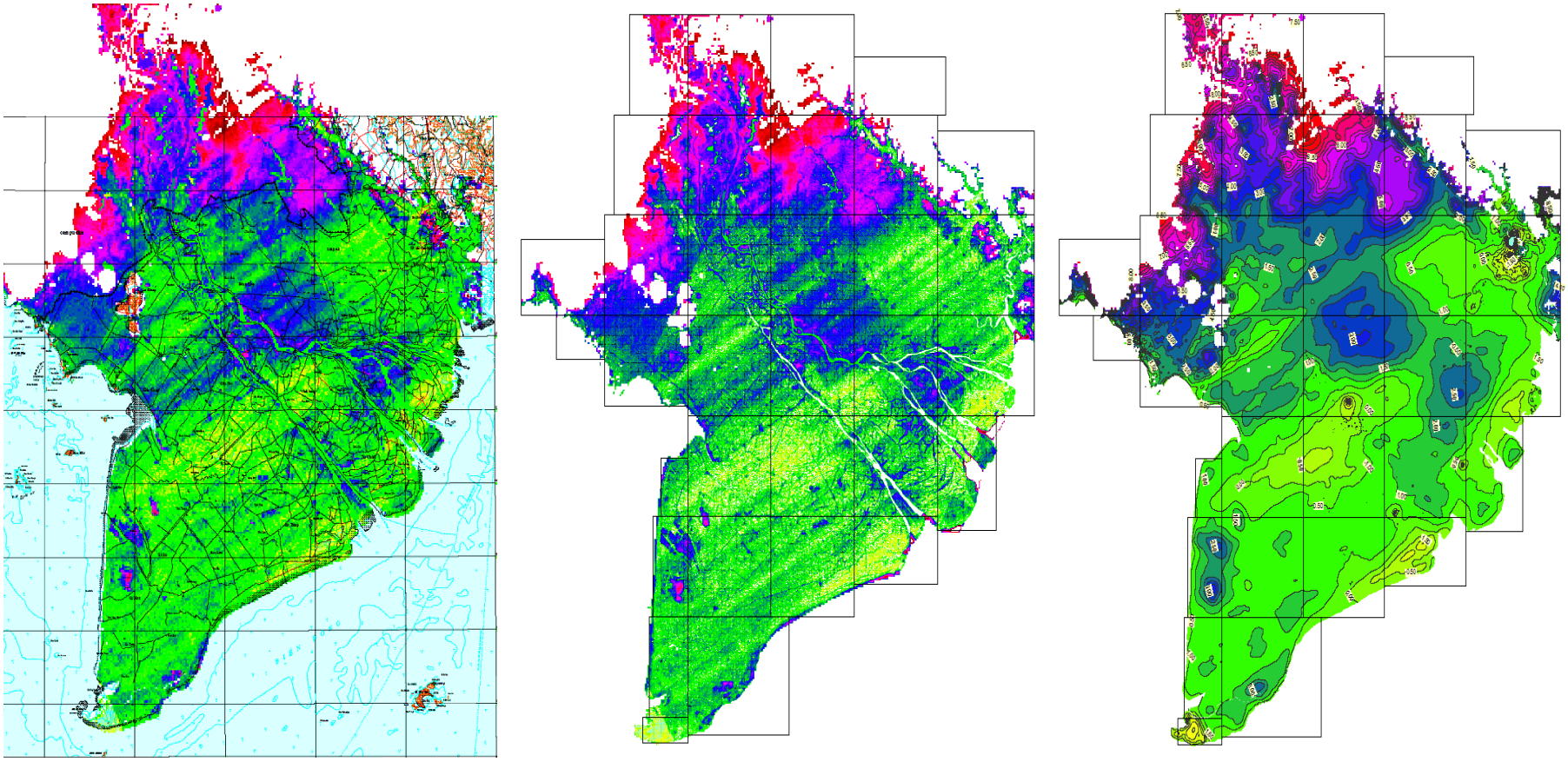

Fig. 3-7 (left) Simulated phreatic heads for the entire Mekong Delta (1,000 x 1,000 m^2) and (middle/right) the 33 submodels used to compute at a scale of a 100 x 100 m^2.

3.5 Conclusions

A supra-regional 3D groundwater flow model for the whole Mekong Delta was established using iMOD. By the entire Mekong Delta model with different grid sizes (1000x1000 m^2 and 100x100 m^2) and 8 layers, groundwater head distribution was calculated, which showed fairly good agreement with the observed values. The findings from the results of model simulation are as follows:

(1) The constructed model for the entire Mekong Delta was flexible to generate high resolution model grids everywhere when needed, and flexible to use or start with a coarser model grid. Also, the model reached the conceptual consistency over time for any part of the area within their administrative boundary.

(2) Base on the model, credible forecast can be made for the future GW situation under present and future GW abstraction with the specific cases in the local areas. However, the additional information and new data are required for updating of the model on regular basis.

(3) The small grid should require quite huge computational time, though it can represent the exact locations better than the coarse grid. In the meantime, as the iMOD can easily generate higher resolution grids everywhere inside, the groundwater head distribution calculated by the model can be utilized as the boundary condition and the initial condition for higher resolution modeling of certain areas. Thus, the entire Delta model was established as a startup model for more detailed analyses in the following chapters.

CHAPTER 4. IMOD MODELING FOR ANALYZING IMPACTS OF GROUNDWATER PUMPING IN THE URBAN AREA OF MEKONG DELTA

4.1 The case study and background

From the past until now, surface water has been used as the main water source of the living and production activities in the MD. For the reason that there are many branches of Mekong and Bassac River and network of canals, people can access the water easily. Unexceptionally, the study are locates in middle of MD has accessed to water from Bassac River (Fig. 4.1). However, the population growth and rapid development in the study area cause high water demand in recent years. In addition, waste water and changing of hydrological regime have impacted on quality and quantity of surface water. Therefore, it could not meet for domestic use and the effective using of domestic and industrial supply has been limited due to river/canal water quality degradation (Tuan et al., 2007). Since the last ten years, GW (GW) has

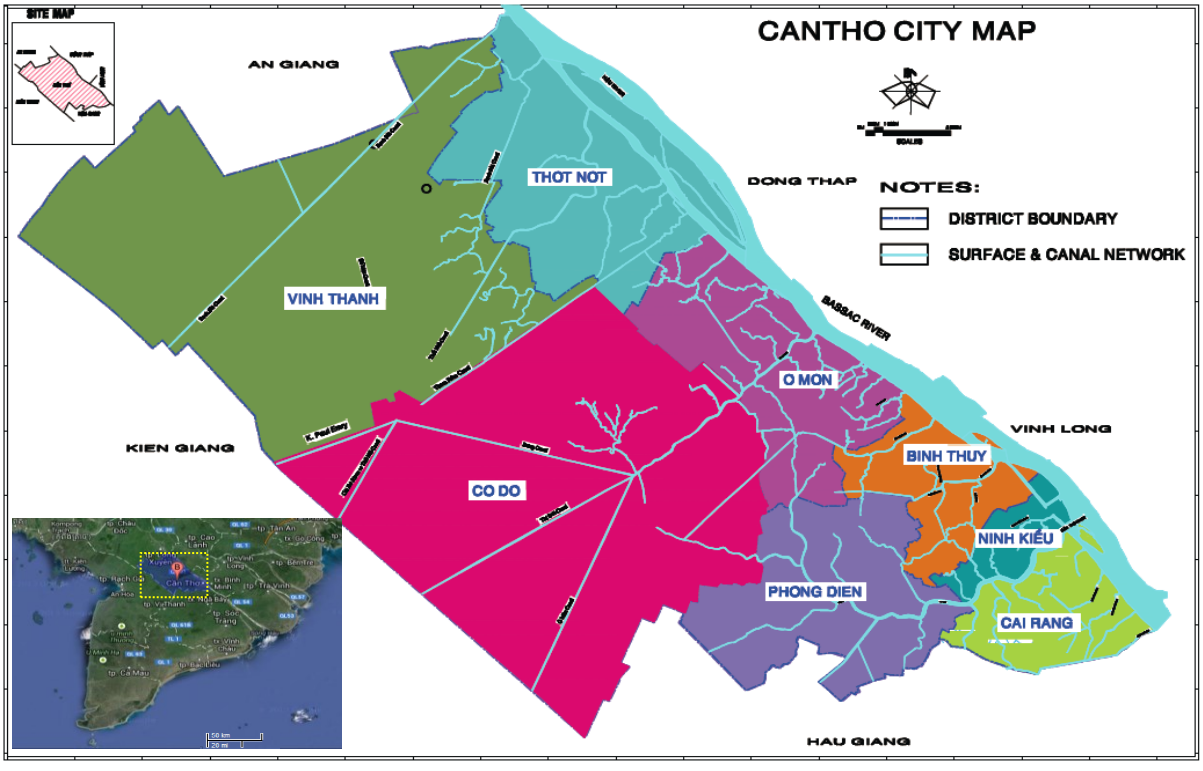

Fig. 4-1 CanTho city & canals network map (DOC, 2011)

considered as an option of fresh water use in the study area. Trend of GW use has increased strongly in the study area because its quantity and quality are more stable than surface water (Thomas, 2008). Because of its availability, GW is convenient resources to access for purposes of water usage. It has led to large scale GW developments in the study area (IUCN, 2011). However, the GW drawdown phenomenon is clear observed in the study area. It shows the drop-down at the observation wells in Can Tho city from 2000 to 2009 (DONRE 2012), especially at the aquifer where the most of depths of pumping wells are located in. GW pumping can cause the cone of depression that may form the zones, where will be vulnerable to impacts of pumpage (USGS, 1997). These zones relate to land subsidence issues and they have been reported widely in some studies (Syvitski, Kettner et al, 2009). Moreover, land subsidence has also been recognized through primary studies in the urban areas of MD (Fujihara et al., 2015). It is necessary to find a proper modeling tool for GW assessment under pumping impacts in the study area and it is very essential as a first step of aquifer response evaluation

4.2 Objectives

This part aims at (i) developing the steady state GW model in the study area, CanTho city, middle part of Mekong Delta; (ii) applying the calibrated model to simulate the GW heads; (ii) Simulating of spatial GW heads distribution of the aquifer includes GW pumping stations for domestic and industry was conducted as expecting on the developed conceptual model; (iii) the model was used to predict the GW decline based on the trend of increased pumping until 2035 and (iv) modeling in 3D to evaluate the formation process of cones of depression under current and increased pumping operation on GW resources in the CanTho city.

4.3 Model building

4.3.1 Model construction

The construction of the GW flow model of the iMOD requires the definition of the conceptual model, the model domain with flow boundary conditions and the aquifer properties.

Conceptual model

The conceptual model approach involves usage of the GIS tools to create the model of the site being modeled. The data are then assigned to the grid. To enable studying GW potentiality in the study area, the conceptual model has been constructed by the result of MD model and it based on the geology formation which was defined by borehole data provided by Division for Water Resources Planning and Investigation for the South of Vietnam (DWRPIS, 2009) to create hydro-geological profiles.

MD region is characterized by the presence of alluvial aquifer and aquifer sediments (Anderson, 1978) which are represented by borehole wells test data. Therefore, total of 5 hydro-geological cross-section profiles was set by connecting corresponding interfaces between the boreholes (Fig. 4.2). Based on those constructed profiles, aquifer layers were interpolated by Kriging method. The confining layer represent largely low hydraulic conductivity units, such as clay and split that impede the flow of water between aquifers whereas the aquifer layers is termed aquifers because they have physical properties that allow for the storage and flow of water between the grains of sediment.

Model domain

The simulation procedure was started by dividing the iMOD domain into a suitable grid pattern on which all the input items are performed via input menus. The total surface area of the model domain reaches 5760 km2. The computational grid for the aquifer domain in the study area is divided into 576054 cells. The dimension of the cell nodes reaches 100m for the cultivated and reclaimed areas (Fig. 4.2).

Boundary conditions

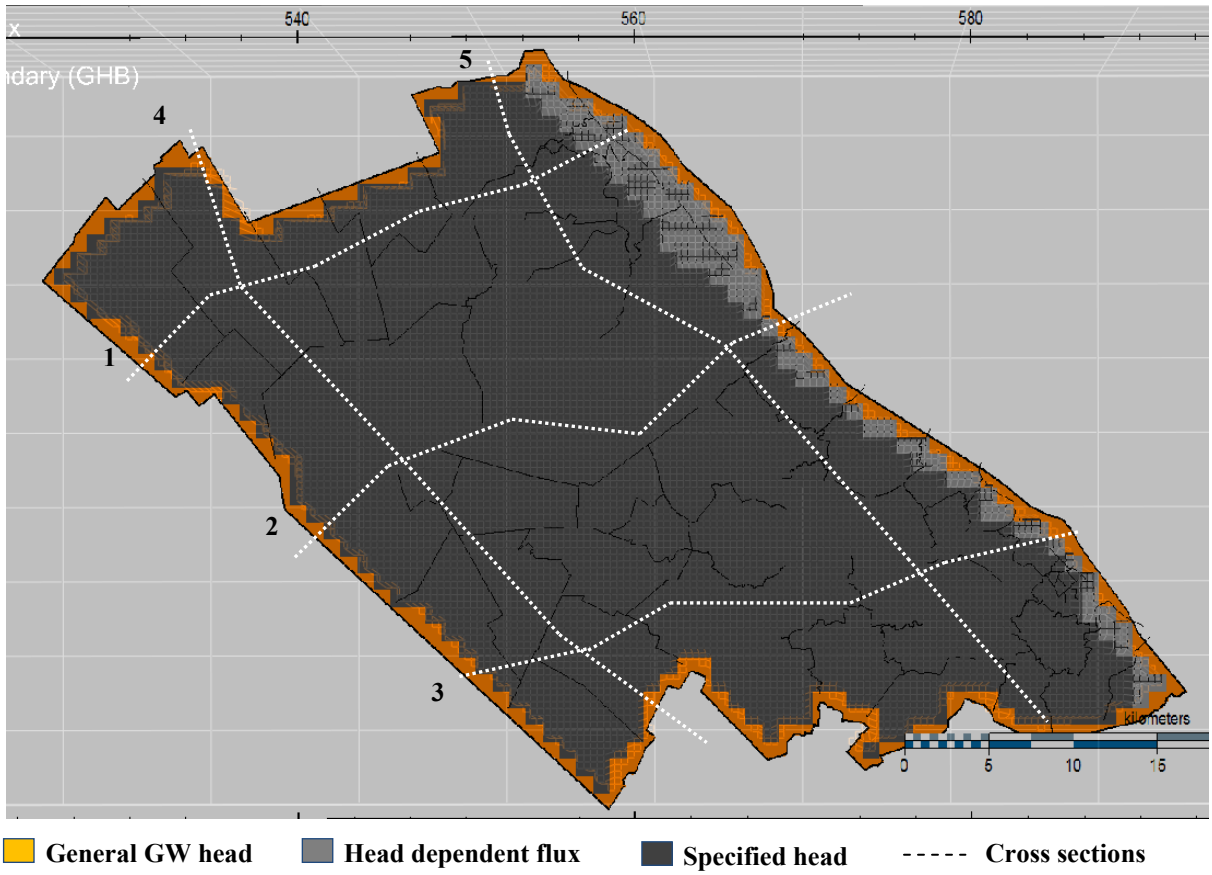

Fig. 4-2 Cross sections & The constructed model domain grid and the boundary conditions

For calculating GW flow in the aquifers of a region, conditions at the study area's boundaries must be given. In this numerical model, boundary conditions are defined: (i) specified head represents the area can be impacted by pumping; (ii) head dependent flux represents the surface water area for the Bassac River and (iii) general GW head boundary (GHB) presents the boundary along the edges of the model domain. Because the entire MD has been simulated on a coarse scale of 1000 m x 1000 m, by a simulation network of 308 columns and 410 rows in iMOD and the layout of the 33 sub-models was primary developed to create a final model result for the entire MD at a scale of 100 m x 100 m. Those values were initially set for the GHB cells. This value was adjusted during calibration.

Initial GW head distribution

The GW level measurements through 14 observation wells in model domain during January, 2009 were used to construct a contour map for the initial GW head distribution. Therefore, all subsequent simulations were started from the January 2009

heads as the initial condition. Compilation of comprehensive GW head data in the study area began at that time.

Drainage and surface level

It were analyzed based on digital elevation map (DEM) optimization with resolution of 90m x 90m was applied to extract the existing drainage features and to evaluate the head of surface water bodies provided by College of the Environment and Natural Resources (CENRes), CanTho University. Further this resulted flow direction operations which follow the existing drainage pattern with corrected DEM in which existing drainage feature are more pronounced. Because the DEM scales in 90m x 90m resolution whereas the model has 100m x 100m resolution, the adjusted irregularly spaced point data were interpolated with 100m x 100m and converted into ASCII file for iMOD's input. It has been used to update the top of the hydrological system as well as the drainage levels throughout the study area.

4.3.2 Model input

Hydraulic parameters were determined by aquifer pumping test conducted by DWRPIS and Haskoning Company in 2000 for all layers. Evaluation of aquifer properties is based on the pumping test analysis which is given on Table 4.1. These determine how easily water moves through the aquifer, how much water is stored, and

Table 4-1. Hydraulic parameters from pumping test for aquifers in the study area

ID	Coordinates			Aquifer (m)			KD (m^2/d)	C (day)	S	C*S (day)
	x (m)	y (m)	z (m)	From (m)	To (m)	D (m)				
860-CT	1106561.00	589306.00	2.000	66.0	91.0	25.0	529.0	22.9	0.00843	0.1930
861-CT	1104608.90	578867.90	1.400	81.0	105.0	24.0	755.0	179.0	0.00148	0.2649
862-CT	1108200.00	575970.00	0.900	79.0	99.0	20.0	896.0	464.0	0.00104	0.4826
863-CT	1111136.00	571326.73	1.210	113.0	140.0	27.0	369.0	471.0	0.00143	0.6735
864-CT	1117683.56	568581.52	1.740	82.0	100.0	18.0	4949.0	231.0	0.00200	0.4620
866-CT	1106368.32	584397.47	1.450	88.0	112.0	24.0	911.0	38.4	0.00183	0.0703
867-CT	1107619.85	585211.16	3.300	69.0	112.3	43.3	844.0	35.0	0.00194	0.0679
868-CT	1109116.25	585597.66	3.900	97.0	122.0	25.0	844.0	18.3	0.00211	0.0386
869-CT	1111525.00	584335.00	2.200	128.0	148.0	20.0	120.0	2.9	0.00199	0.0057
871-CT	1116109.10	578733.10	0.950	127.0	146.0	19.0	1800.0	confined		

how efficiently the well produces water. Aquifer properties were addressed by the results of pumping test data at ten locations in the study area. The analyses were obtained as mathematical solution of Theis, Cooper Jacob straight line and recovery methods. For the model input, the parameter to be estimated and distributed across the model grid is either transmissivity or hydraulic conductivity which are constant within a given grid cell. The corresponded hydraulic parameters are interpolated and preliminarily categorized by Kriging method and mapping. These zones will be optimized during calibration process (Fig. 4.3).

Rainfall is the main recharge of shallow or unconfined aquifer. The rainfall data of rain gauge stations have been collected and analyzed. The mean annual precipitation has a bimodal distribution with most of rainfall occur during rainy season from May to November. Generally the entire city receives an annual average rainfall depth has decreased in recent five years (2008 - 2012), from 1230 mm to 1530 mm (DONRE, 2012). Interpolation techniques, ordinary Kriging method and the empirical

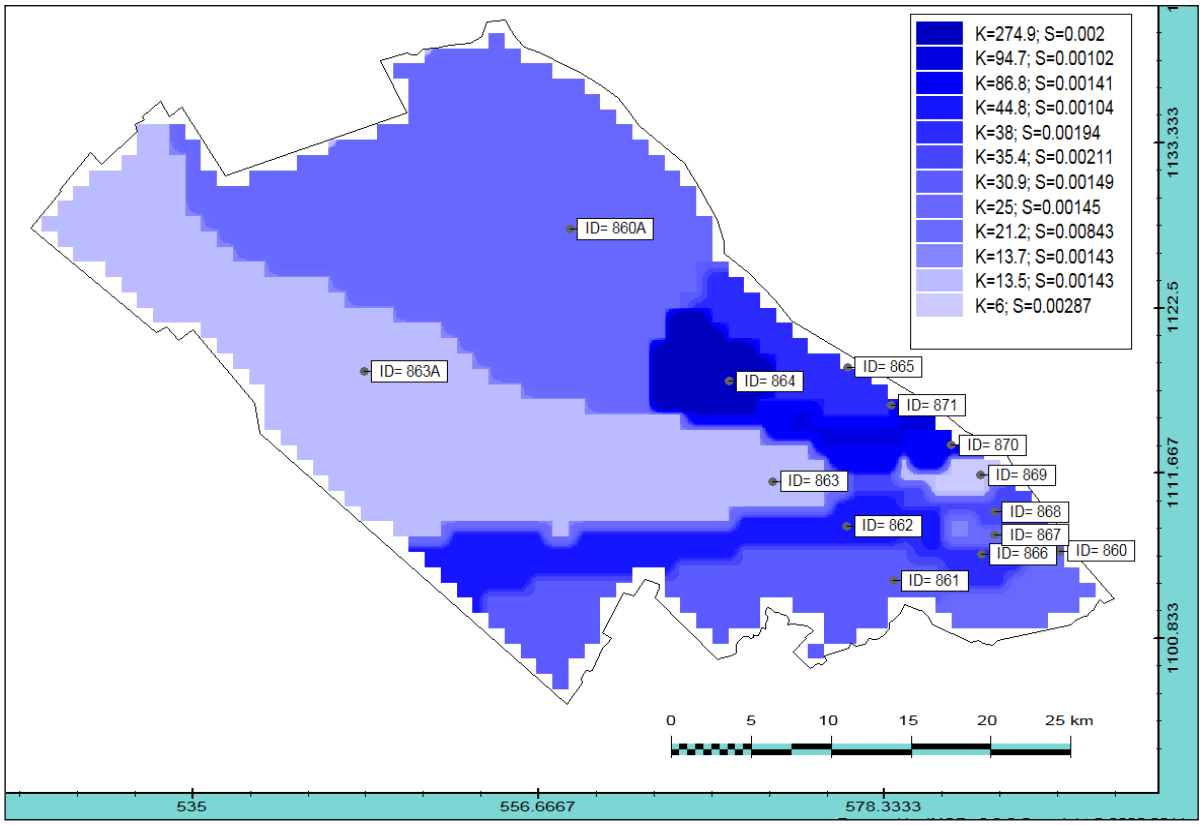

Fig. 4-3 Results of the optimised hydraulic parameter zones

relationship between the GW level and rainfall (Korkmaz, 1988) were applied to study the spatial distribution of the recharge within the model area.

Evaporation describes the water loss of shallow GW that will occur under a given climatic condition. Recent research has demonstrated that evaporation of GW can play a significant role in the local water cycle, especially in dry season (Korkmaz, 1988). Evaporation data were collected from meteorological station locates in the city. The trend of evaporation is increasing in recent 10 years and the highest evaporation is reported during the months of February, March and the lowest in September and October (DONRE, 2012). This value is calculated by input data of the evaporation coverage and the depth to the GW level estimated by iMOD during the period of running the model. The input data include: (i) the potential ET value per cell, for which the average open pan evaporation (ETO) was assumed; (ii) The extinction depth of evaporation of GW, which was assumed at 3 meter depth below the surface; and (iii) The surface elevation, which is the same as top elevation of the first layer in the GW model and is therefore imported in the evaporation package of the iMOD module per grid cell.

4.4. Model calibration and sensitivity analysis

Proper model calibration is important in hydrologic modeling studies to reduce uncertainty in model simulation (Engel et al., 2007). Measured GW levels collected on January, 2009; May, 2010 and December, 2011 were used to calibrate for the current condition. In this study, steady steady-state calibration for the current condition was conducted through a trial and error process, in which the initial estimates of the aquifer system were iteratively adjusted over reasonable ranges to improve the match between simulated and observed GW levels. Measured and calculated GW head of 14 observation wells in the study area (Fig 4.4) served as calibration targets for the model. There are basically two methods of model calibration: trial and error adjustment and automated parameter optimization (Anderson et al., 1992). Generally in GW modeling, root mean square error (RMSE) value reflects accuracy of model through the difference between measured and calculated GW heads. Ideally, the normalized RMSE of model-calculated GW heads

at calibration points should be less than 10 % and Nash-Sutcliffe's coefficient of efficiency should be around of 0.75:1 for a good model (Lutz et al., 2007). In order to obtain the acceptance model, calibration was carried out based on adjusting: (i) GHB value and (ii) hydraulic conductivity and storage coefficient.

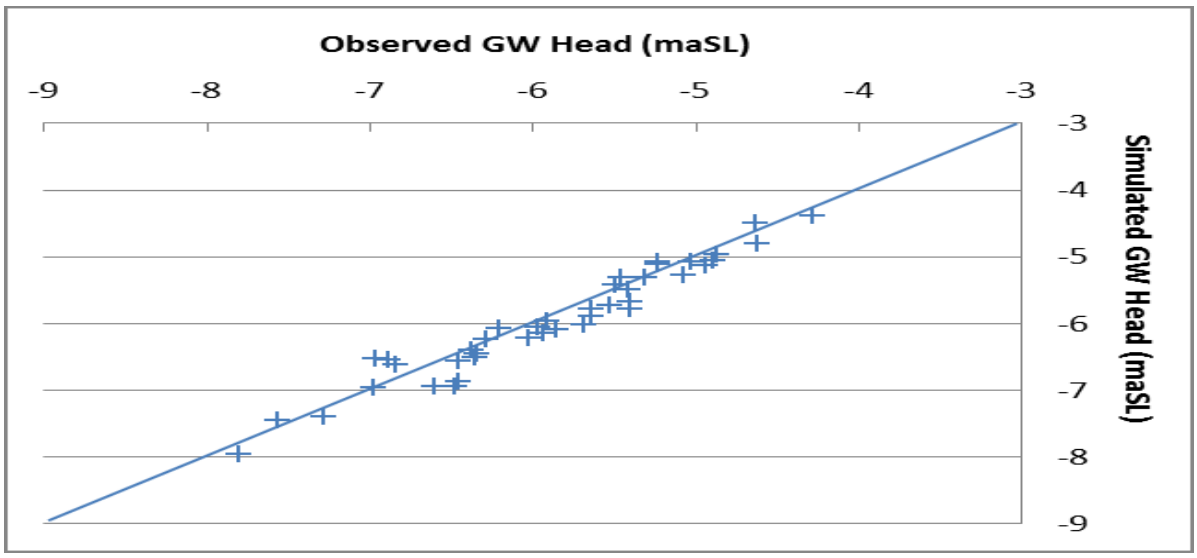

Fig. 4-4 Comparison of simulated vs. observed head: steady state

Table 4-2. Model evaluation results

Wells	Jan,2009			May, 2010			Dec, 2011		
	Observed Head (maSL)	Calculated Head (maSL)	Residual (m)	Observed Head (maSL)	Calculated Head (maSL)	Residual (m)	Observed Head (maSL)	Calculated Head (maSL)	Residual (m)
QT11A	-4.28	-4.38	-0.1	-5.03	-5.07	-0.04	-4.94	-5.14	-0.2
BS01A	-5.46	-5.32	0.14	-6.03	-6.21	-0.18	-5.69	-6.02	-0.33
QT12A	-5.31	-5.31	0	-5.97	-6.06	-0.09	-5.41	-5.79	-0.38
BS02A	-5.53	-5.73	-0.2	-6.36	-6.52	-0.16	-6.29	-6.23	0.06
QT09A	-5.41	-5.67	-0.26	-6.38	-6.40	-0.02	-5.94	-6.15	-0.21
QT16A	-6.84	-6.61	0.23	-7.57	-7.45	0.12	-7.81	-7.96	-0.15
BS04A	-6.60	-6.95	-0.35	-7.29	-7.39	-0.10	-6.89	-6.54	0.35
QT06A	-5.08	-5.28	-0.2	-5.64	-5.78	-0.14	-5.49	-5.42	0.07
BS03A	-6.21	-6.07	0.14	-6.98	-6.96	0.02	-6.34	-6.46	-0.12
BS06A	-6.46	-6.87	-0.41	-6.48	-6.94	-0.46	-4.63	-4.49	0.14
BS05A	-6.46	-6.57	-0.11	-6.97	-6.52	0.45	-4.87	-4.97	-0.1
QT10A	-5.24	-5.12	0.12	-5.92	-5.96	-0.04	-4.62	-4.81	-0.19
QT18A	-4.90	-5.06	-0.16	-5.64	-5.88	-0.24	-5.86	-6.09	-0.23
QT17A	-5.24	-5.08	0.16	-5.64	-5.78	-0.14	-5.42	-5.49	-0.07
	RMSE = 3.72 %; MAE= 0.18 m; NSE = 0.92			RMSE = 3.32 %; MAE= 0.16 m; NSE = 0.94			RMSE = 3.7 %; MAE= 0.18 m; NSE = 0.94		

The primary changes made to hydraulic parameters (K, S) during calibration were adjustments to values assigned to individual K and S zones, rather than adjustments to the spatial sizes and shapes of the zones. Through the calibration process, as these initial values were found not to give appropriate results, the hydraulic parameter values were optimized to obtain good agreement on GW head distribution; Fig. 4.3 shows the results of the optimized K and S zones for abstracted aquifer.

Model calibration results were evaluated qualitatively by comparing contoured maps of calibration target GW levels to the GW head observations. The error in the simulation heads were also quantified by determining the RMSE, MAE for the model residuals (target head – model head). During model evaluation steps, simulated heads are slightly greater than observed heads on average. However, the calibration for GW level falls within acceptance ranges, that is, RMSE is about 0.21m and less than 10 percent (average for 14 observation wells). The simulated steady state heads had a mean residual of 0.17m. The high value of Nash-Sutcliffe's coefficient of efficiency (0.92-0.94) between simulated and observed heads indicates that the calibrated model can be accepted as a good GW model of the study area (Table 4.2 and Fig. 4.4)
The purpose of sensitivity analysis is to observe the model response to the variation in GHB and hydraulic conductivity. Sensitivity of the model was evaluated by RMSE after multiplying each parameter a time by 0.4 to 1.6 of the initial value and model's run-file. The RMSE related to each run were plotted against the multiplying factor. As

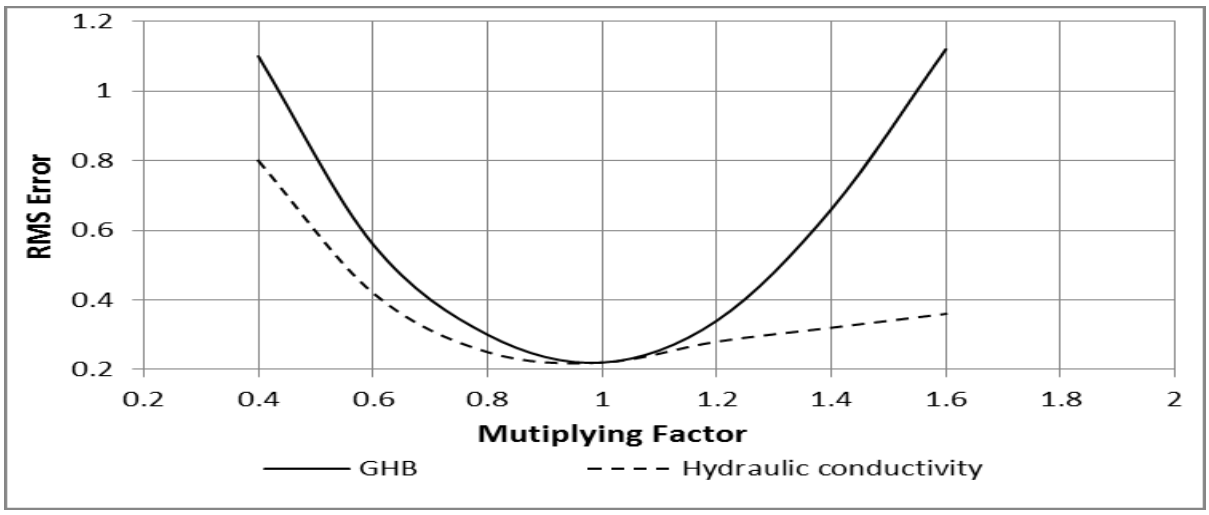

Fig. 4-5 Sensitivity analysis

the results, in case of the changes in factor of hydraulic conductivity, RMSE responses were less than the changes in factor applied to GHB cell values. The GHB was shown to be the higher sensitive parameter than hydraulic conductivity (Fig. 4.5).

4.5. Model simulation

4.5.1 Simulation of current pumping

GW pumping

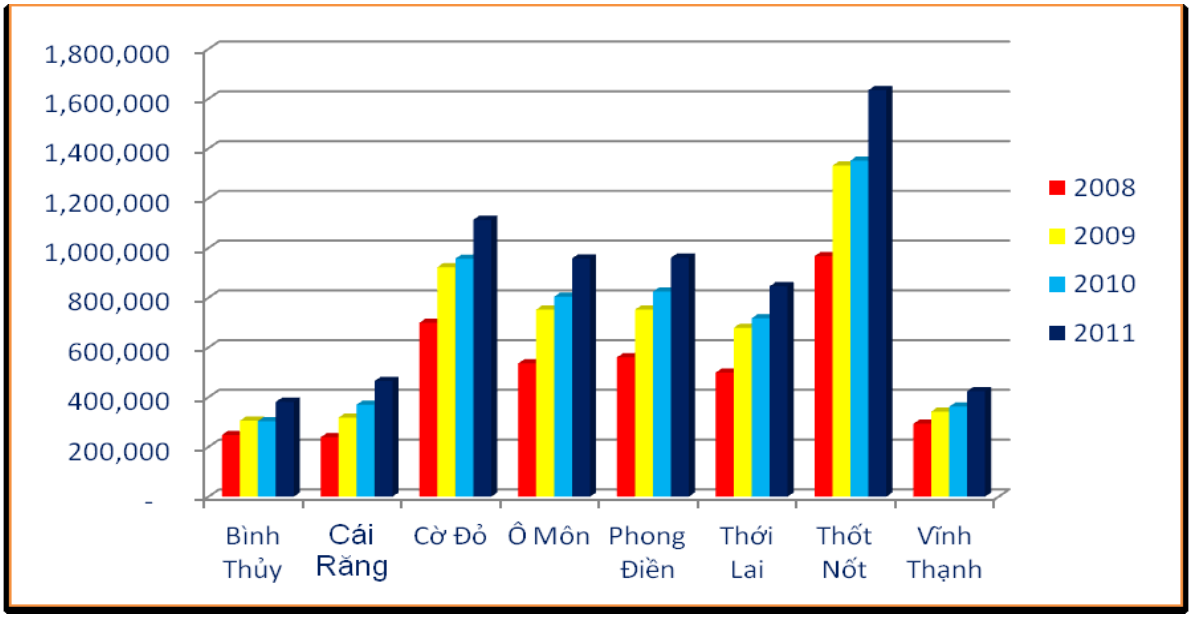

Fig. 4-6 GW demand for centralised domestic water supply (m^3/year)

The investigation on wells distribution was conducted in 2011 and it revealed that high capacity extraction wells are centralized domestic water supply stations and industrial supply stations, and the low capacity wells belong to households. The observed data in the past ten years indicated a significant trend of lowering of GW level, especially in Pleistocene aquifers (abstracted aquifer). According to result of hydrological profiles, Pleistocene aquifer is distributed at depth of 100m to 250m where pumping wells are located in. Centralized domestic water supply stations mainly are located at Binh Thuy, Cai Rang, Co Do, O Mon, Phong Dien, Thot Not, Thoi Lai and Vinh Thanh. Based on collected data from Center for Water Supply and Environmental Sanitation of Can Tho city (CWSES), the result of demand of GW was analyzed and synthesized. The chart in Fig. 4.6 shows GW exploitation for domestic

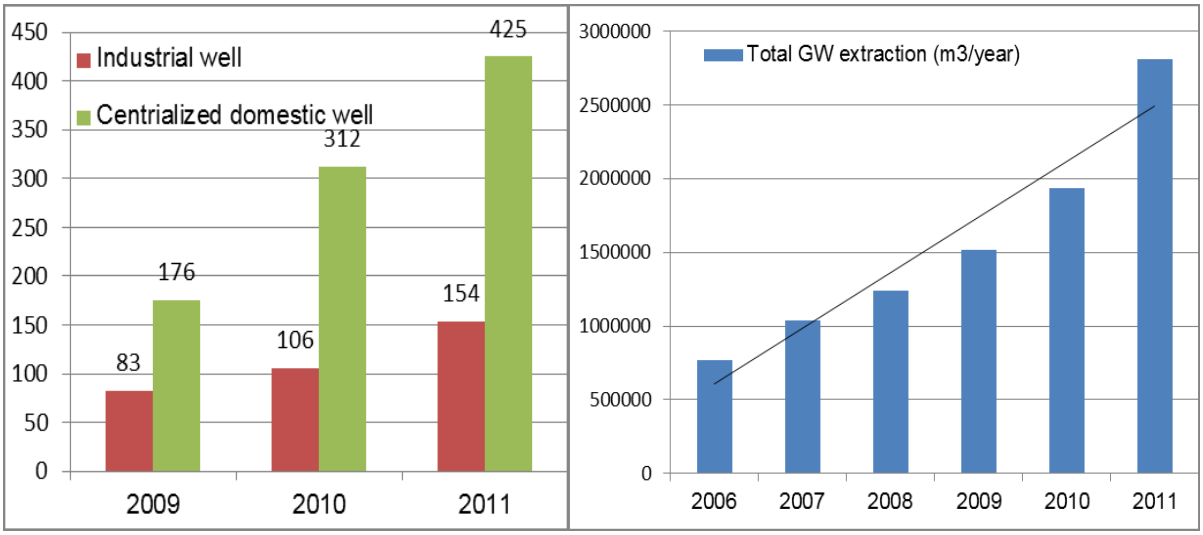

Fig. 4-7 GW demand for industry and abstraction well development

use has been increased year by year. It shows the highest GW demand in Thot Not district.

In recent years, industry has been promoted and expanded in CanTho city. There are three industrial zones in Can Tho: TraNoc 1, TraNoc 2 and ThotNot. TraNoc industrial zone has officially operated since 1990 and is fully covered by factories at the present. Water supply sources for industrial production are river and GW. However, in order to meet high quality requirement of production, most of factories use GW for production processes. Capacity of exploitation wells is very high; (50-100) m3/h; and trend of GW demand has increased year by year (Fig. 4.7).

The well package of model input is designed for outflow through pumping wells. Most of them are equipped with electric pumps and their coordination was examined by DWRPIS. Pumping parameters as depth, capacity and pumped schedule were provided by CWSES and IZA. In order to estimate the amount of pumping in reality, 30 typical wells were investigated and measured in 2011. Such data of each abstraction well as ID, coordination, depth and pumping capacity obtained by the above investigation was handled by the well package for model input. Each well was designated with its properties on cell basis in the model grid. All abstraction wells were assigned into model domain by programming (Fig. 4.8)

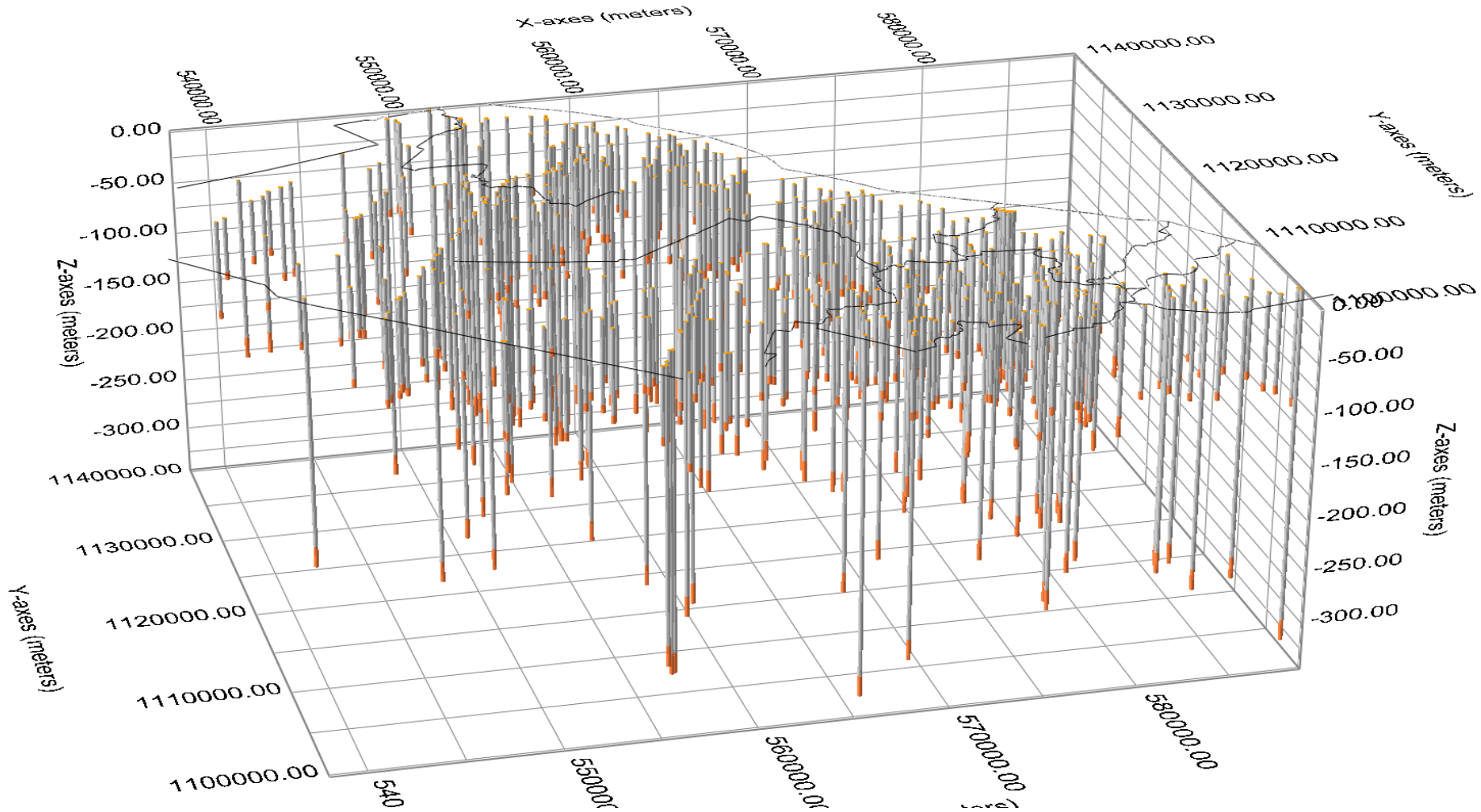

Fig. 4-8 Current distribution of pumping wells in Can Tho city

Simulation results

Fig.4.10 shows the simulation of the spatial distribution of the simulated heads (100m x 100m) at the abstracted aquifer (100m to 250m). The comparison between the simulated and observed heads is presented with GW drawdown areas of decline coincident with the wells serving in the 14 observation points (Fig. 4.9). The results show visualized movement of GW heads and aquifer responses under current pumping in the CanTho city. Generally, 1/2 area of the abstracted aquifer in the city is declined below – 5.0 meters (mSL) by the current pumping impact. If the growing pumping is maintained in the future, this area will be larger than current situation.

Land subsidence occurs when porous formations that once held water collapse, which results in the surface layer settling. This may occurs where the city was built on unconsolidated land such as Mekong Delta. The excessive GW pumping may cause significant increasing land subsidence rates in the city that exceed the rate of sea level rise (Fujihara et al., 2015). Based on simulation results, two zones of GW drawdown are developed in a part of: ThotNot, BinhThuy, NinhKieu and PhongDien (Fig 4.1 & Fig 4.10) by GW pumping. These zones may know as vulnerable zones to land

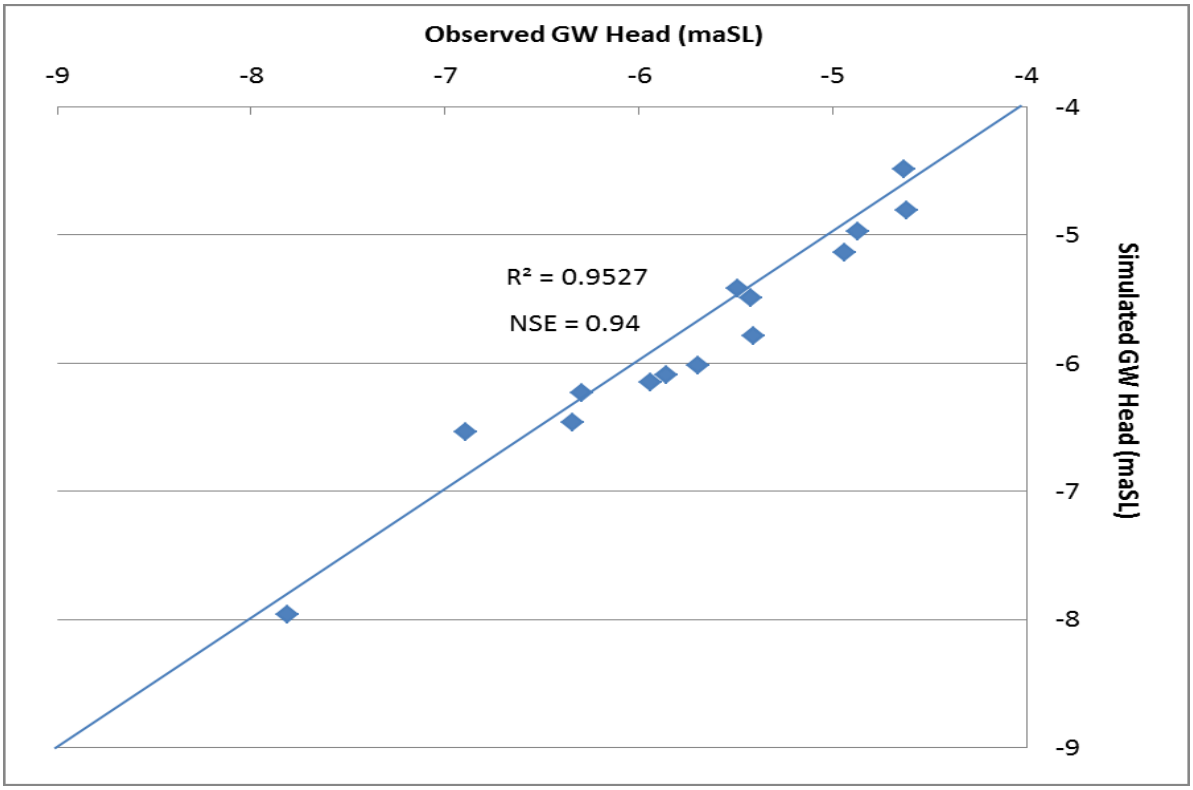

Fig. 4-9 Comparison of simulated vs. observed GW drawdown by current pumping

subsidence. The land subsidence rates also highly relevant to GW drawdown rates and it is one of factor that contributes to water level rise and flood magnitude, resulting in inundations that have been severe in the city, especially in Tra Noc industrial zone (BinhThuy) and the urban zone (NinhKieu). Fig 4.10 shows the extended trend of the area of GW drawdown for these zones may occur in South and West side of the city.

4.5.2 Predicted effects of increased pumping

Because assessment tools as a decision support system are still limited, there are some constraints for local government to project GW resources planning. Therefore, GW management frameworks are carried out just on experience basis (IUCN 2011). However, to meet the increased water demand in the future, CWSES projected that the distribution net of GW supply station will be extended which means the amount of pumping will increase.

Based on the current trend of GW use provided by CWSES, this simulation projected that the increasing pumping by approximately 100 percent in 2035. Moreover, because the city government recommends limitation of GW use for industry water supply in the future, projected increasing of GW demand for industry will be 50 percent in 2035.

Therefore, to understand how this increased pumping may affect GW flow, we assumed that this increased demand will be supplied by existing wells (Fig. 4.8), and simulated the increased water demand by increasing concurrently the pumping rate for all centralized domestic water supply station by 100 percent and industrial supply by 50 percent. Because it is certain that new wells will be installed to meet the increased demand, and because the locations of these new wells cannot be predicted, the results are highly speculative. The simulation of spatial GW heads under current pumping (Fig. 4.10) will be assigned to initial conditions for the predicted effects of increased pumping. GHB conditions for the city boundary were not changed for this simulation.

The effects of increased pumping make additional areas of GW decline in the city, resulting in 2/3 area with GW level of -5.0 meters (mSL) is predicted by future pumping (Fig. 4.11). Comparison of predicted water levels during increased pumping to current pumping results indicates that the average head decline in the city aquifer

will be approximately 2.0 meters (Fig. 4.10 & Fig. 4.11). The maximum head decline which occurs at ThotNot is around 4 meters to 5 meters and PhongDien is around 3 meters to 4 meters (Fig. 4.12). Effects of increased pumping in the CanTho city aquifers indicate maximum additional drawdown to be in the range of a few meters.

To figure out the reason of the strong GW drawdown and highest decline occurs in ThotNot anh PhongDien, the 3D-simulation of zone A and zone B (Fig. 4.11) were conducted under current and increased pumping. The visualized simulation of 3D in Fig. 4.13 points out the cones of depression has been developed by impact of densest abstracted wells in these zones. There are the correlation between drawdown magnitude and pumping wells distribution. The results imply that wells distribution has been planned inappropriately which means that distance of pumping wells is quite close. Therefore, the cones of depression are overlapped and it makes highest decline of GW and changing of the direction GW flow into South-West side of the city (Fig. 4.13). The interference will reduce the water available to each well and well interference can be a problem when many wells are competing for the water of the same aquifer, particularly at the same depth.

The new wells will likely to be installed by water utilities at additional locations. Therefore, their locations should be planned. In order to evaluate how reasonable distances of these wells are, the model can be used for illustrative and discussion purposes to reach wells planning purposes.

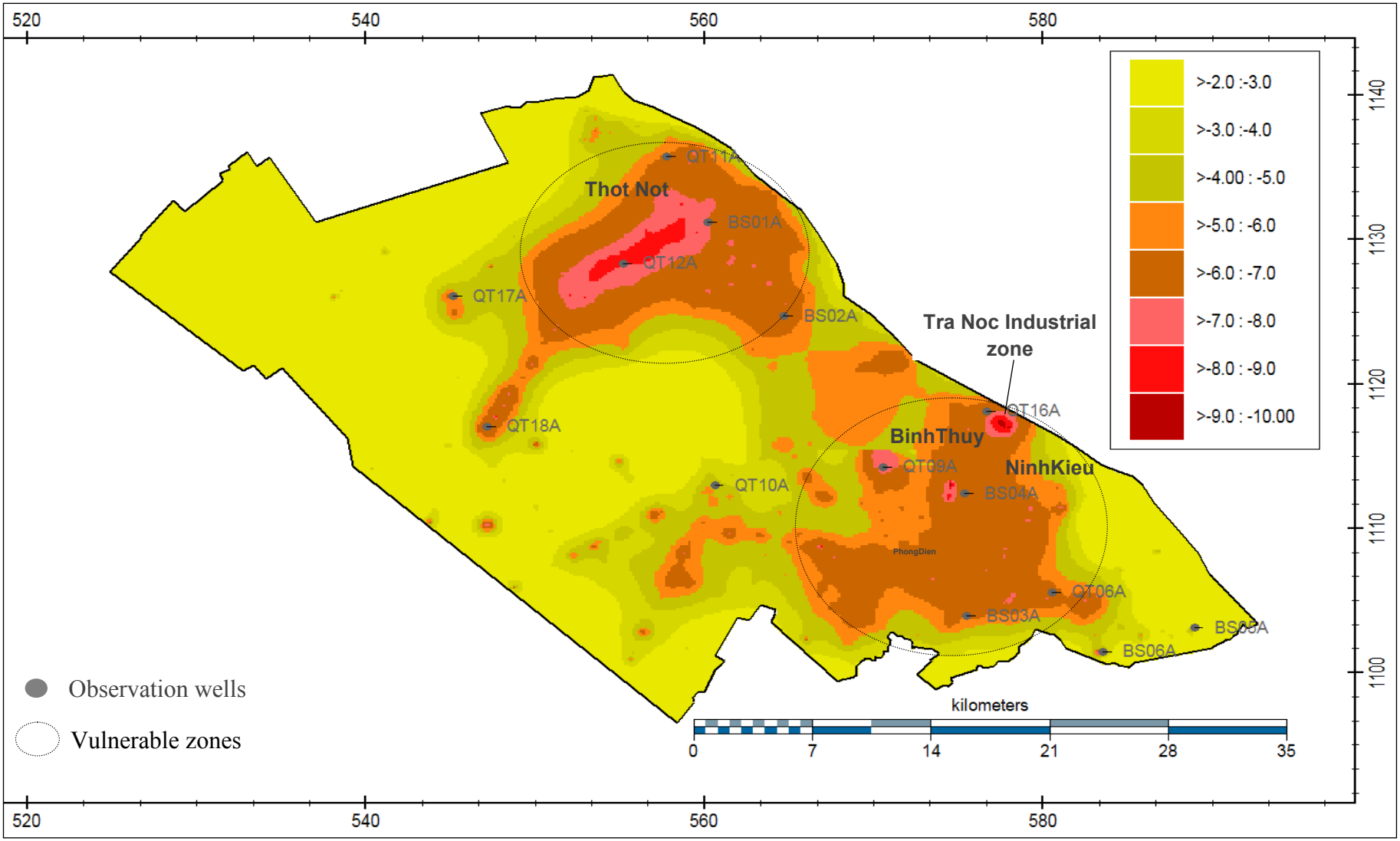

Fig. 4-10 Simulated map of spatial GW heads (maSL) at 100mx100m.

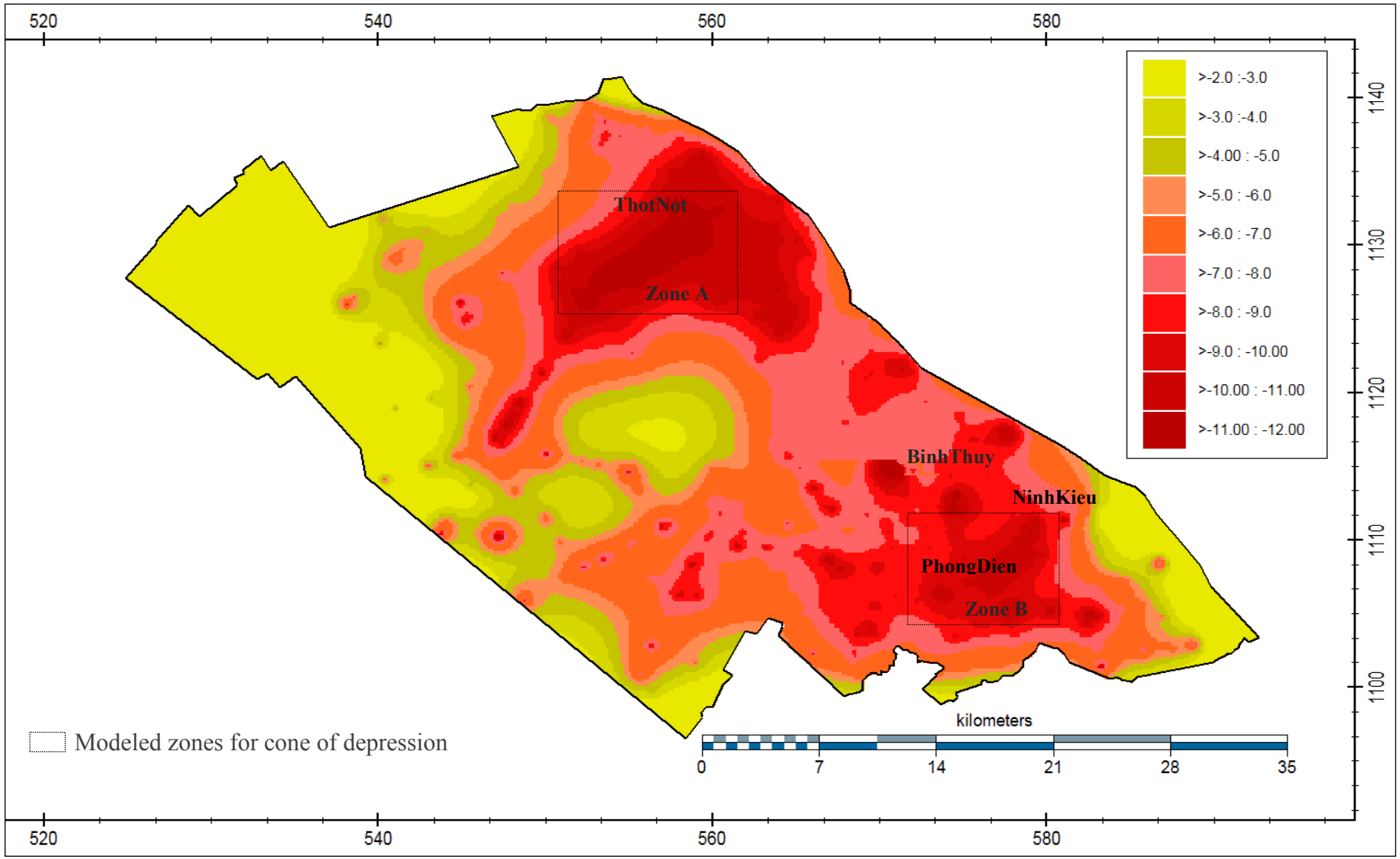

Fig. 4-11 Model computed heads for the aquifer under increased pumping in 2035

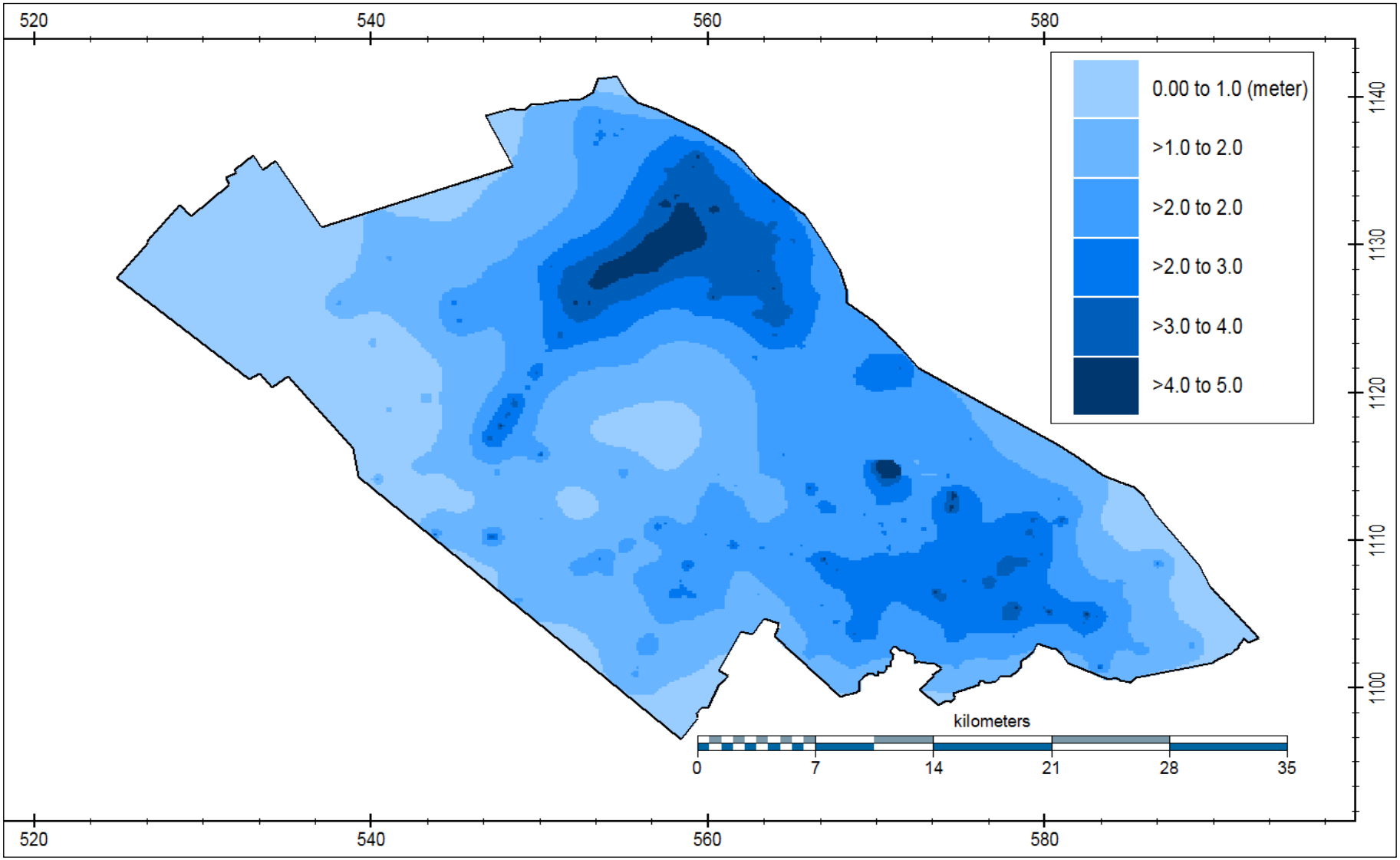

Fig. 4-12 Predicted differences in GW heads between current and increased pumping

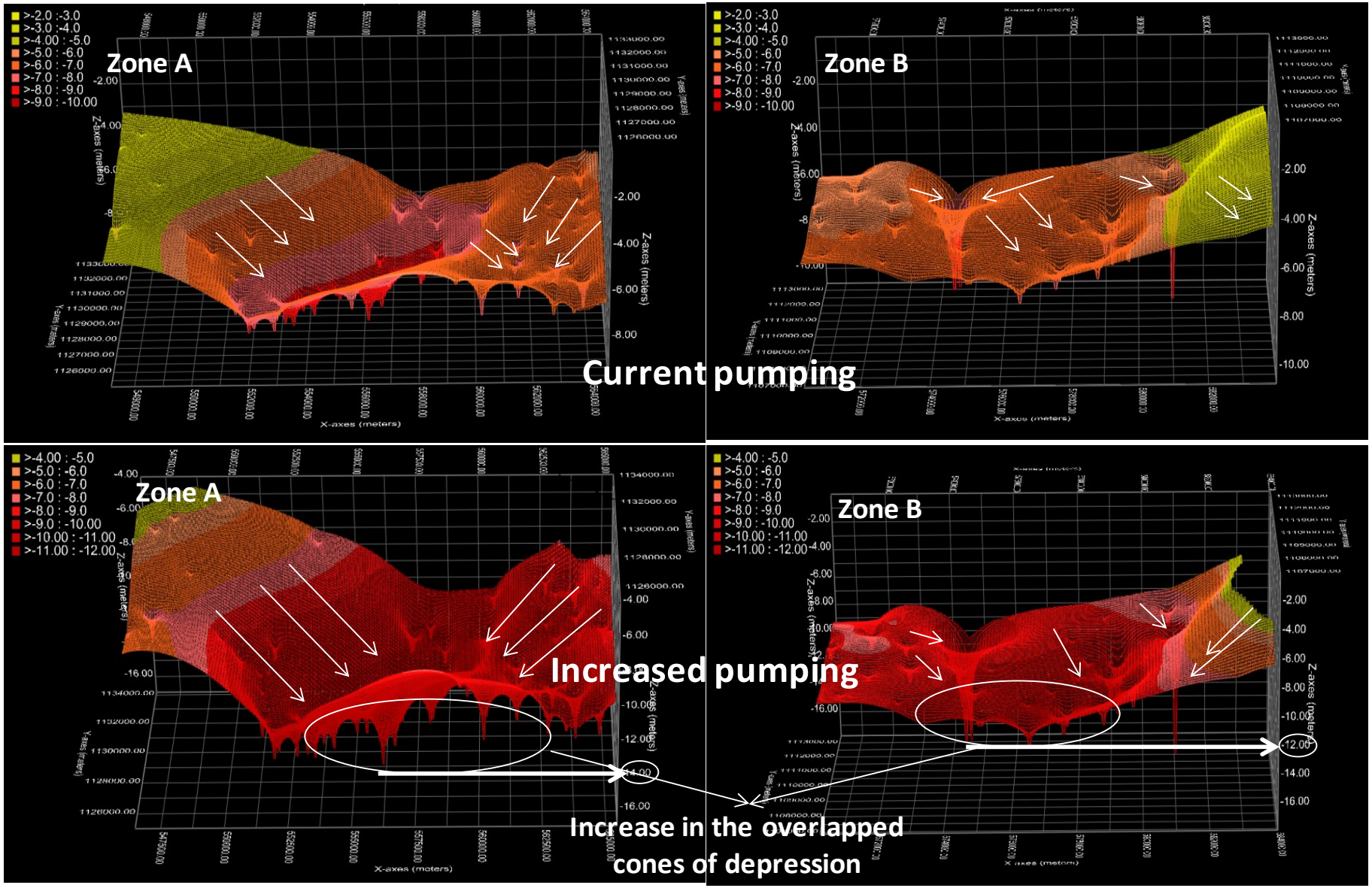

Fig. 4-13 Formed cones of depression 3D-simulation between current and increased pumping

4.6. Conclusions

GW is a critical source of water in CanTho City, the capital of Mekong Delta. It is supporting human economic activities such as domestic and industrial water supplies as well as sustaining aquatic ecological systems. GW simulations using numerical models are now the state of the practice for professional and research assessments of GW availability and sustainable water use for the city. For such practical usage, a GW model for CanTho City was built up using iMOD.

To construct the numerical model, the hydrological profiles data, digital elevation map and the results of the entire Delta model were compiled and analyzed for setting up the model concept and boundaries. The necessary data for the model input such as aquifer properties, hydraulic parameters, locations and amounts of pumping wells, and meteorological data were compiled and initially assigned to the grid scheme of the model. The calibrated model could show good agreement between calculated groundwater heads and the observed ones at 14 monitoring wells. It was confirmed that the established model can work properly to evaluate the human or natural impacts. From the calculated spatial distribution of groundwater heads, the zones of serious groundwater drawdown were identified as depression cones, and it was clarified that those zones are deeply affected by dense distribution of groundwater pumping stations for domestic and industry.

As more increased demand on groundwater for water supply is expected in the city, the model was also used to predict the future groundwater decline based on the trend of increase in pumping until 2035. As the result, the areas of GW decline are expected to be significantly increased by the projected pumping. These areas are also addressed and known as vulnerable zones to land subsidence. The formation process of depression cones with the increase in pumping was also depicted in 3D graphics. From these results, the serious impacts of increase in pumping were clearly shown.

Generally, the model was established as the first assessment tool for GW resources in CanTho City. Its results allow the stakeholders to evaluate how well their interests would fare in terms of the available GW resources. People are able to see which areas

may be more vulnerable to GW exhaustion and its process under pumping impact. The Water Authority and the conservation groups are more interested in how modeling outputs represent a potential aquifer recovery.

However, model predictions are only as good as the information used to construct and calibrate models. In this regard, there are several improvements to numerical models that could make results more useful for water management. There are very few pumping test and borehole structure data have been made. The analyses on these data indicate that the up-middle aquifer may not be a fully confined system and there may be some connectivity between the upper and lower aquifers. To clarify the details of the geo-structures to know the connectivity, detailed reliable drilling records and pumping test data should be required to enhance the information of the aquifer system including the connectivity and its behavior. Another possible source of inaccuracies is related to such input data as estimates of pumping. GW pumping rates used in this model are averages computed from incomplete water-use records. These data are inadequate for future work that simulates transient responses of aquifers to seasonal and annual changes in climate and pumping. Accurate and complete water pumping records for large capacity water wells are needed to allow any model to simulate field conditions of head and flow.

CHAPTER 5. IMOD MODELING FOR GROUNDWATER MANAGEMENT IN THE COASTAL AREA OF MEKONG DELTA

5.1 The study area

Soc Trang is one of coastal provinces of the Ca Mau peninsula in Mekong Delta, Vietnam and locates at the Bassac River mouth area. Its East side borders Bassac River and the South side borders East Sea with around 72 km of coastal line. Total of area is 3.331,76 km2 includes the Soc Trang city and ten districts (Cu Lao Dung, Ke Sach, Long Phu, My Tu, My Xuyen, Nga Nam, Thanh Tri, Chau Thanh, Vinh Chau and Tran De), (see Fig. 5.1)

Surface water resources is distributed by canal network of about 2,5 to 3,0 km/km2

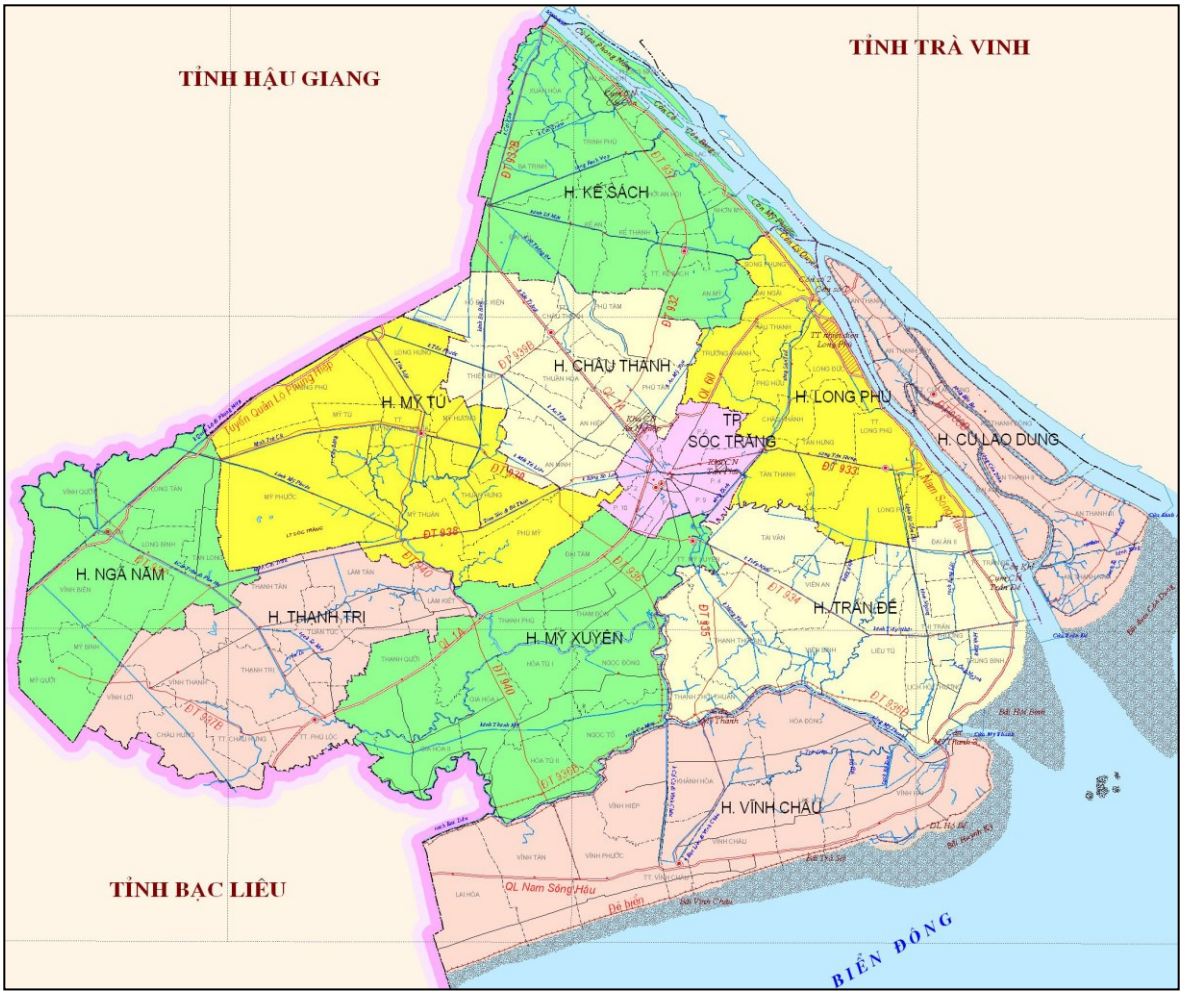

Fig. 5-1 Administrative map of Soc Trang (DONRE, 2012)

evenly in Soc Trang. Although there are many canals that connect to rivers, but canal water is low quality due to impacts of untreated waste water from human activities, salinity and acid sulphate (DONRE, 2012). In addition, Soc Trang locates in downstream part of the Bassac River and its surface water resources have been influenced by the Bassac River (Fig. 5.2). The sediment contamination and pollution in the river reach are of higher levels compared to river reaches of middle stream and upstream. Besides that, population growth of urban zones and rapid development of industrial and agricultural production cause high water supply demand. Moreover, complex changes of rivers pollution and the Bassac river discharge by impacts of upstream activities are obstacles to effective water supply for local people.

Fig. 5-2 The study area in Mekong Delta (modified from Google Earth image, accessed on Dec. 2015)

5.2. Backgrounds

Since a part of GW there is brackish and saline, GW is not always so suitable for drinking water and irrigation unfortunately (Nam et al., 2013), but a big amount of GW has been drawn for various purposes in the study area. From monitoring of GW levels for the past several years in the study area, a phenomenon of GW drawdown caused by excessive GW use has been observed clearly, especially in the aquifers where GW has been abstracted (DONREs, 2012). In addition, our previous study in 2013 showed saltwater intrusion into aquifers resulting in significant deterioration of the GW quality in the study area (Nam et al., 2013), and it was considered to be caused by the GW table drawdown. The study area is now facing a number of critical GW management problems with respect to meeting water needs, avoiding water right disputes and environmental deterioration (DONREs, 2012). Although legal documents regarding GW management have been issued, there are some constraints for the effectiveness of GW management planning, because the GW potential of the aquifer underlying MD is still greatly unknown due to lack of GW technical assessment (Boehmer, 2000; Phuc, 2008). Therefore, GW management frameworks are carried out just on experience basis (IUCN, 2011). A development or application GW model is considered very essential in scientific approaches for GW management in the future.

5.3 Objectives

This study aims at establishing a GW model for the 100-meter aquifer of a coastal area of the Mekong Delta, and applying it to simulation of the GW heads under possible changes in rainfall and GW management in the future. The model, iMOD, was calibrated using historical data of GW level and model input requirements. It was confirmed that the calibrated model could work properly to reproduce the distribution of the GW table and its response. For scenario setting, several cases of future rainfall conditions for the period from 2015 to 2035 were set up based on the downscaled output from the global climate model with bias correction. For each of the combinations of climatic conditions and pumpage, model simulation was carried out to estimate GW tables

5.4. Model building

5.4.1 Theoretical background

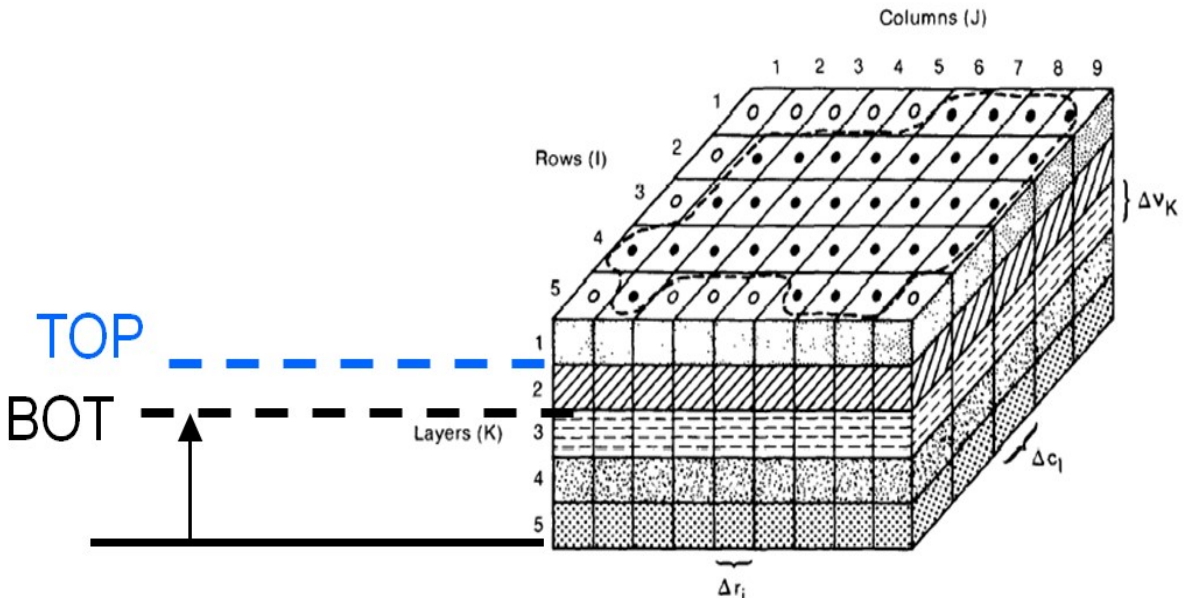

Fig. 5-3 Three-dimensional grid (McDonald, 1988)

Numerical models provide the most general tools for quantitative analysis of GW applications (Charies 1980). To develop a numerical model of an aquifer, the concepts and laws that control the physical processes of the system should be translated into mathematical equations with partial differential equations. This model is designed in the same way as other numerical models of GW to simulate aquifer systems in which: (i) saturated flow conditions exist, (ii) Darcy's Law applies, (iii) the density of ground water is constant (USGS, 1997). The GW flow equation is derived by mathematically combining the water balance equation with Darcy's Law in three dimensions as follows:

$$\frac{\partial}{\partial x}(K_x\frac{\partial h}{\partial x})+\frac{\partial}{\partial y}(K_y\frac{\partial h}{\partial y})+\frac{\partial}{\partial z}(K_z\frac{\partial h}{\partial z})=S_s\frac{\partial h}{\partial t}-W$$

Where, x is the Cartesian spatial coordinate x, y, z; h = h(x,t) is hydraulic conductivity as a function of x, y, z; S_s is Specific storage; W is source (positive) or sink (negative)

The iMOD requires the value of horizontal grid spacing to be determined, whereas vertical grid spacing is estimated from supplied values of the bottom by hydrological structure of each layer (Fig. 5.3).

5.4.2 Model concept and building

Fig. 5.4 presents a schematic view and steps of complementary building of the model.

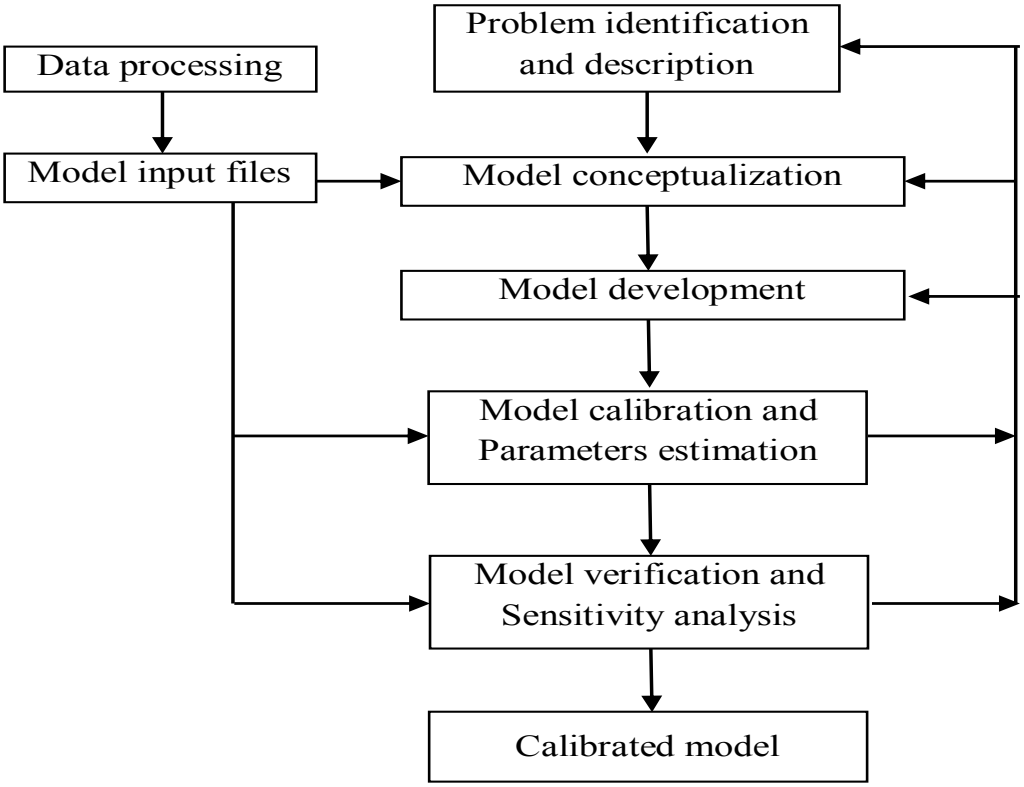

Fig. 5-4 Modelling steps (modified from McKinney et al. (1994))

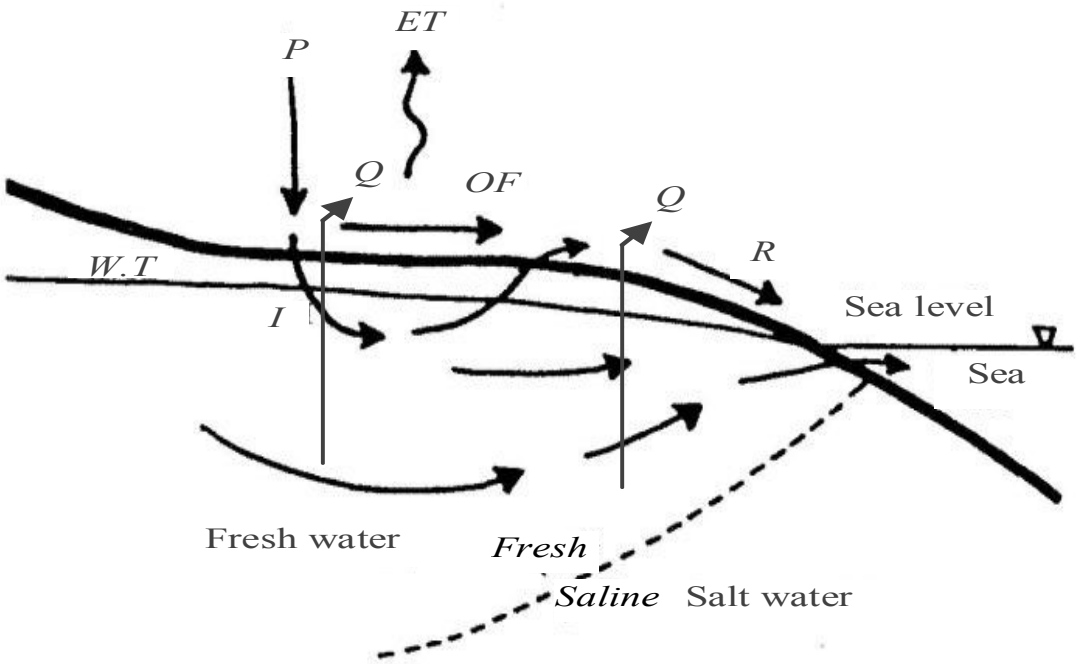

Fig. 5-5 Simplified conceptual model of hydrogeologic system of the study area

Conceptual model

The first step for the model building is to define the conceptual model for the coastal area in this study, that is, how the hydrological system works actually (Fig. 5.5). The conceptual model approach in this study involves the use of GIS tool in the map module. The location of sources/sinks, layer parameters such as hydraulic conductivity, model boundaries, and all other data necessary for the simulation have been defined at the conceptual model level in map form.

To complete the conceptual model, borehole data were used to create 3D hydro-geological profiles between represented boreholes (Fig 5.7). The cross section in Fig 5.6 shows the soil stratigraphy data from available drilling boreholes. These cross

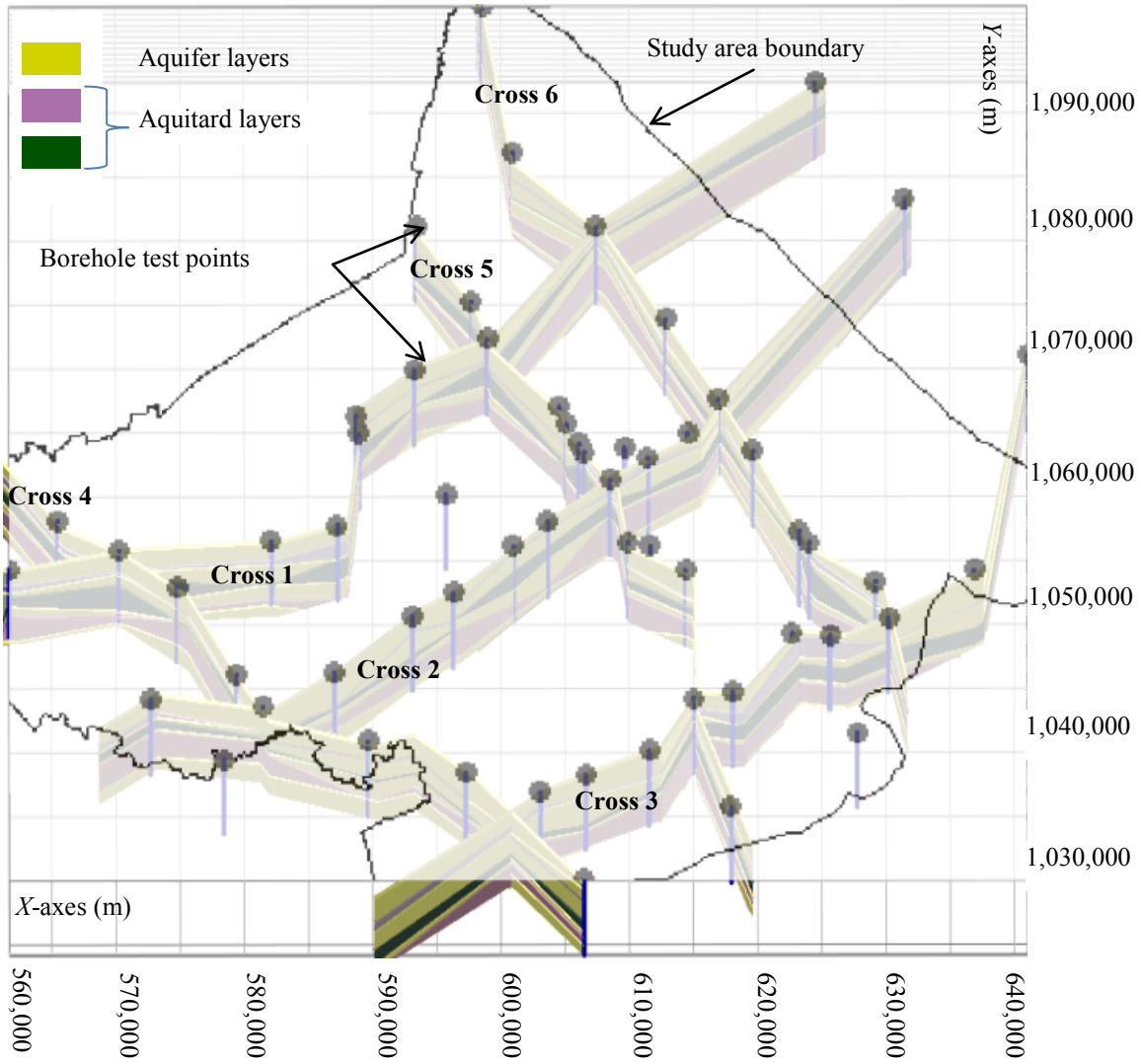

Fig. 5-6 Constructed hydro-geological profiles for the model input

sections were converted to solids which were used to interpolate the elevation data (bottom/top) of each layer for this numerical model.

Because most of the drilling boreholes do not reach the bedrock, mapping the entire depth of the aquifer system is difficult. However, 100-meter aquifer is known as the most productive GW reservoir in MD (Eugene, 1971) and most of the abstraction depths of the wells are from 80 m to 120 m (DONREs, 2012). Therefore, the 100-meter aquifer was constructed in the model structure (Fig. 5.6).

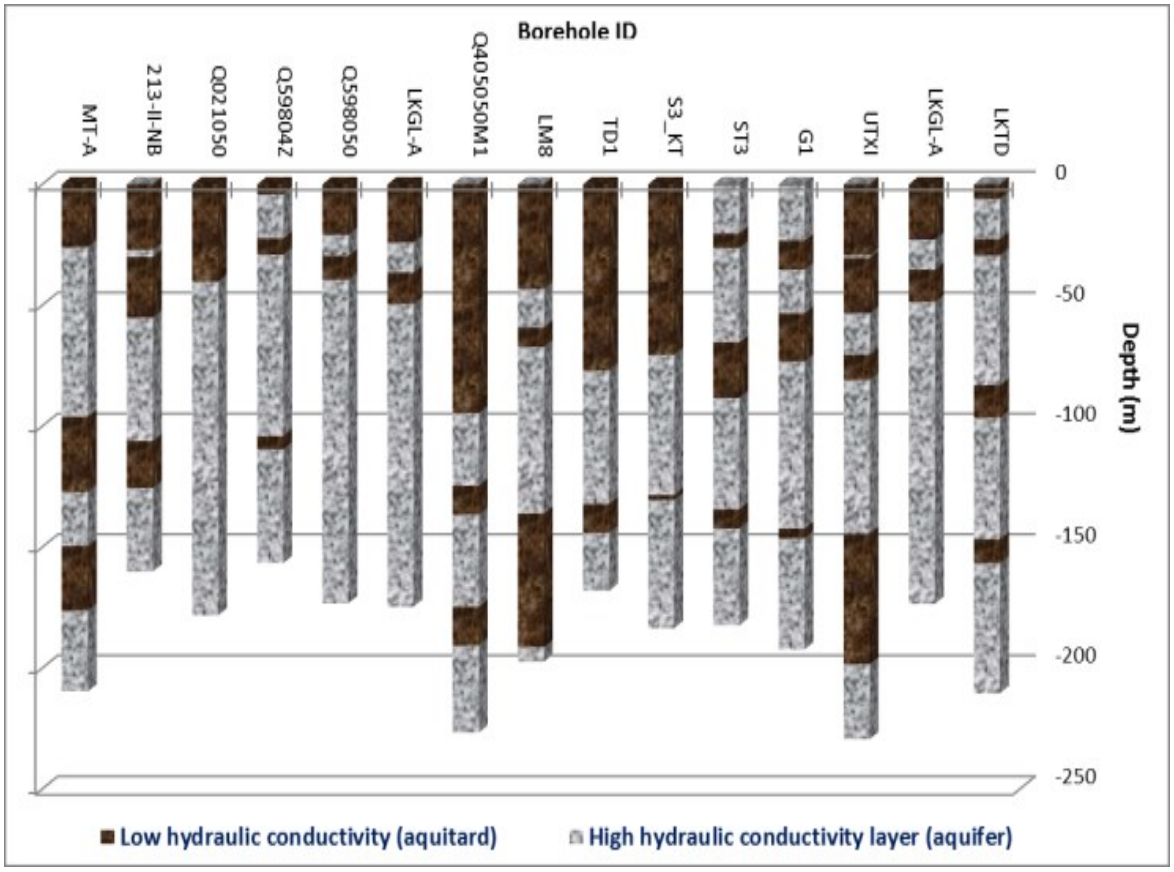

Fig. 5-7 Geological formation from typical borehole wells

Model Domain and Discretization

Based on data availability and hydro-geological conditions in the study area, the model employed a grid size of 100 × 100 m, totaling 5,295,683 cells. As the collected ArcGIS maps were in different grid sizes and different coordinate systems, pre-processing was performed using ArcGIS, MapInfo. Then, the iMOD tools were applied to create input files. Based on data availability and considering the dynamic

behavior of GW level, a month was chosen as the time step within which sea level is assumed constant.

Initial Conditions

For running the GW model in dynamic mode for long term simulation over 21-years (1994-2014), the initial conditions of the GW system were crucial. The historical data showed that compilation of comprehensive GW head data in the study area was begun in January 1994. As the pumpage of GW was not yet so big before that, the measured GW levels in January 1994 was considered relatively steady as the long-term average reflecting the pre-development stage. Therefore, all subsequent simulations were started from the January 1994 heads as the initial condition.

Boundary Conditions

For calculating GW flow in the aquifers of a region, conditions at the region's boundaries must be given. In this numerical model, boundary conditions are defined as specified heads and head dependent flux for the model domain, while the sea area is defined as constant head equal to the average sea level of 0.0 m (Fig. 5.8).

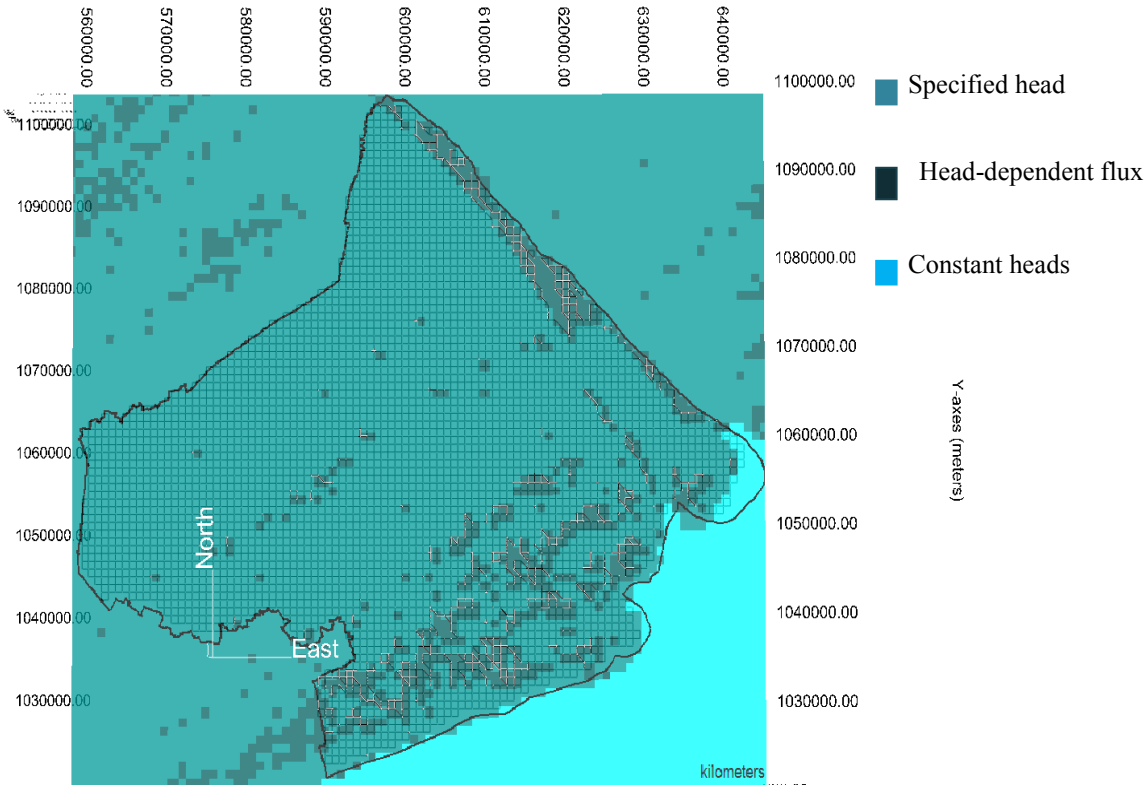

Fig. 5-8 Defined boundary condition in model domain

The river reach of the Bassac River within the model area is a major surface water area. The river water levels are relevant to the GW table of the shallow (or unconfined) aquifer (Anderson and Woessner, 1992). Hence, the river/canal surface areas were defined as head dependent flux. Cross sections of the rivers/channels and water levels were provided by College of the Environment and Natural Resources (CENRes), CanTho University. Flux into the aquifer was estimated by iMOD functions based on Cauchy's equation.

The aquifer system was built by boreholes test data provided by Division for Water Resources Planning and Investigation for the South of Vietnam (DWRPIS). Since alluvial basin aquifers in the coastal area of MD range from unconfined to confined (Boehmer, 2000), the aquifer layers were set by connecting corresponding interfaces in between the boreholes. A total of 6 hydrogeological profiles were built in the model domain by combining interpolation and provided geological sections from DWRPIS (Fig….). Incorporating more detail was also taken into account: such as out wigging of aquitards as well as a local modification of interfaces in between boreholes.For determining drainage of the model domain, the digital elevation map (DEM) of the model area with a resolution of 100 × 100 m was constructed by interpolation with Kriging method from investigation data provided by DWRPIS. It was converted into an ASCII file for iMOD input and used to define the top of the hydrological system, as well as the drainage levels throughout the model area.

Hydrological System

Hydraulic properties of each cell were initially assigned by interpolation of aquifer properties estimated using available field data (at nine points) from several investigation campaigns performed by DWRPIS and Haskoning B.V. Consulting Engineers and Architects, which involved borehole tests, pumping tests, lithological logs and geophysical methods. According to the field test results, there are two high conductivity layers from surface to 120 m depth. The hydraulic conductivity values of the upper layer (unconfined aquifer) ranged from 10 m/d to 90 m/d and for the lower layer (100-meter aquifer) from 23 m/d to 70 m/d, while its values of storage coefficient were from 0.4 × 10-3 to 0.2 × 10 -2.

GW Abstraction

The well package of iMOD is designed for outflow through pumping wells. Intensive pumping has significantly altered the GW system over the past two decades, practically becoming the sole aquifer output under current conditions. More than 8.5 thousand private abstraction wells and hundreds of pumping stations are situated in the study area (Fig. 5.9). Most of them are equipped with electric pumps and their coordination was examined by DWRPIS. In order to estimate the amount of pumping, such pumping parameters as depth, capacity and pumped schedule were investigated and measured in 2014. Such data of each abstraction well as ID, coordination, depth and pumping capacity obtained by the above investigation were handled by the well package for model input. Each well was designated with its properties on cell basis in the model grid. Under the present condition, pumping of GW for domestic and agricultural use is the main discharge of the GW system with an amount of 348,226 m3/d (DONREs, 2012).

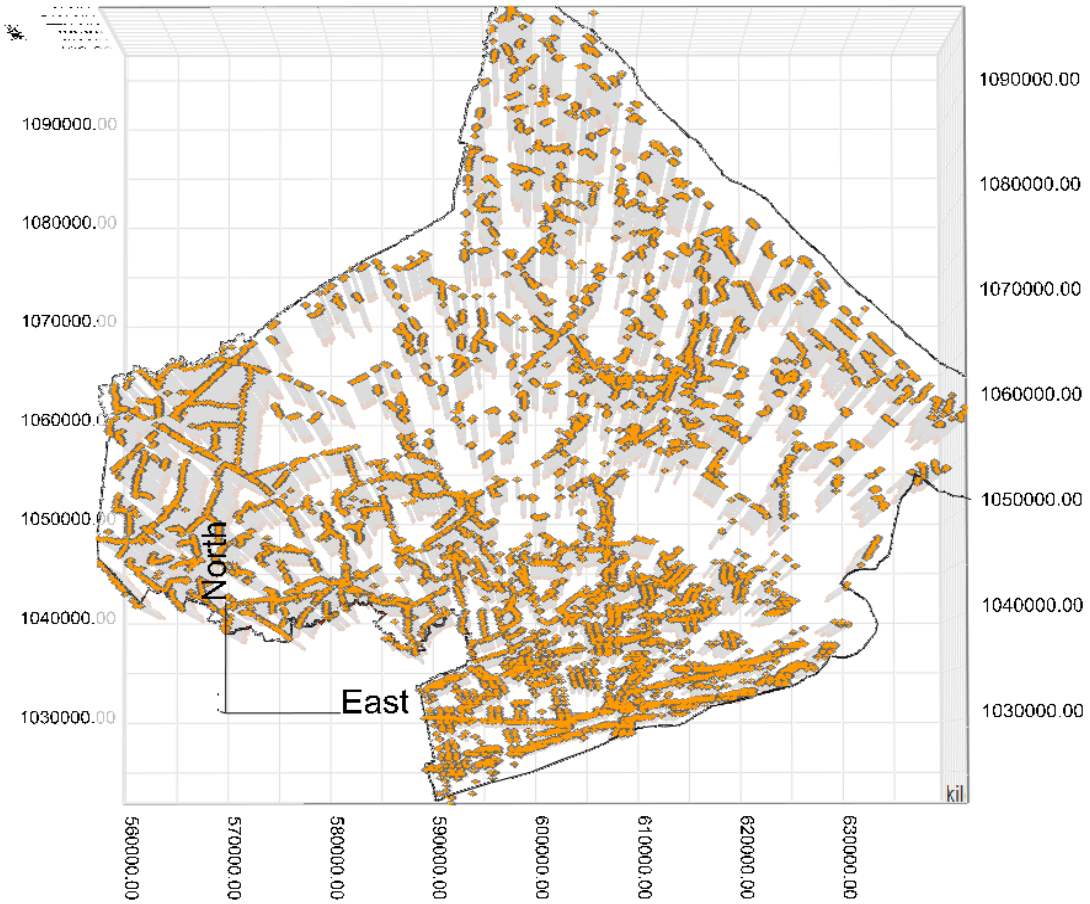

Fig. 5-9 Pumping wells distribution developed by programing in the study area

Recharge

According to the calibrated GW model for the entire MD region (Boehmer, 2000), the actual recharge of GW by rainfall and streams proved to be much lower than the potential recharge of MD. The recharge in most of the delta ranges from 0.01 mm/d to 1 mm/d, or 1 to 20% of rainfall, whereas it ranges from 0.2 mm/d to 0.8 mm/d in the study area. Measurements of GW level fluctuation along with precipitation events can be a practical method of estimating temporally and spatially variable GW recharge rate (Korkmaz, 1988). In the study area, most of rainfall occurs during the rainy season from May to November, and monthly precipitation has a bimodal distribution. Generally the study area receives from 1,600 mm to 2,230 mm of annual rainfall (DONREs, 2012). Because the conceptual model was developed to mainly focus on 100-meter aquifer (abstracted aquifer), the main source of water entering the model domain is from the top surface boundary condition, namely recharge from precipitation through infiltration into the sub-soil. The rainfall and GW levels were monitored periodically once a month from 1994 (unaffected duration by pumping) by Department of Natural Resources and Environment of SocTrang (DONREs). The linear regression model for the relationship between recovery of the GW level (ΔH) and total precipitation (Rt) during wet periods (Korkmaz, 1988) was employed to estimate the recharge rate. The average recharge in the study area was found as 0.62 mm/d, or 12.4 % of rainfall.

Evaporation

The evaporation in the model is corresponding to water loss of the shallow GW that should occur under a given climatic condition. It is calculated by input data of the evaporation coverage and the depth to the GW level estimated by iMOD during the period of running the model. The input data include: (i) the average open pan evaporation (ETO) whose values have been collected and calculated from meteorological station in the study area (DONREs, 2012); (ii) the extinction depth of evaporation of GW, which was assumed at 3-meter depth below the surface; and (iii) the surface elevation, which is the same as top elevation of the first layer in the GW model and is therefore imported in the evaporation package of the iMOD module per grid cell.

5.4.3 Model Calibration Process

For model calibration, the model parameters were adjusted so that calculated GW heads would get good agreement with a set of historical data (Lutz, 2007) and consistency with the common understanding of the GW system. Since GW head data were available at two long-term observation wells (1994-2013 and 2000-2013) managed in the nation level and twelve short-term observation wells (2010-2013) managed in the local level in the study area (the location of these wells are shown in Fig. 5.13), these data were utilized for model calibration. Analysis of the difference between measured and computed heads give an indication as to which parameter must be adjusted in order to minimize this difference. In this study, calibration for steady-transient state condition was conducted through a trial and error process, in which the initial estimates hydraulic conductivities and storage coefficients of the aquifer system were iteratively adjusted over reasonable ranges to improve the match between simulated and observed GW levels (Fig. 5.10). Calibration was carried out for the long-term observation wells for the period from 1994 to 2014. The model was calibrated by adjusting pumping rates of abstraction wells and recharge rates in wet and dry periods.

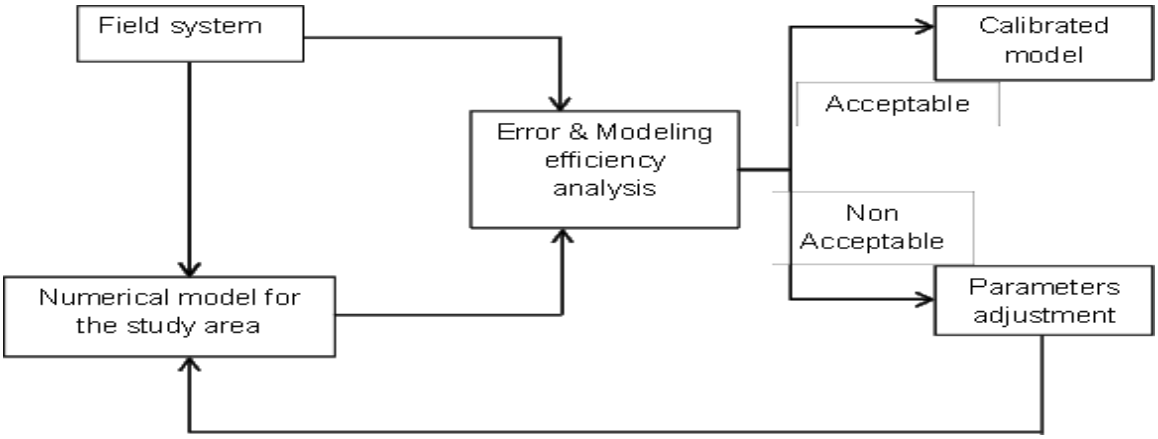

Fig. 5-10 Trial and error calibration procedure (Anderson 1992)

5.5. Scenario setting for model application

According to the hydrogeological property of the 100-meter aquifer in the study area, the two main factors affecting the GW balance are recharge from precipitation as source and pumpage as sink. In the period 1970-2007, rainfall tended to increase in

the whole MD by an average increase of 95 mm per year (MONRE, 2010), along with the lengthening of rainy season. With average annual rainfall of approximately 1,700 mm, the rate of rainfall increases over the 38 years period (1970-2007) was 5.5 %. The outcome of the future rainfall simulation for MD also shows rainfall increase in rainy season (June to November) and rainfall decrease in dry season (December to May) (MONRE, 2010). Regarding pumpage, during the last two decades, a large number of GW abstraction wells have been installed in the aquifer (DONREs, 2012). For GW management planning, the future scenarios to be examined need to consider the two factors (Fig. 5.11).

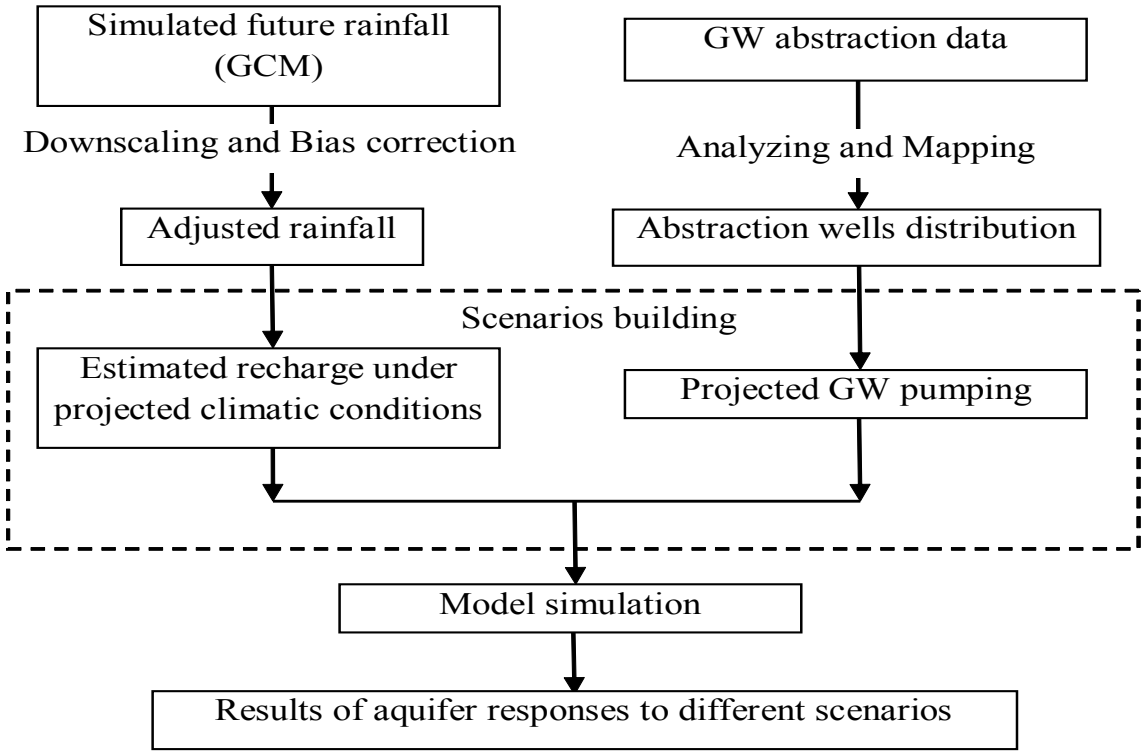

Fig. 5-11 Schematic chart of model application

5.5.1 Rainfall Series Generation

The rainfall time series observed at the meteorological station close to the long-term GW monitoring station of Q598030 located in the middle of the study area was selected as the representative of the whole study area to be used for simulating the GW levels from the past to the present. Meanwhile, the precipitation forecast for the

future was estimated by the downscaled GCM model for the whole Mekong basin with a resolution of 20 km × 20 km up to 2035, which was downscaled using Met Office's PRECIS regional climate model (Providing Regional Climates for Impacts Studies) from the GCM by the Southeast Asia START Regional Center. However, there were significant differences between the observed rainfall and the model estimates for the present condition. Therefore, based on the bias correction method (Piani et al., 2010), the daily rainfall series for the future 21-year period (2015-2035) was adjusted by considering the difference in the present 20-year period (1980-1999) rainfall series (Fig. 5.12). The estimated monthly rainfall series from the daily adjustment were used for the model.

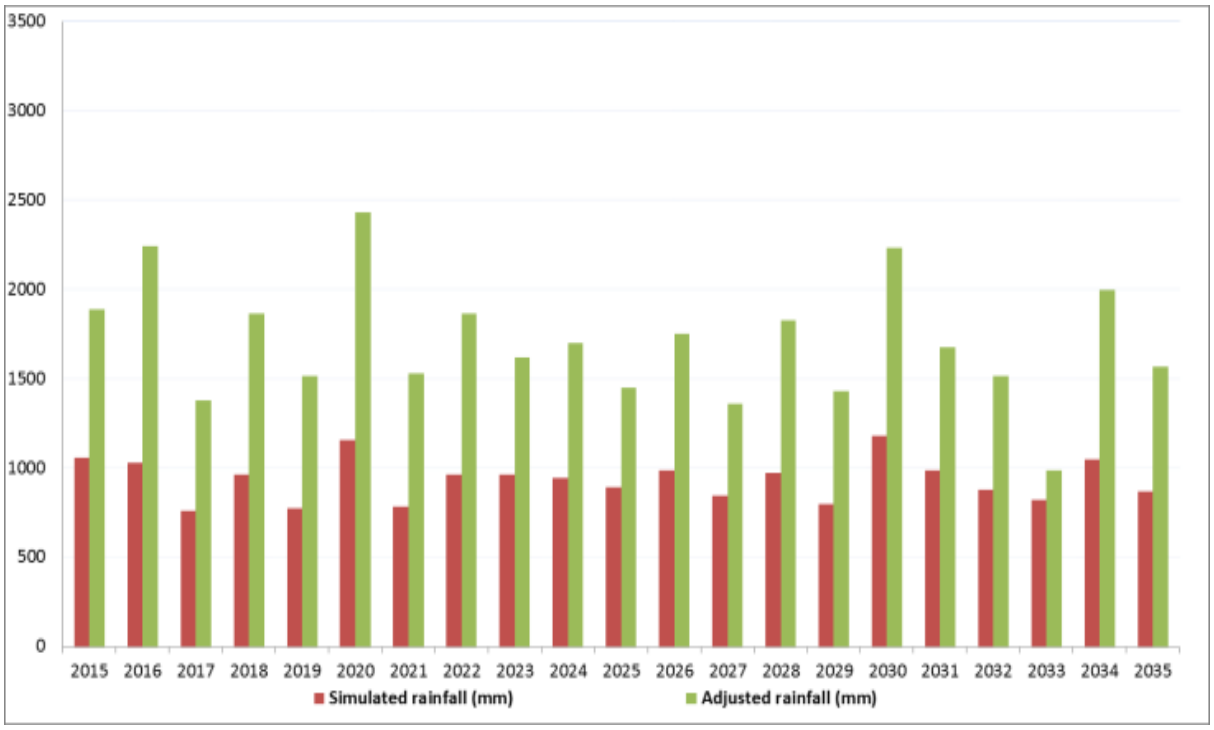

Fig. 5-12 Simulated & Adjusted future rainfall trend

5.5.2. GW Management (Driver 1-3)

Three cases, Driver 1 to 3, are taken as the future levels of GW abstraction (Table 5.1). First, Driver 1 is the case where the current GW abstraction level should be maintained. Meanwhile, the increasing population and industrial production will increase water demand and consumption. According to the projections on future trends of water demand and consumption made by experts and stakeholders, for the

Table 5-1 Driver and scenario assumptions

	Management options	***GW abstraction***
1	Baseline situation	Abstraction is maintained
2	Increased supply	Increasing of 1.8 % per year
3	Conservative policies	Reducing of 1 % per year
	Future climatic conditions (annual rainfall)	*Recharge by rainfall*
A	Historical base-case condition (1,911 mm)	Recharge by historical rainfall of 21-year period (1994-2014)
B	Future rainfall condition (1,985 mm) with average increasing of 13 % for the medium emission (ADB, 2013)	Recharge by simulated future rainfall of 21-year period (2015-2035)
C	Minor dry condition	Reduction in recharge by 5 % loss (*Re*) of future rainfall (*Rt*)
D	Major dry condition	Reduction in recharge by 15 % loss (*Re*) of future rainfall (*Rt*)

period of 6 years (2015-2020), the total GW demand is predicted to increase from 348.226 m3/d to 379.916 m3/d in the study area (DWRPIS, 2012), which means 1.8% increase per year in average. Thus, in Driver 2, GW abstraction rates for domestic, industrial and agricultural supply were set up with this 1.8% increase (Table 5.1). In case GW abstraction will increase corresponding to the future water demand and it will exceed the potential GW supply, some technologies must be applied to save water or utilize other water resources. Otherwise, closure of wells in operation and their geographical reallocation may be necessary, and anyway, GW management should focus on reducing the quota of GW abstraction. Under this assumption, Driver 3 was set as the case that GW abstraction should be reduced by 1% per year from the previous year. This would help avoid the decline of GW levels and protect limited water resources of the aquifer.

5.5.3 Future Conditions of Rainfall and Recharge

Four conditions related to the future climate were considered, such as: (A) Historical base-case condition which maintains the present annual rainfall with the present recharge rate; (B) Future rainfall condition which has the increased rainfall predicted by the GCM with the present recharge rate; (C) and (D) Lower recharge conditions which assume some reduction in recharge despite the increased rainfall. We considered the conditions (C: 5% rain loss) and (D: 15% rain loss) to be examined because of possible decrease in recharge rates due to increase in evapotranspiration and increase in rain loss for intensified rainfall events. Besides the future increase in total rainfall, the GCM forecast is also showing extremization of weather which includes increased frequency of heavy rains and lengthened dry spells. Accordingly, possible decrease in recharge despite the increased rainfall should also be examined.

5.5.4 Scenario Building

Combination of the three GW management options and the four future climate conditions produces 12 possible cases. Among them, two sets of scenarios were chosen to fit the two main focuses of the scenario simulations. The focuses are: (i) Evaluation of transient responses to the GW management options under the present and the future climate, and (ii) Assessment of GW system responses under the recharge reduction conditions.

For the first focus (i), the scenarios A1, B1, B2, and B3 were simulated. In the scenario A1, the current rainfall condition (1994-2014) and GW management of Driver 1 are assumed (baseline case—the status quo scenario); while the future rainfall condition predicted by GCM is assumed for B1, B2 and B3 with the GW management of Driver 1 for B1, Driver 2 for B2 (risk scenario), and Driver 3 for B3 (sustainable scenario) respectively.

For the second focus, the three scenarios C2, D2, and D3 were simulated, where the possible reduction of recharge from rainfall is considered. The cases C2 and D2 which assume increased GW pumping (Driver 2) are considered rather risky cases, while D3

is expected to contribute to alleviation of the situation with the decrease in pumping (Driver 3).

The following parameters were used while studying future management scenarios: (i) All the parameter values and assumptions used for the hydrogeological characteristics of the aquifer remain the same as present, and (ii) The GW levels computed by the calibrated GW model for Dec. 2013 were used for initial conditions.

5.6. Model Results

5.6.1. Calibrated Hydraulic Conductivity (K)

The hydraulic parameters package of iMOD handled input values for each model cell of the two layers in the model domain. The data of the investigated nine wells with

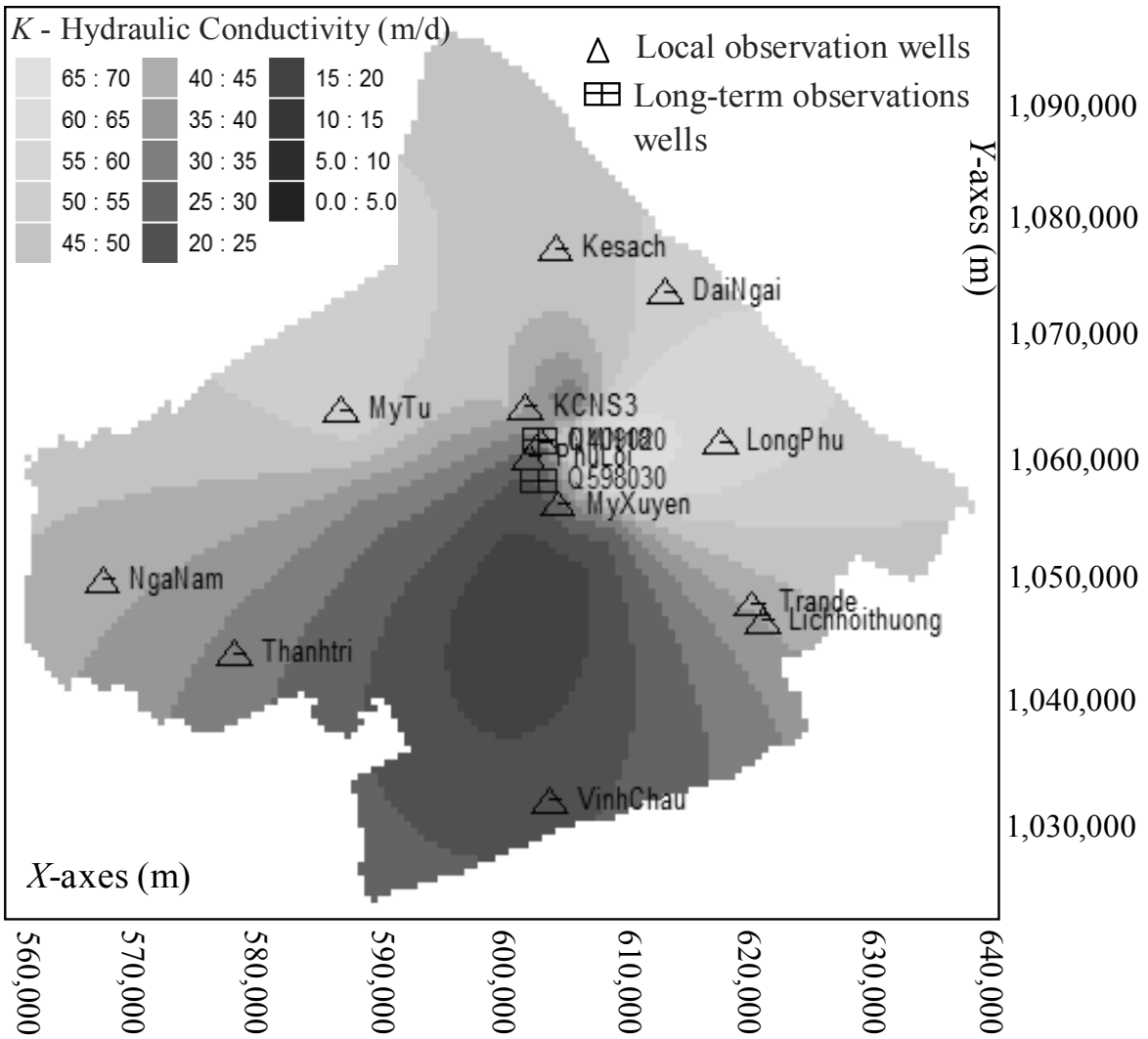

Fig. 5-13 Optimised *K* values (m/d) and monitored points

pumping test were utilized for a spatially distributed series of cells within a layer or zone containing defined values for those parameters. The hydraulic conductivity (K) between the pilot points was determined by interpolation of the Kriging method as tentative values for model cells. Through the calibration process, presents the hydraulic parameter values were optimized from the tentative values to obtain good agreement on GW heads of the 100-meter aquifer at the observation well points as shown in Fig. 5.13.

5.6.2. Calibrated GW Model for the Study Area

The measured GW levels of twelve local and two long-term monitoring wells in the study area were used to calibrate the model. The error in the simulation heads were quantified by mean residuals and root mean square errors (RMSE) in the calibration process, and finally the model performance was evaluated by Nash-Sutcliffe's coefficient of efficiency (NSE). The first phase of calibration with the steady state model was performed by adjusting values of hydraulic conductivity to obtain good agreement between simulated GW heads and observed ones at the 12 local observation wells. Fig. 5.14 shows the map of the spatial distribution of the simulated heads (100 m × 100 m) of the 100-meter aquifer on Dec. 2013. The calibrated model still shows a mean residual of 0.5 m, and the tendency that the calibrated model calculates the heads slightly lower than the observed ones was recognized. This defect is considered due to the inaccuracy of pumping estimation. However, the result with respect to GW heads of the 12 wells shows the high value of NSE (Fig. 5.15). It indicates that the calibrated model can be accepted as a good GW model of the study area (Anderson and Woessner, 1992).

In the second phase, transient simulations for the period from 1994 to 2014 have been carried out. The GW contour maps at January 1994 obtained by the steady state simulation were used to define the initial condition of the hydraulic heads. The model was calibrated by adjusting pumping rates and recharge rates to obtain good agreement of GW head fluctuations with the observed values at the two long-term observation wells for the calibration period. The results of the transient simulation showed the trend of GW drawdown at the 100-meter aquifer for the past decades in

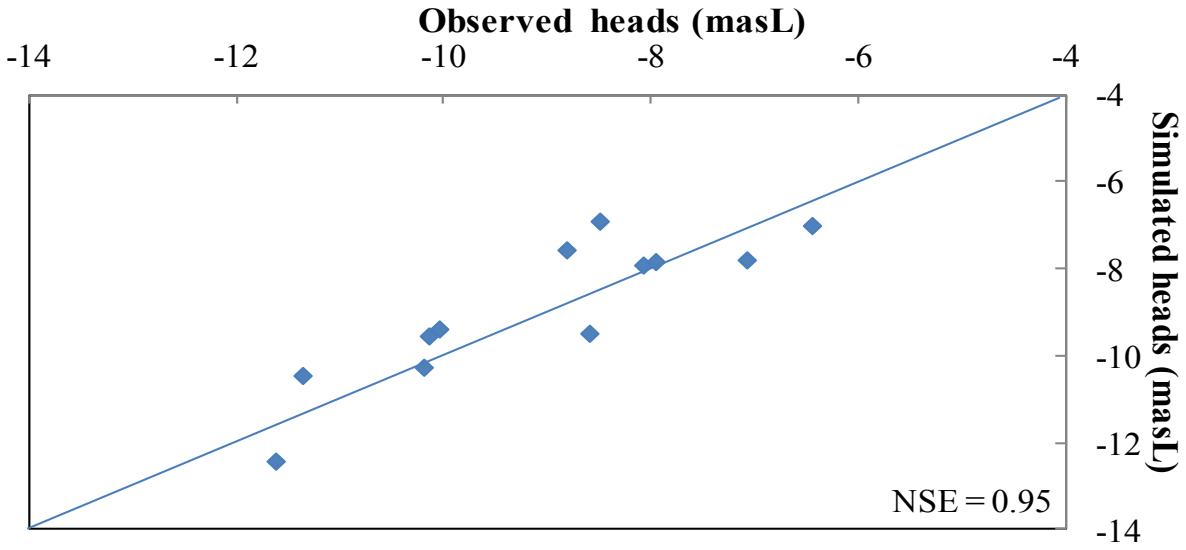

Fig. 5-14 Plots of simulated versus observed GW heads on Dec. 2013 at 12 local observation wells

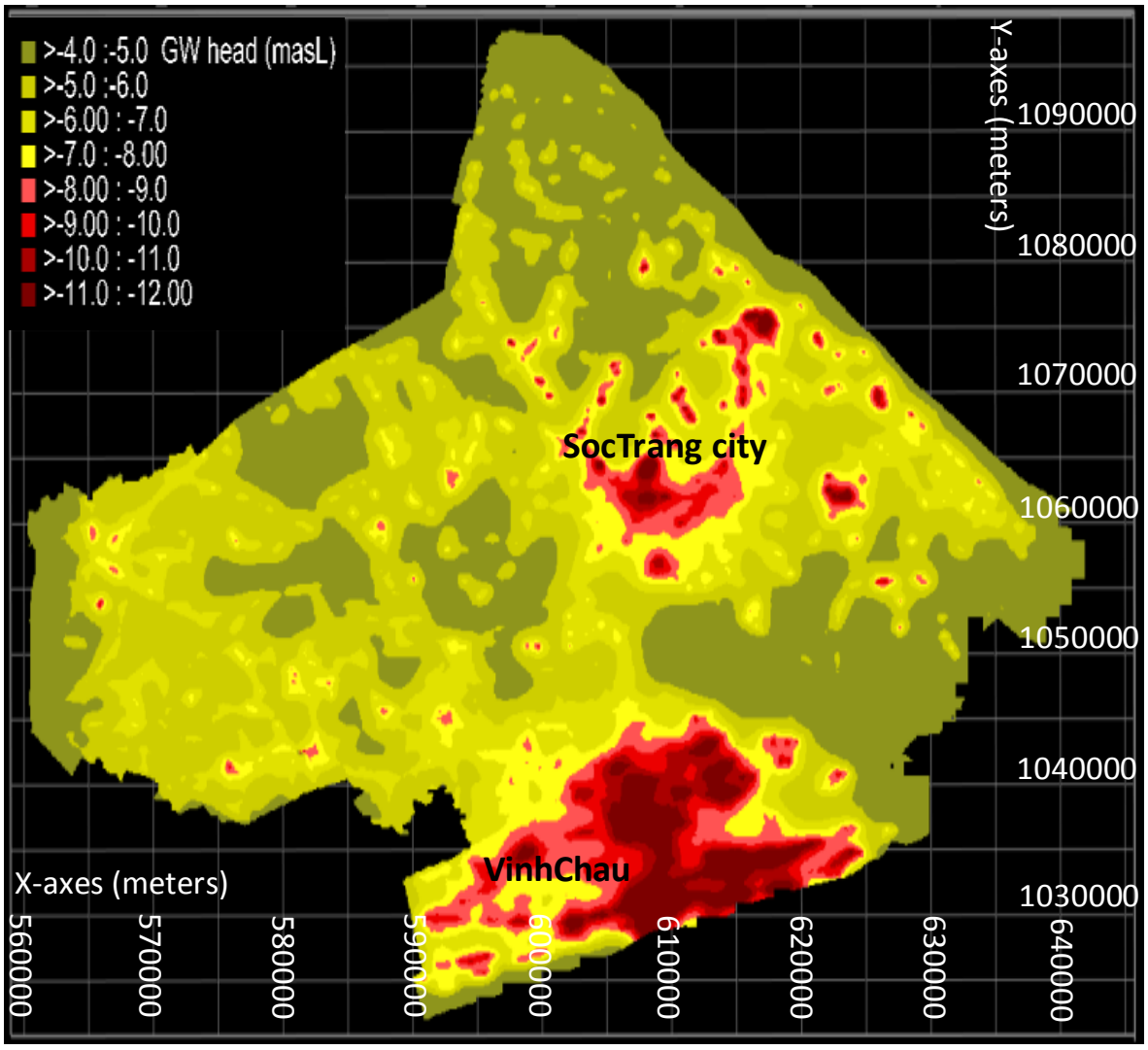

Fig. 5-15 Simulated spatial distribution GW head on Dec. 2013

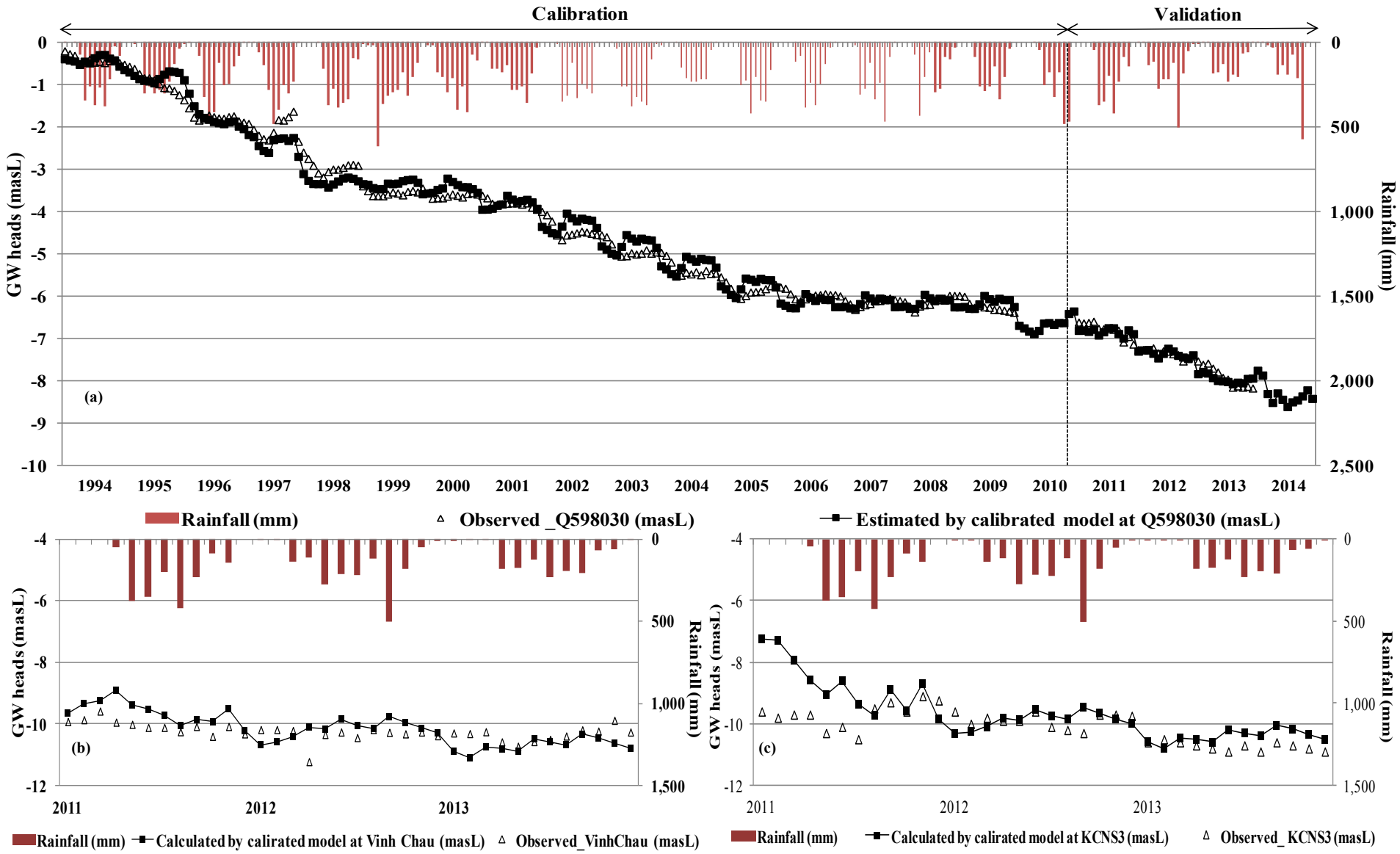

Fig. 5-16 Simulated vs. observed GW heads at: (a) long-term well; (b) local well in the central district and (c) local well in the coastal

the study area (Fig. 5.16). The simulation result of GW drawdown at the long-term observation well shows fairly good matching with the measured one with a very high value of NSE (Fig. 5.17), though simulated drawdowns at the some local wells (DaiNgai, LongPhu, Kesach, MyTu, Thanhtri) were somewhat less than observation. The mean RMSE was about 0.62 m (average for 14 wells) and residuals were within ±0.6 m. Besides the drawdown trend, the seasonal fluctuation of GW levels was also well expressed by the simulation. The long-term decline in GW levels is considered due to over-exploitation of GW resources. Though GW levels recover in the rainy season, the recovery cannot catch up with the depletion by pumping. Such phenomena can be well presented by the model simulation and the GW dynamics simulated by the model were consistent with observations. Therefore, the established model was expected to be a useful tool for examining various GW management options under different climate factors in the future.

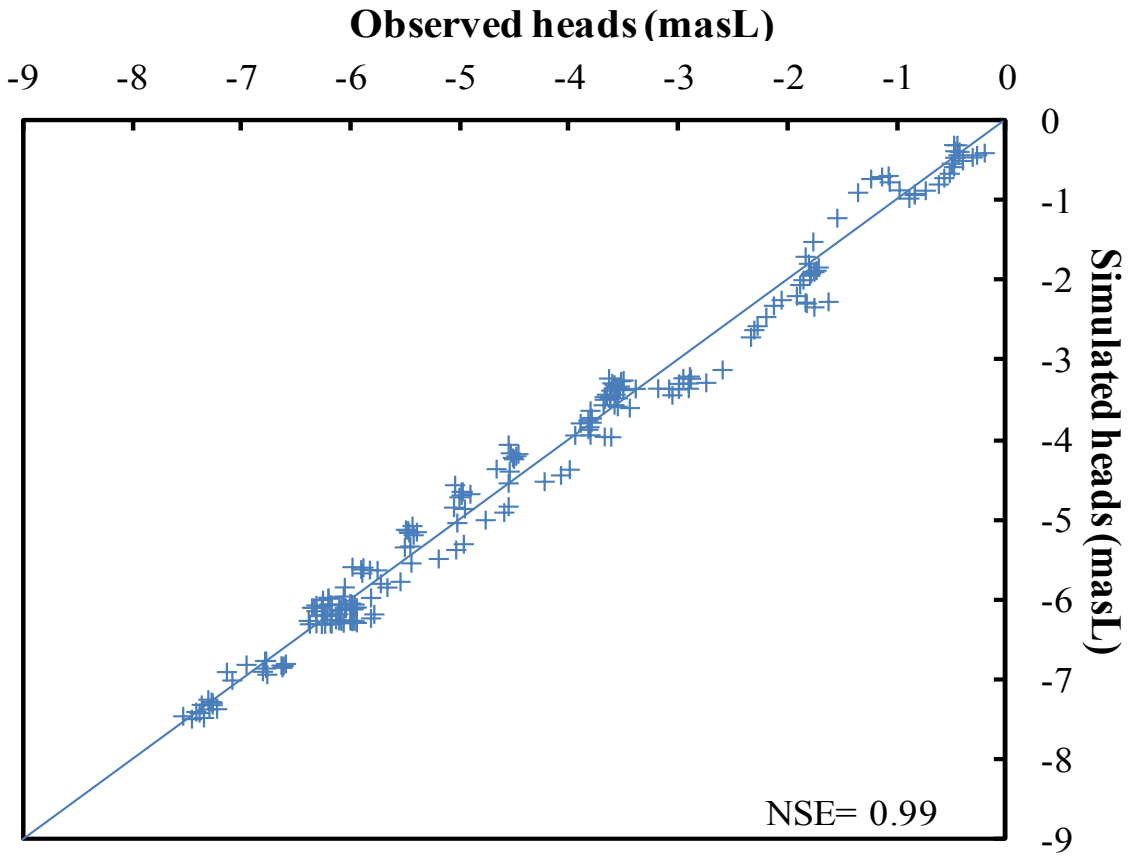

Fig. 5-17 Plot of simulated versus observed GW heads on the period of 1994-2013 at long-term well

5.6.3. Sensitivity Analysis

The purpose of sensitivity analysis is to observe the model response to the variation in uncertain parameters. The results can be used to identify sensitive input parameters for the purpose of guiding for the calibration such as aquifer parameters, pumping rate, recharge and boundary conditions. Among the model parameters, hydraulic conductivity, recharge rate and discharge (pumping) rate were selected as the most uncertain parameters. During this analysis the calibrated value for the aquifer parameters and the boundary conditions are systematically changed with plausible range (Anderson and Woessner, 1992). Sensitivity of the model was evaluated by RMSE after multiplying each parameter a time by 0.4 to 1.6 of the original value and model's run-file. The RMSE of each run was plotted against the multiplying factor. As the result, the factor of recharge was shown to be the most sensitive parameter and the second is pumpage (Fig. 5.18). These factors are the main water balance components and their impacts therefore should be assessed in the model application.

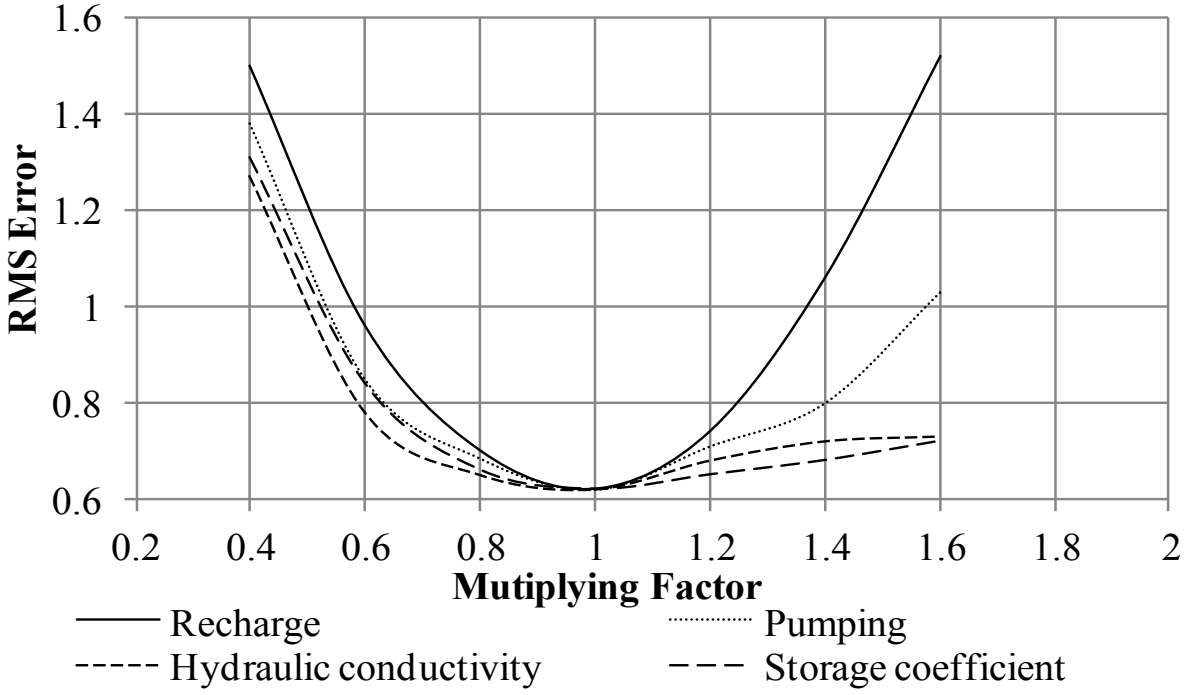

Fig. 5-18 Results of sensitivity analysis

5.6.4. Aquifer Response to Scenario A1, B1, B2 and B3

Because most of the centralized water supply stations are located in the central district, the Q598030 well was chosen to predict aquifer response to the different scenarios.

The baseline scenario (A1) assumed that the current climatic and rainfall conditions continue to be the same for the future 21 years period 1994-2014 and the current GW abstractions be maintained. As the graph indicates slight decline of GW heads (Fig. 5.19), some imbalance between recharge and discharge (pumpage) was recognized. According to this result, if the current recharge and the current GW abstraction continue, there will be an overall GW level decline by around 0.05 m per year in the urban zone of the study area.

Simulation for Scenario B1 examined the condition of maintaining the current GW pumpage under the future rainfall predicted by GCM for the 21 years period 2015-2035. The simulation results indicated that GW levels are mostly stabilized for the whole period with repeating slight drops and recoveries in each year (Fig. 5.19). This means Scenario B1 has smaller risk of GW depletion than Scenario A1, thanks to the future rainfall increase in the rainy season.

For Scenario B2, which assumed 1.8 % per year increase in GW pumping under the future rainfall, the simulation results showed significant decline in GW levels through the simulation period. This result implies that aquifer depletion is taking place, because GW is withdrawn faster than it is recharged by precipitation. The graph shows that if GW abstraction increases, the GW levels will be lowered by around 2 m in the middle of the study area and 3.5 m in the coastal districts where abstraction wells are densely located. In this scenario, there is no development of abstraction wells was assumed, the decline therefore is smaller than the historical period (1994-2014) (Fig. 5.16 (a)).

In Scenario B3, which assumed 1% per year reduction in pumping for water supply, the benefit of GW resources protection with sustainable policy was tested. According to the results for this case, since the discharge by pumpage becomes smaller than estimated recharge from rainfall, the GW levels can recover up to about 1.0-1.5 m in

2035. Thus, the proposed 1% per year reduction in pumping was considered as a sustainable policy option that can significantly reduce the risk of GW depletion and help protect the scarce GW resources. However, it would probably take long time to implement such policies effectively.

5.6.5. Risk (C2, D2) and Sustainable (D3) Scenarios

The risk scenarios of C2 and D2 assumed increased GW abstraction (Driver 2) under minor (C2) and major (D2) reduction in recharge due to increased rainfall loss and uncertainty of rainfall. Simulations for these scenarios were carried out in order to depict aquifer response to the unsustainable condition in terms of spatial distribution of GW heads. The map of spatial distribution of simulated GW heads (100 m × 100 m) in 2035 (Fig. 5.20) showed an intense and continuing decline of the GW heads, whose pattern represented the clear impact of decreased recharge and increased pumping. If these conditions occur in the future, significant depletion of the GW aquifer could appear in most of the area by 2035. It was also shown that evident decline ranging from -8.0 m to -14.0 m might be observed in the middle and the coastal areas which have intensive pumping. Under Scenario D2, people in these areas would be most immediately vulnerable to water scarcity. Since the study area is coastal lowland of MD, the simulation results for both C2 and D2 imply that further drawdown of the GW table can cause land subsidence and salt intrusion in near future. Therefore, it can be concluded that increasing pumping rates will be risky considering the uncertainty of the future climate.

In simulation for Scenarios D3 (Fig. 5.21), the effect of "sustainable policies" (Driver 3) under the lowest recharge condition (D) was examined where the total amount of pumping water during the period 2015-2035 is reduced by about 11%, as the result of the assumed 1% reduction of pumping rates every year. The result showed that the simulated GW levels in 2035 can recover to higher levels than those calculated for Dec. 2013 (Fig. 5.14) even under the reduced recharge condition. In this condition, GW heads were found to be stabilized as the current levels with values of -10m to -11m and -11m to -12m in the middle and the coastal zones of the

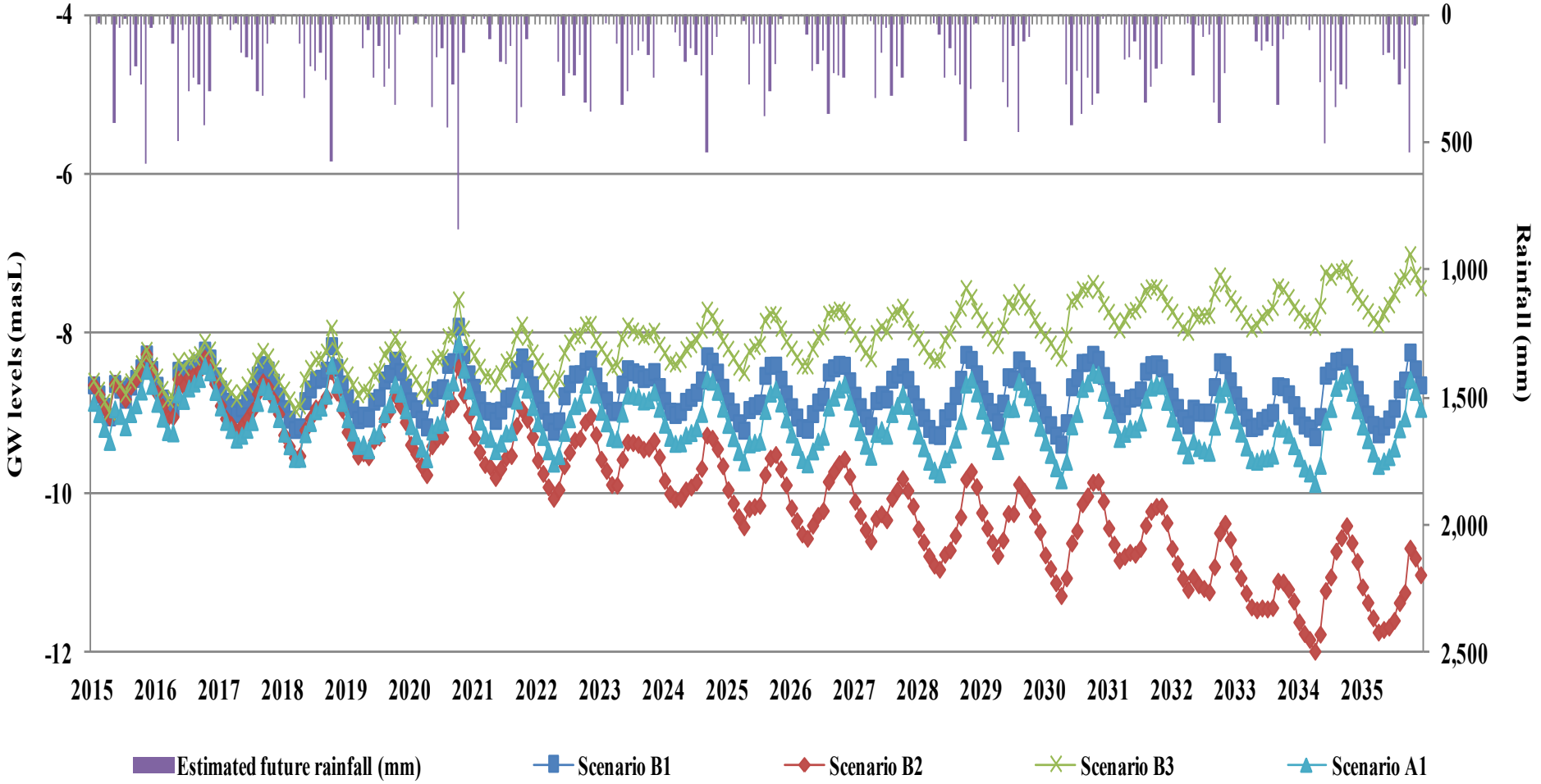

Fig. 5-19 Simulated GW heads at Q598030 for transient management scenarios (Scenarios of B1, B2, B3 with recharge calculated by estimated future rainfall; Scenarios of A1 with recharge calculated by current rainfall)

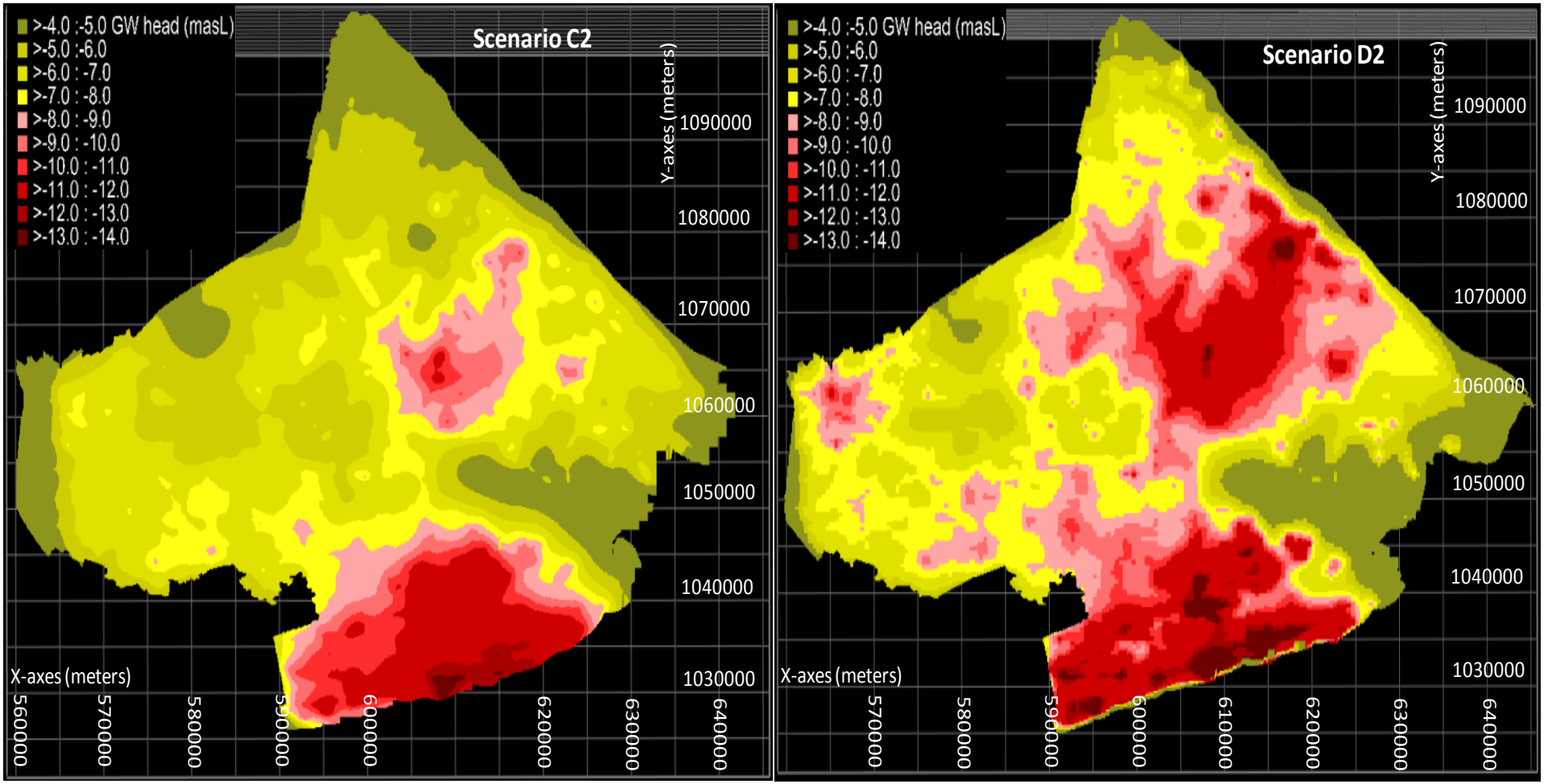

Fig. 5-20 Spatial distribution of simulated GW head of risk scenarios of scenario C2 and scenario D2 in 2035

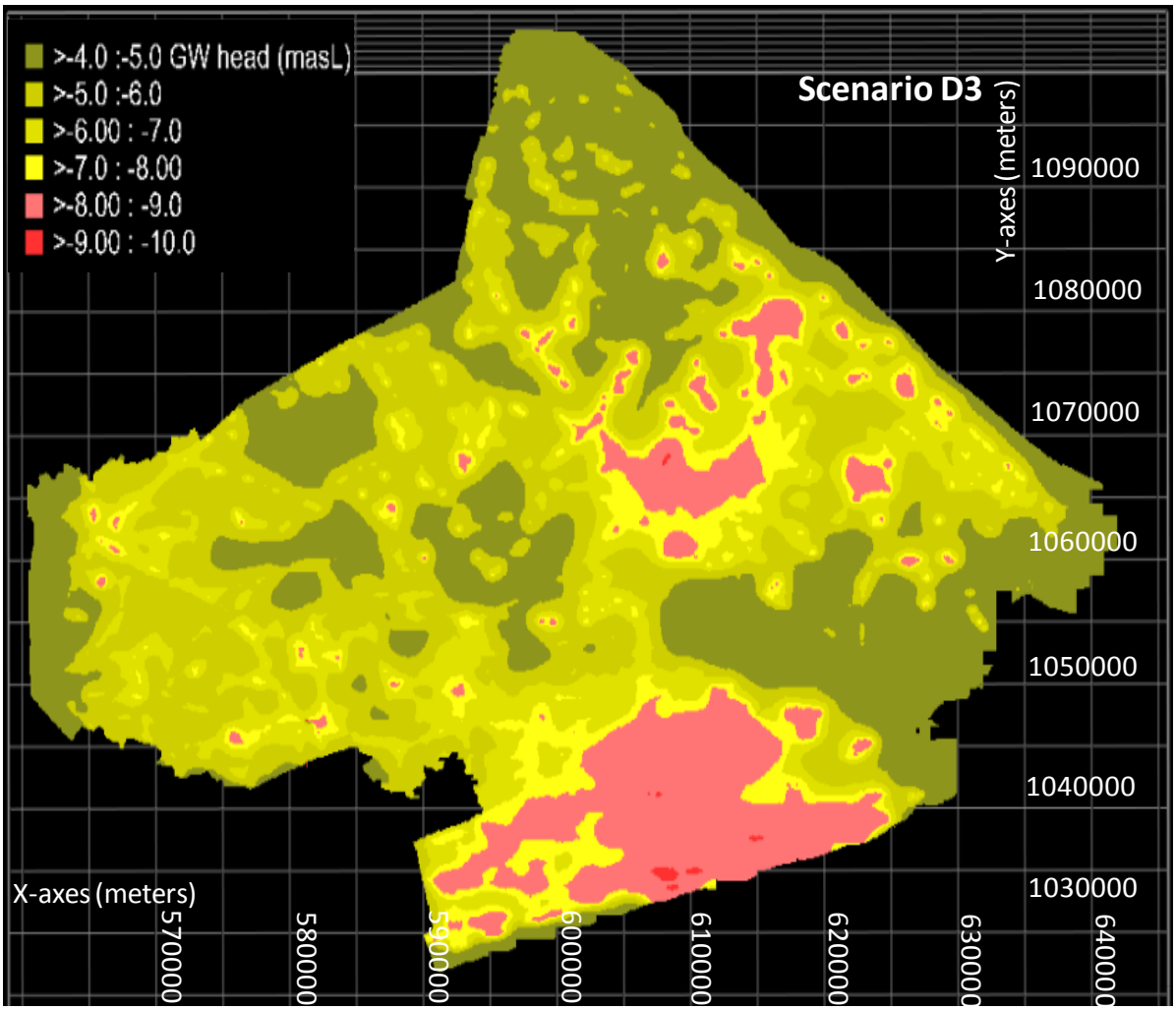

Fig. 5-21 Spatial distribution of simulated GW head of "sustainable policies" scenario D3

study area, respectively. In addition, a tendency of flattening out the GW heads for the whole area was recognized in Scenario D3, when compared with C2 and D2 (Fig. 5.20 and Fig. 5.21). These results imply that the improved GW management to save pumping can work quite effectively to prevent the GW aquifer from depletion.

5.6.6 Uncertainty

Although the established GW flow model can be useful tool for investigating aquifer response, it is a simplified approximation of the actual system and is based on average values and some estimated conditions. In addition, GW monitoring system in the study area is now still being established and optimized. There are some constraints to construct the appropriate GW model, uncertainty identification is therefore important in case the model is employed to analyze impacts from GW extraction. The

uncertainty associated with this model may be due to several factors, which include: (i) the errors and uncertainty in the data; (ii) assumption used to construct the model; (iii) pumping rate and recharge estimation; (iv) lack of uniqueness and reliability in the calibrated hydraulic conductivity values; and (v) uncertainty of GCM prediction.
The accuracy of model predictions depends on availability and accuracy of the input data to be used to calibrate the model. Particularly in areas having sparse or no data, the accuracy of the model may be degraded. To clarify the details of the geo-structures and to enhance the information of the aquifer system, more detailed reliable drilling records and pumping test data should be required. Another possible source of uncertainty is related to such input data as estimates of pumping and wells distribution. Despite the efforts of investigation of wells, it was difficult to get full data of the wells for the model, because many of those wells working for agricultural and domestic use are not metered. Therefore, the assumed rates of GW pumping may be overestimated or underestimated compared to the real pumping.

5.7. Conclusions

A GW flow model based on iMOD was established for the coastal area of MD. The model was calibrated with the observed GW heads at several wells in the study area for the past years. The calibration results showed fairly good agreement between calculated GW heads and observed ones with respect to both spatial distribution and temporal fluctuation. It was confirmed that the established model can work properly to reproduce the GW heads of the aquifers and to represent the behaviors of the aquifers. We ran the GW flow model for simulating various scenarios for 2015-2035 in order to examine the effects of the possible future change in rainfall and GW abstraction managements on the GW resources. Through the scenario simulation, the model predicted what is likely to happen on the GW aquifer for each scenario. As the results of the simulation on different scenarios (A1, B1, B2, B3), the transient aquifer responses during period simulation of 2015-2035 were addressed and the following points were clarified:

(1) Under the baseline scenario (A1) assuming that the current climatic and rainfall conditions continue to be the same as that of the 21 years period 1994-2014

and the current GW abstractions be maintained, slight decline of GW heads was recognized. In this scenario, namely if the current recharge and the current GW abstraction would continue, an overall GW level decline by around 0.05 m per year in the urban zone of the study area was expected.

(2) Simulation results for the condition (B1) of maintaining the current GW pumpage under the future rainfall predicted by GCM indicated that GW levels would be mostly stabilized for the whole period with repeating slight drops and recoveries in each year. This means that if future rainfall increase as predicted by GCM, the risk of GW depletion might be smaller than present.

(3) In case of the scenario (B2) assuming 1.8% per year increase in GW pumping under the future rainfall, the simulation results showed significant decline in GW levels over the simulation period. This result implies existence of big imbalance between GW recharge and discharge.

(4) In the scenario (B3) assuming 1% per year reduction in pumping for water supply, the results showed that the GW levels could recover up to about 1.0-1.5 m by 2035. The proposed 1% per year reduction in pumping was considered as a sustainable policy option that can significantly reduce the risk of GW depletion and help protect the scarce GW resources.

(5) Considering the uncertainty of the future climate, simulations for the risk scenarios (C2, D2) assuming increased GW abstraction under minor (C2) and major (D2) reduction in recharge due to increased rainfall loss and uncertainty of rainfall were carried out in order to depict aquifer response to the risk conditions in terms of spatial distribution of GW heads. Also for examining the sustainable GW management policy to overcome the risk, another scenario (D3) assuming reduction in GW abstraction was simulated and predicted by the model in 2035. From the results of these simulations, the following points were found:

(i) The map of spatial distribution of simulated GW heads in 2035 for both C2 and D2 showed an intense and continuing decline of the GW heads, whose pattern represented the clear effect of decreased recharge and increased pumping. If these conditions occur in the future, significant depletion of the GW aquifer might appear in most of the area by 2035.

(ii) The simulation result for the scenario (D3) assuming 1% per year reduction in GW pumpage showed that the simulated GW levels in 2035 could recover to higher levels than the present ones even under the reduced recharge condition. From this, the improved GW management to save pumping was considered quite effective to prevent the GW aquifer from depletion.

CHAPTER 6 LAND SUBSIDENCE MODELING FOR MEKONG DELTA

6.1 Background

It has been reported that most of land subsidence in low lying land have been caused by excessive GW extraction. In 1960s to 1970s in Japan, a big amount of GW was taken for satisfying the growing water demand for industrial and domestic water use, and it had resulted in serious land subsidence in the urban areas such as Tokyo and its surroundings (Nakajima et al, 2010). In order to avoid the risk of the land subsidence, the Japanese government implemented the regulation on GW use in the urban areas, in which the government tried to control major GW use and conversion of GW use to surface water use was promoted. After this regulation, land subsidence has now mostly stopped in Japan.

When we look at Mekong Delta, it is most likely that the rapidly growing GW use should cause serious land subsidence also in Mekong Delta (Philip et al, 2017). Particularly because of its vast low lying land feature, land subsidence in Mekong Delta may lead to decisively serious devastation. In the areas where GW pumping is resulting in subsidence at levels affecting the existing management area, additional land use planning (Phien-wej et al, 2006). Relationship between GW level decline and the rate of subsidence has been observed for some years in various places in Mekong Delta. The phenomenon can cause to other associated problems, such as changes in elevation and gradient of stream channels, ill drainage, and other water transporting facilities, damage to civil engineering structures, private and public buildings, etc. Especially, the salt intrusion in the coastal area, Sea level rise along the east coastal area of Mekong Delta has also been observed for some time and has averaged 2.9 mm/year (MONREs, 2012). A combination of sea level rise and land subsidence could cause a serious increase in frequent flood inundation and result in tidal encroachment onto lowlands in a coastal community.

For such serious risk of land subsidence, however, observation of land subsidence in Mekong Delta has so far been very poor. However, to understand and visualize the

relationship of land subsidence and GW levels, the first attempt in this study performed the modeling of land subsidence due to GW withdrawal and its application to the Mekong Delta.

A thorough modeling of subsidence has been performed, with particular concerning to the case study in the middle and coastal of Mekong Delta. The area of modeling, CanTho city and Soc Trang city, is interested by a lot of water supply wells, which have been installed since 10 years ago. GW withdrawal for domestic, industrial and agricultural employment has induced remarkable ground surface settlements. The model parameters was optimised by the data on ground surface settlements has been gained by Interferometric SAR (InSAR) for 5 years (2006-2010).

6.2 Model Description

6.2.1 Approach of Modeling

The thickness of a confined aquifer is maintained with the balance between the outer pressure from the gravity of the upper soil layers and the inner pressure of the aquifer water. Therefore, reduction in the inner pressure caused by extraction of GW from the confined aquifer will cause contraction of the thickness of the aquifer. That is the process of land subsidence and it is considered a phenomenon containing both reversible and irreversible factors. Namely, the recovery of land surface elevation cannot catch up with the recovery of GW level to the past level. For example, in the correspondence between the seasonal fluctuation of GW level and that of land surface elevation, even if the GW level returns to the same level as the past, the land surface elevation cannot be back to the past level.

For such partly irreversible phenomena, it is known that the theory of rheology is effectively applicable, where the reversible factor is expressed by elasticity and the irreversible factor is expressed by plasticity or viscosity. Here in this study, the three-factor rheology model to be mentioned below was employed to simulate the land subsidence in Mekong Delta.

6.2.2 Rheology

The aim of rheology is to examine the influence of a load on work of various materials considering also of the duration of such a load. The name rheology originates from Greek words rheo (flow) and logos (science). Sometimes rheology is treated as an independent field of science that encompasses such special issues as: resilience theory, plasticity theory, or mechanics of viscous liquids. Models of the aforementioned ideal materials are treated as special cases of a more general rheological model. Such a division is a result of the interdisciplinary significance of rheology.

Materials exhibiting rheological properties are subjected to the same general laws of mechanics as the rest of materials. Differencesin their mathematical description lie in formulating appropriate constitutive equations which include an additional independent variable: real time.

Rheology is of a huge practical significance in numerous fields of technology, including compression of soil analysis, for rheological properties are exhibited by soil characteris. Those properties become visible to various degrees depending on the type of soil and conditions of any given soil or land.

6.2.3 Three Factor Rheology Model

Rheology model is the simple structural models, the aim of which is to interpret fundamental properties of materials in terms of physics, are used in the literature on rheology. A spring is a model of an elastic material that subjected to the Hooke's law. As a model of viscous liquid it is possible to consider a silencer, presented asa perforated piston moved in a cylinder filled with viscous liquid. As a result of the applied force, the silencer performs a movement, velocity of which

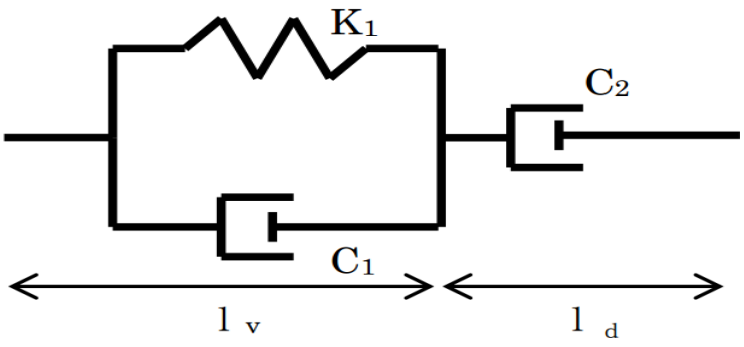

Fig. 6-1 Three factor Rheology Model

is proportional to the amount of the force. A parallel combination of an elastic element and a viscous one forms a model of viscous-elastic material (Kelvin-Voigt).

A three factor Reheology model was developed to estimate land subsidence caused by excessive GW exploitation (MORITA et al, 2014). GW-related subsidence is the subsidence (or the sinking) of land resulting from GW extraction, and a major problem in the Makong Delta as rapid urbanization zones and developing areas without adequate regulation and enforcement, as well as being a common problem in the developing countries. One estimate has 80% of serious land subsidence problems associated with the excessive extraction of GW making it a growing problem throughout the world.

In order to express the characteristics of ground subsidence, using a three-element model that can designate the amount of return displacement and residual displacement independently. The concept of the three-factor model consists of the Voigt part and the damper part, which are characterized by following parameters:

(1) the elasticity coefficient k1 and the viscosity coefficient c1 of the Voigt part;

(2) the viscosity coefficient c2 of the damper part.

The equations of the model are as follow:

The force acting on Voigt section: $fv = - k1(Lv - L) – c1\ Lv$

Force acting on damper part: $fd = - c2\ Ld$

Balance of forces : $f = fv = fd$;

This differential equation was solved using the Euler method. The value of f represents the relationship between the GW level and the ground force with:

f = ground pressure - GW level (pressure head)

Balance of length: $L = Lv+Ld=(k1\ (L - Lv - f)/c1 -f/c2$

Where Lv is the length of the Voigt part, Ld is the length of the damper part and L is the total length; For applying it to land subsidence, the thickness of the soil layer is represented by "L"; Groundwater level is interpreted to the working force on the soil layer

6.3 Model Application for Land Subsidence in Mekong Delta

6.3.1 Estimation of Three factors Values

To find out the optimised values of three factors: (i) the elasticity coefficient (k_1), (ii) the viscosity coefficient (c_1) and (iii) the viscosity coefficient (c_2) for the model is important to reduce uncertainty in model simulation. In order to estimate the these factors for land subsidence model, the type of optimization target is the observed land subsidence of INSAR during the period of five years (2006 – 2010) for whole Mekong Delta. Optimization steps as the figure following:

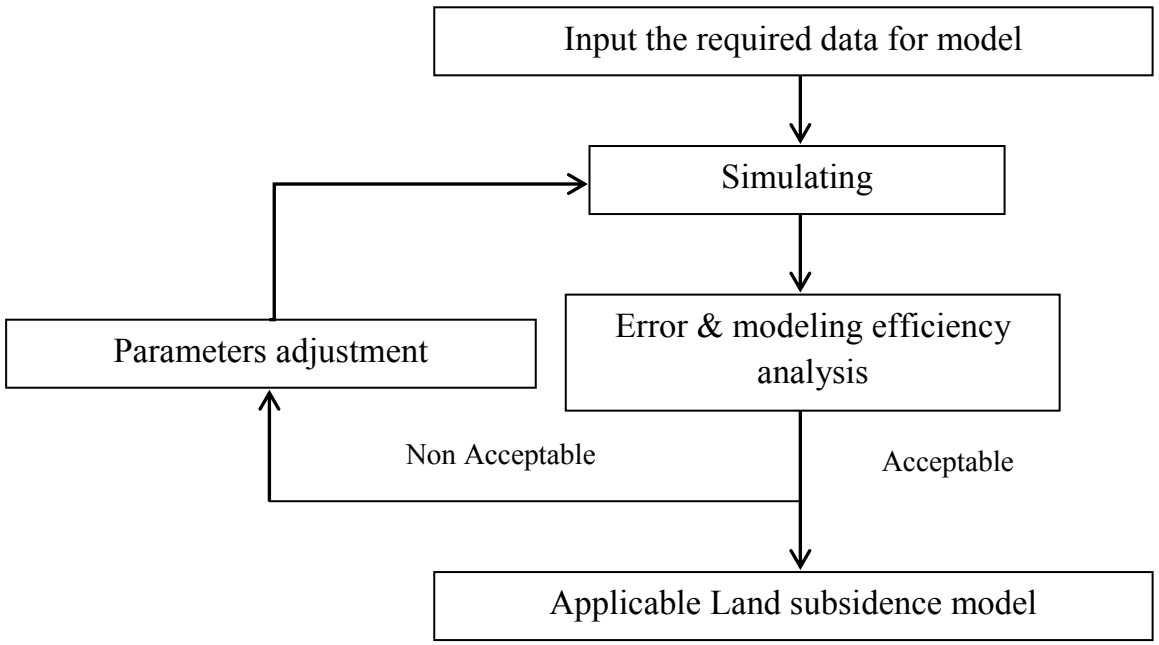

Fig. 6-2 Processes of estimation of three factors values

Table 6.1 shows the applicable paramerter values of thress factors during the adjusment steps.

Table 6-1 Parameter values at different application

Locations	K1	C1	C2
Previous research in Tochighi, Japan (Morita, 2014)	0,45	0,25	67
Applicable values for Mekong Delta, Vietnam.	0.5	0.35	87

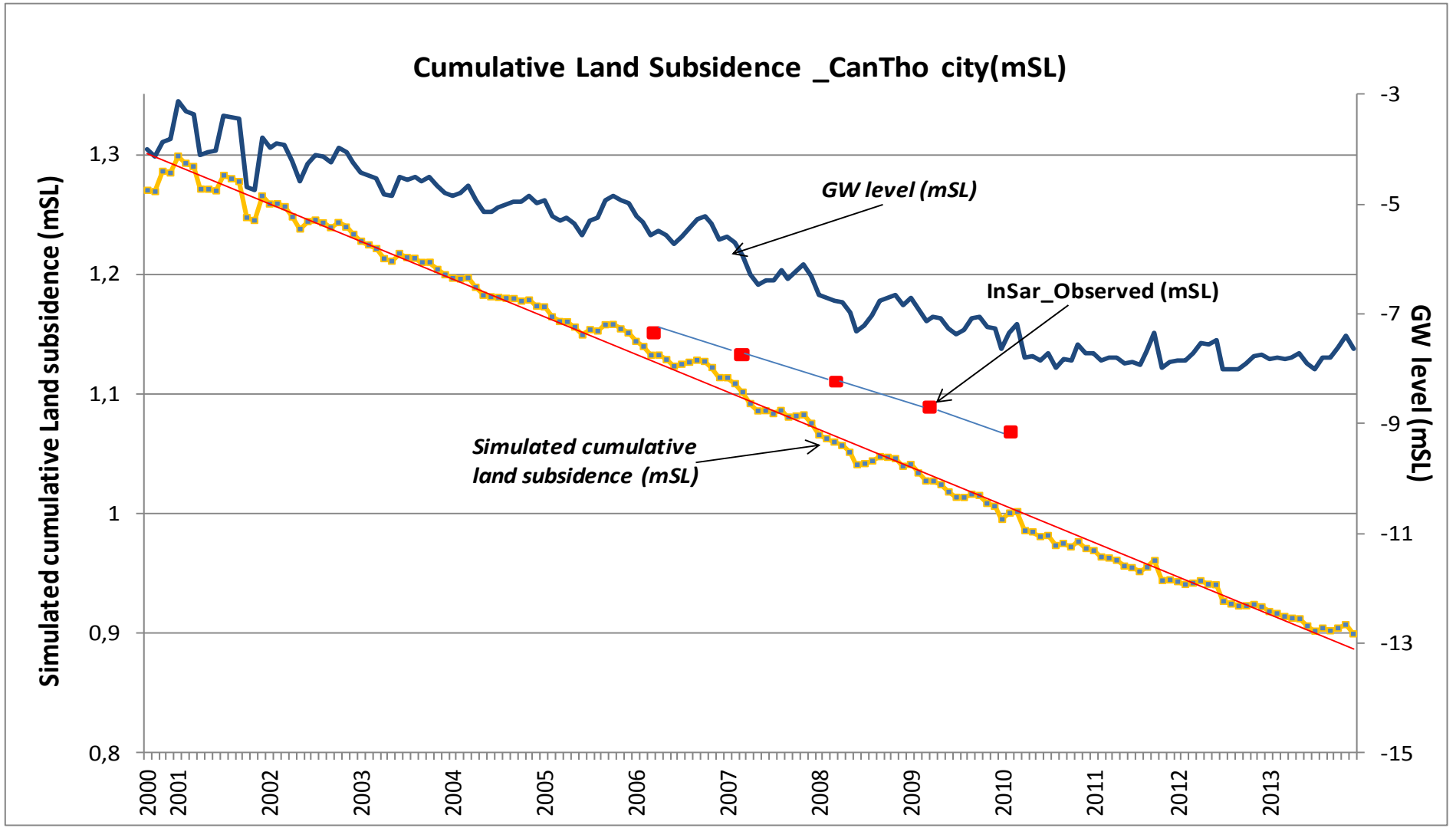

Fig. 6-3 Long-term transient simulation of cumulative land subsidence (mSL) in the period of 2000-2013 of Can Tho city

6.3.2 Simulation Results and Discussion for the Can Tho city

The Fig. 6.3 shows the relation between GW head, which is measured as GW levels at the long-term obsevation well (QT16A, see Fig. 4.10) in TraNoc industrial zone of CanTho city, and subsidence, which is typically analyzed as land subsidence at land surface by the InSAR method. Given the current trend of decreasing GW level, the long-term transient simulation of 14 years (2000-2013) was conducted to find out the current land subsidence situation in Can Tho city. It was found that the cumualtive land subsidence in Can Tho city was about 36 cm over the 14 years which means 2.6 cm per year of land subsidence rate.

Because of the limitation of the soil propertises testing, a match between simulated and measured subsidence should be improved by the futher detailed data for the model (Fig. 6.4). Thus, it does not necessarily indicate that the factors controlling subsidence are accurately represented by the model.

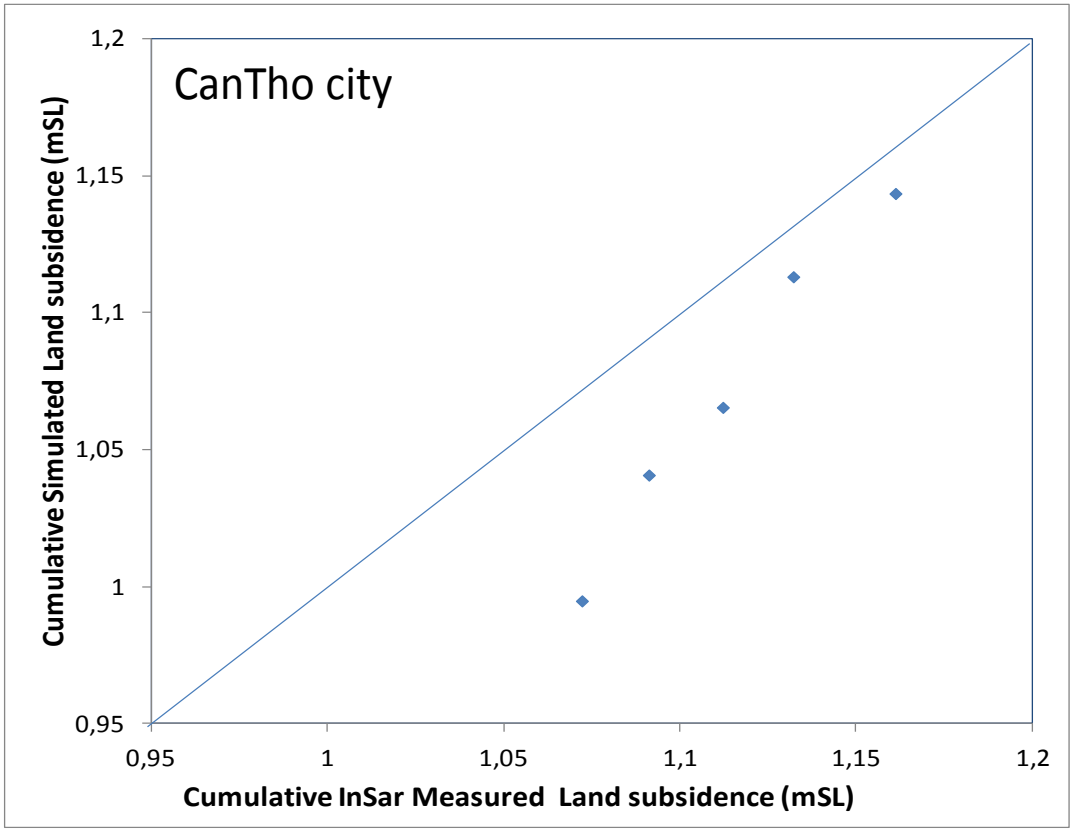

Fig. 6-4 Cumulative simulated vs. observed land subsidence in Can Tho city

6.3.3 Simulation Results and Discussion for the Coastal area of Mekong Delta

In the fisrt simulation, the model is appled to estimate land subsidence rate concerning historial observed GW level from 1994 to 2014 and the output modeled GW level of each scenarios in SocTrang. The Figure 6.6 shows the current rate of land subsidence is 3 cm/year. It implies that changes of GW heads in the aquifers, which are confined by thick clay layers, can lead to cumulative land subsidence was about 65 cm. Meanwhile, simulation for future rainfall (Scenario B1 in chapter 4) indicated that the land subsidence is lighter than the current by around 2.7 cm per year which means around 60 cm of the cumulative land subsidence (Fig. 6.7). Thus, in increasing recharge condition has smaller subsidence risk than the current. In this case, the model shows a fairly good macth between simulation and observed-InSAR from 2006 to 2010 (Fig. 6.5)

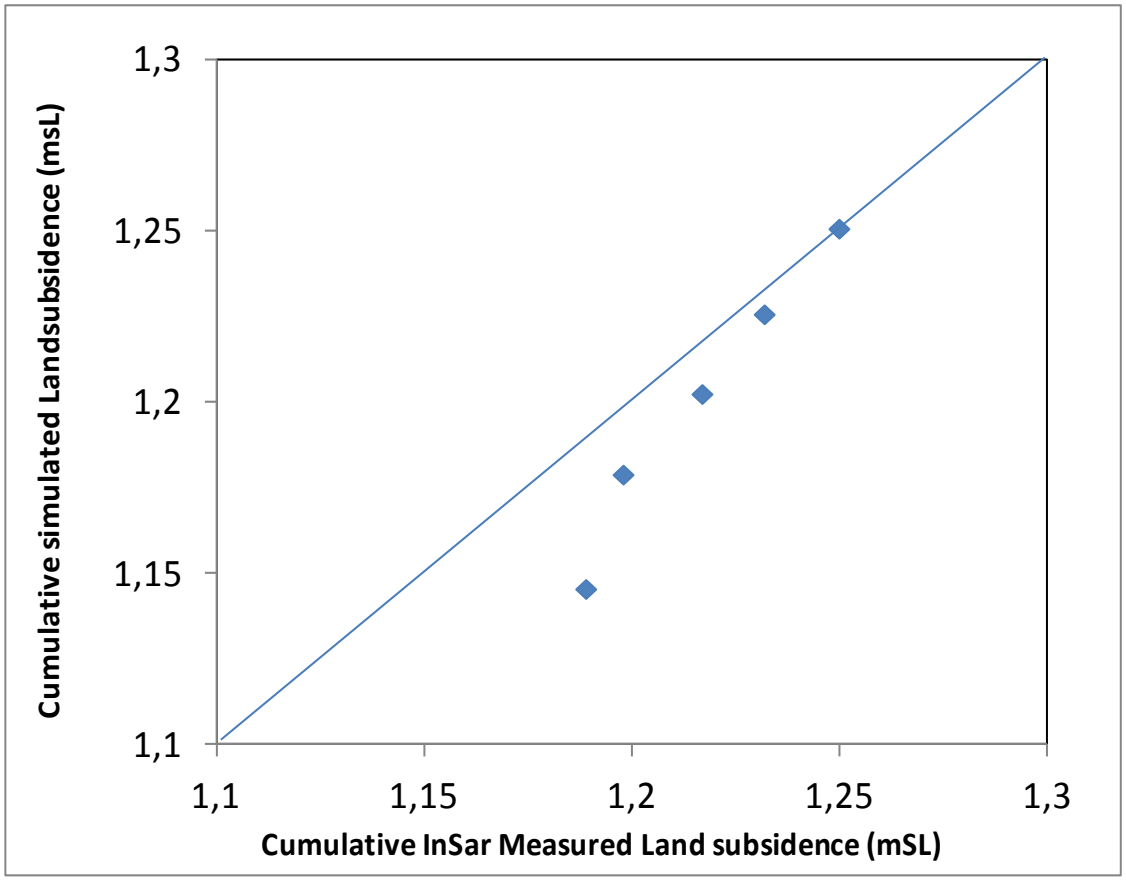

Fig. 6-5 Cumulative simulated vs. observed land subsidence in SocTrang city

To evaluate the land subsidence in the next 21 years, the model was applied corresponding simulated GW levels of the scenarios in Chapter 4. For the baseline scenario (A1), if the current recharge and the GW abstraction will be kept as the current pumping, there will be an land subsidence by around 2.85 cm per year. Meanwhile, the simulation results showed significant land subsidence through the simulation period with rate of 3.4 cm per year in case of the increasing GW pupmping (Scenario B2). It implied that if GW abstraction increases, the cumulative land subsidence will be around 71.4 cm in SocTrang in 2035 (Fig. 6.7).

In sustainable policy condition (Scenario B3), which assumed 1% per year reduction in pumping for water supply. According to the results for this case, since the GW levels can recover up to about 1.0-1.5 m in 2035, the rate of land subsidence is smallest value with 2.5 cm per year (Fig. 6.7)

From the calculation it is found that the rate of subsidence is directly controlled by the fall of GW level, the saturated thickness of aquifer and the hydrogeological characterist ics of the aquifer

As the results, the estimated land subsidence in the coastal area of Mekong Delta may cause several problems. Potentially the most devastating problem occurs in flat-lying coastal areas where loss of ground elevation may either cause inundation or increase the potential for flooding by tides and storm surges. When flooding becomes severe enough, expensive flood-control works or even abandonment of the affected land becomes necessary. A second problem may be caused when the magnitude of subsidence is large and the subsidence area is small or narrow.

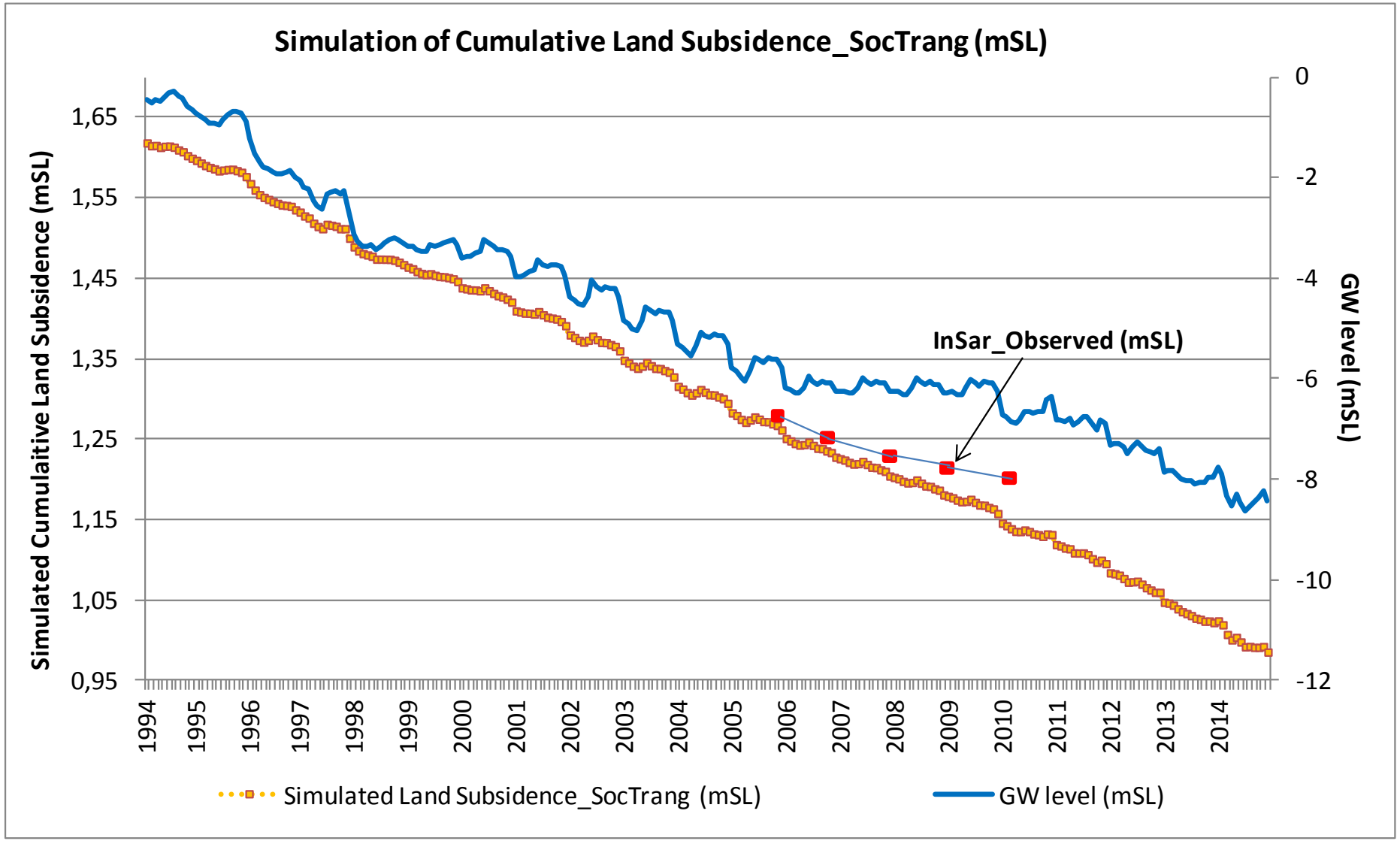

Fig. 6-6 Simulation of cumulative land subsidence (mSL) in the coastal Mekong Delta of Soc Trang.

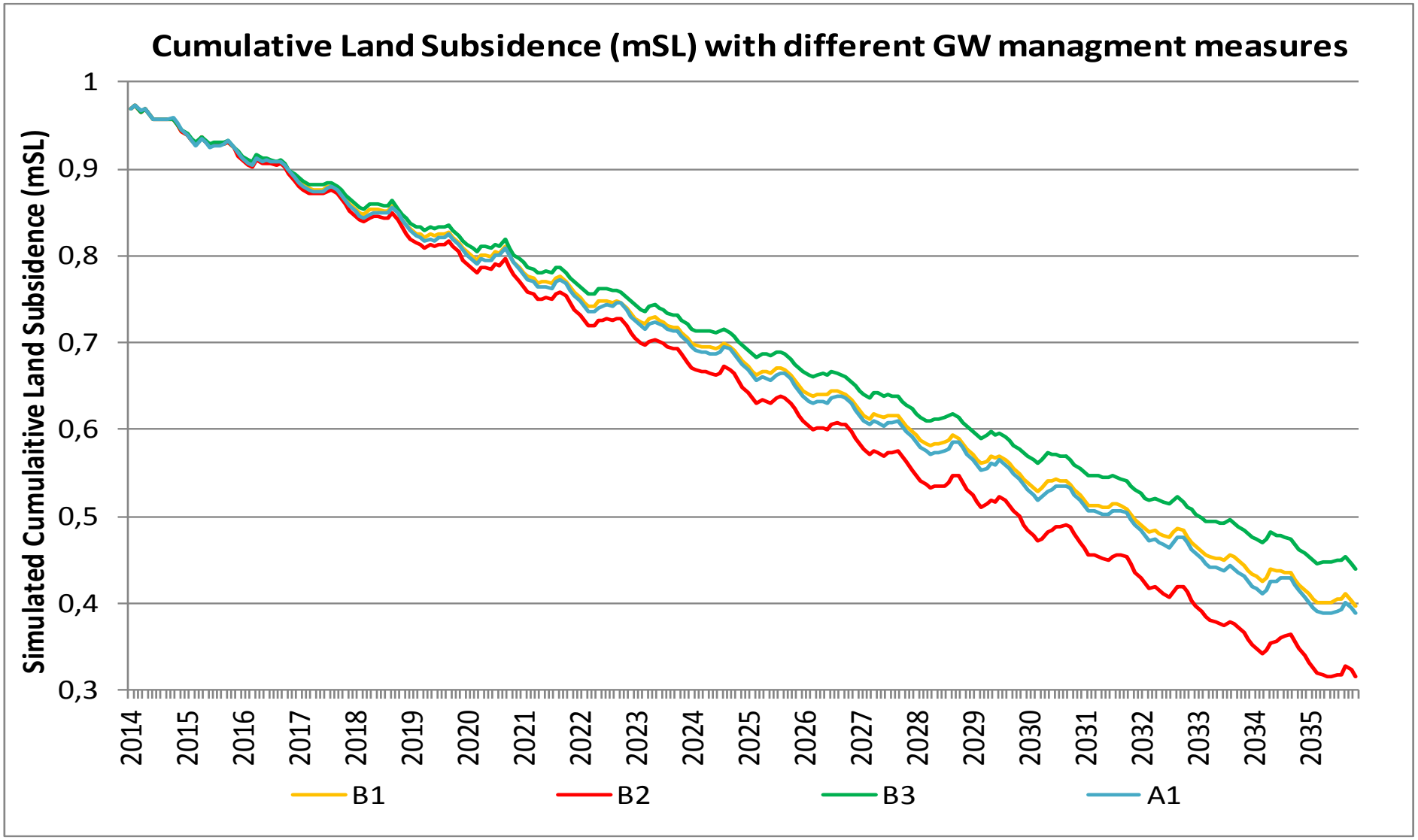

Fig. 6-7 Simulation of cumulative land subsidence (mSL) with different groundwater management and rainfall conditions.

6.3.4 Model Limitation

The issues of land modelling are very complex and specific. There is no universal model that would equally consider all properties ofthe material. Depending on the accepted theoretical model, various models of displacement may be obtained. Land subsidence occurs due to several joint factors: natural soil compaction, soil compaction due to external load, soil compaction due to water extraction, thickness of the clay and thickness and content of filling materials. In this chapter, the model has implemeted by theoretical basics of rheological models that are applied when describing vertical land displacements. The simulated rate of land subsidence of the study areas has been calculated based on lack of observation data. Because of limitation in availability of database, the calculation of land subsidence has been done using some average table values as there is a limitation of getting the materials from different depths beneath the surface to test their hydro-geological properties.

6.4 Conclusions

Land subsidence is a phenomenon which is the result of soil layer compaction associating groundwater table lowering. The three-factor rheology model was applied to simulation of land subsidence in correspondence to the GW decline in two areas of Mekong Delta, the urban area of Can Tho City and the coastal area of Soc Trang.
The model was calibrated to show the same decline slopes between calculated and observed land surface elevations for each area. The results of model simulation showed that the model can perform well to reproduce the land subsidence, though the observed data was very limited. Also, the simulation results as well as the observed data presented well the irreversibility of land subsidence.

From model simulation for CanTho City, the magnatude of land subsidence was well demonstrated as the combinEd action with groundwter drawdown and the land subsidence rate was estimated around 2.6 cm per year.

In land subsidence modeling for SocTrang, model simulations were carried out first for the period 1994-2014, and then for the future period 2015-2035 with different scenarios described in Chapter 5. From the model simulation, the cumulated land subsidence from 1994 to 2014 was estimated 65 cm, and if the current GW decline continues for the future, another 60 cm of land subsidence was expected over the next 21 years. In the serious scenario of combining increasing pumping and low recharge condition, model simulation predicted that significant land subsidence be at 71.4 cm in 2035. This is certainly no good news for the coastal areas in Mekong Delta where residents have been trying hard to cope with more frequent tidal floods.

However, the model is the first trying of land subsidence evaluation in Mekong Delta under limited data. Thus, some recommendations are required as flollowing:

(i) Because GW level declines and soil properties can influence land subsidence, it is important to monitor, testing, complie, and interpret them througout the entire Mekong Delta.

(ii) It is possible that water levels may not yet have declined below the preconsolidation head in areas where subsidence has not occurred. Subsidence can be simulated in the model only where inelastic storage is specified; inelastic storage was specified only for areas where measurements have shown that subsidence has occurred.

(iii) The one-dimensional indicated that the delayed flow of the soil layers is an important process in the occurrence of subsidence. Therefore, the model applied for this study may simulate subsidence before it actually occurs.

(iv) Owing to hydrodynamic lag and residual compaction and land subsidence. Additionally, the simulated subsidence is dependent on simulated drawdown in chapter 5. If simulated drawdown does not match actual drawdown, then simulated subsidence would not be expected to match measured subsidence.

(v) The subsidence monitoring needed to address recent and future subsidence issues as well as improve the accuracy of modeling.

Finally, it is expected that the simualtion and prediction of subsidence rates in two case studies be helpful for water and land resource managers, planners, regulators, and administrators to utilize, to manage, and to protect the Mekong Delta resource.

The irreversibility of land subsidence means the difficulty of recovery from the land subsidence that once has happened. Accordingly, countermeasures to cope with the land subsidence must be taken as soon as possible before the serious problems emerge.

CHAPTER 7. CONCLUSIONS AND RECOMMENDATIONS

7.1 Overall Conclusions

This study was designed for supporting the decision makers to formulate the strategies for sustainable GW utilization in Mekong Delta with the five objectives, such as: (i) Constructing the GW model for the entire Mekong Delta; (ii) Assessing the impacts of GW pumping in the typical urban area of Mekong Delta by detailed GW modeling; (iii) Assessing different GW management measures under the possible climate changes in the coastal Mekong Delta by detailed GW modeling; and (iv) Construction a land subsidence model to estimate the subsidence rate corresponding to the decline in GW levels in the two urban areas of the Mekong Delta.

As mentioned below, all of the four objectives were completed, and for overall, it can be concluded that basic GW models for the Mekong Delta were established as useful tools for assessing the current and future statuses of GW, and the approaches for sustainable GW utilization were also presented in this study.

As the results of analyses, it was made clear that the GW use in MD is in over-exploitation and some regulation or conservative measures for GW are required. However, because of the fresh water shortage and the salt intrusion in the Delta, the GW use in the Mekong Delta could not stop. By the modeling method, the study is the first attempt on GW model which has made alternative simulation results in visualized and easy ways to support the sustainable GW utilization/management in context of many impacts on the resource in the Mekong Delta.

For the first objective, the results and conclusions can be summarized as:

(1) The GW model for entire Mekong Delta is flexible to use/ start with a coarser model grid for generating high resolution model grids in any small/interested region

(2) In the model, the detailed structure of hydro-geology was built and hydraulic parameters, digital elevation map of Mekong Delta were processed.

(3) The calibrated model can be used for multi-grid scale for data input processing.

(4) An appropriate model which can provide initial & boundary condition in any interested case study within MD region

For the second objective regarding Can Tho City modeling, the results and conclusions can be summarized as:

(1) A GW models was successfully constructed and calibrated to analyze the impacts of pumping GW in Can Tho city.
(2) The simulation indentified the vulnerable areas of GW decline due to current pumping rate in Can Tho city.
(3) In the projected growing pumping, the simulation showed that the GW decline areas would be larger than current situation about 30%, and the maximum decline was predicted around 4 meters to 5 meters.
(4) Under current pumping, it was found that two cones of depression are forming in the city. It reflects that the extraction wells locations have been developing inappropriately in the city.

The third objective regarding GW modeling for the coastal area, the results and conclusions can be summarized as:

(1) A calibrated GW model for the 100-meter aquifer of a coastal area of the Mekong Delta was established and applied for the simulations of the GW flow with respect to possible changes in rainfall and GW management in the future.
(2) It was confirmed that the calibrated model could work properly to reproduce the distribution of the GW table and its response.
(3) To set up the management scenarios, the future rainfall conditions for the period from 2015 to 2035 were defined based on the downscaled output from the global climate model and modified by bias correction method;
(4) To obtain the sustainable GW management plan and gain a further understanding of the GW resources risks in the future, predicted GW situations and its responses relates to climatic conditions and the amount of pumpage were achieved by model application.

For the fourth objective regarding land subsidence modeling, a basic calibrated three factor model was conducted to estimate land subsidence due to decline in GW tables in an urban area and a coastal area, the results and conclusions can be summarized as:

In urban area of Mekong Delta:

(1) The land subsidence in CanTho city was found in average range of 2.6 cm per year

In coastal area of Mekong Delta:

(2) The cumulative subsidence was estimated of 65 cm (1994-2014), while the next 21 years showed 60 cm under the future rainfall condition(A1)

(3) In case of combining increasing pumping and low recharge condition, significant cumulative land subsidence would be 71.4 cm

(4) A three factor Rheology model was applied for land subsidence due to decline in GW tables in the two urban areas, and the model was proved to perform well.

7.2 Recommendations

The thesis deals with GW modeling. It must be emphasized that modeling in itself is not sufficient to address these challenges. Modeling only constitutes one, among several, sets of tools that can be used to support sustainable water resources management. Computer based hydrological models have been developed and applied at an ever increasing rate during the past four decades. The key reasons for that are: (i) improved models and methodologies are continuously emerging from the research community, and (ii) the demand for improved tools increases with the increasing pressure on water resources.

Although the GW flow models were successfully established and useful tool for examining aquifer response, there are still consisting aspects which should be considered in further studies:

- The analyses on these data indicate that the up-middle aquifer may not be a fully confined system and there may be some connectivity between the upper and lower aquifers. To clarify the details of the geo-structures to know the connectivity, detailed reliable drilling records should be required to enhance

the information of the aquifer system including the connectivity and its behavior.

- Another possible source of inaccuracies is related to such input data as estimates of pumping. It is is based on average values. The complete water pumping records for large capacity water wells are needed to allow any model to simulate field conditions of head and flow
- GW recharge rates in the Mekong Delta have been extensively studied using precipitation-runoff models and are relatively well known. However, local recharge rates should be improved by considering the variations in topography, vegetation, soil characteristics, and the extent of development of the land surface.
- Only a limited number of aquifer tests have been performed in the model area. It is needed that more pumping test should be implemented on the adjacent properties to measure the hydraulic conductivity of the GW zones.
- Monitored land subsidence data is limited for the subsidence model. Its observation should be improved in the areas where GW pumping is resulting in subsidence at levels causing damage.
- There are many water resources problems that require a more realistic linkage between surface water and GW. Understanding how surface water levels are related to adjacent aquifer systems is important for example, for the management of wetlands, rivers and canals in Mekong Delta. Whether a river flood at times of heavy rain or not will often impact on the surrounding GW levels. In this study, for these situations it is desirable to consider surface and GW as interconnected and to develop the modeling tools to describe their interactions. The holistic concept reflecting a close connection between surface water and groundwater is emphasized in the policy and management of groundwater resource development, protection and quality conservation.
- GW quality degradation owing to intensive pumping is reported in some studies. Recognition of the impact of intensive abstraction is nearly almost based on hydraulic phenomena. However, subtle changes in the GW chemical composition caused by pumping may often be observed before becoming

evident from GW level decline, especially salt intrusion of GW in coastal zones. Therefore, the first study step of this thesis on GW quality assessment was implemented in Vinh Chau, a coastal zone of Mekong Delta (see Appendix A). The further steps will be targeted on the specific GW quality problem caused by intensive pumping by modeling method. Most often, GW quality is affected by saltwater intrusion into coastal aquifers, by the downward and upward influx of poor water quality from superposed and underlying aquifers into exploited aquifers or by the discharge of polluted surface water into phreatic aquifers

ACKNOWLEDGMENTS

I would like to express my grateful thanks to my advisors Prof. GOTO Akira and Associate Prof. OSAWA Kazutoshi and Associate Prof. KATO Tasuku for their initiation for the outline of my research and continued support, with valuable comments and encouragement for the study.

I gratefully acknowledge all organizations and individuals who directly or indirectly supported me in my study. I am very grateful to FOLENs project for giving me the opportunity to participate in the valuable training. I greatly acknowledge Detares for proving me the software. I would like to extend my gratitude to the staffs and student of Department of Environmental Engineering, Faculty of Agriculture, and Utsunomiya University for their kind support during my stay in the Utsunomiya University.

My earnest thanks go to my beloved parent, my mother and father, and my brother for their continuing support and patience over the years. Without their unconditional love and understanding, none of this would have been possible.

Last but not least, I would like to extend my deepest appreciation to my beloved wife and my son and my daughter for their patience, encouragement and sacrifices to help me achieve my objectives.

REFERENCES

1. ADB: Asian Development Bank. (2013). Climate risks in the Mekong Delta, 5-24.
2. Anderson, M. P. and Woessner, W. W. (1992). Applied groundwater modelling, Academic Press, 20-256.
3. Alley, W. M., and Leak, S. A. (2004). The journey from safe yield to sustainability. Ground Water, Vol. 42, No.1, January-February, 12-16
4. Anderson, H. R. (1978). Hydrogeologic reconnaissance of the Mekong Delta in South Vietnam and Cambodia. USGS Water Supply Paper: 1608-R.
5. Atilla, J. (1998). Management of shared groundwater resources: the Israeli-Palestinian Case Booj
6. American Public Health Association (APHA). (1995). Standard Methods for the Examination for Water and Wastewater (19th edition). Byrd Prepess Springfield, Washington.
7. Berendrecht, W. L., Snepvangers, J. C. (2007). Methodology for Interactive Planning for Water Management. MODSIM 2007 International Congress on Modelling and Simulation. Modelling and Simulation Society of Australia and New Zealand. L. Oxley and D. Kulasiri: 74-80. ISBN: 978-970-9758400-9758404-9758407.
8. Boehmer, W. (2000). Ground Water Study Mekong Delta, Modelling report, HASKONING B. V. Consulting Engineers and Architects, in association with DWRPIS for the South of Vietnam and ARCADIS Euro consult, Royal Haskoning, 3-45.
9. Brown, J. (1996). Geochemical modeling of groundwater, vadose and geothermal system book.
10. Danh, V. T. (2008). Household Switching Behavior In The Use Of Groundwater in The Mekong Delta, Vietnam, Cantho University, School of Economics and Business Administration. Cantho city, Vietnam: Economy and Environment Program for Southeast Asia (EEPSEA).
11. DEVC: Department of Environment in Vinh Chau, Soc Trang province. (2011). Annual environment report, 25-104.

12. Devendra, D., Shriram D., and Atul K. (2014). Analysis of Ground Water Quality Parameters: A Review. Research Journal of Engineering Sciences. ISSN 2278 – 9472. Vol. 3(5), 26-31
13. DGMS. (2004). Research of geological structure and classification of N-Q sediments in Mekong Delta, Edited by Nguyen, H. D., DGMS [Division for Geological Mapping for the South of Vietnam].
14. Doneen, L. D. (1964). Notes on Water Quality in Agriculture, Department of Water Science and Engineering, University of California, Water Science and Engineering, p. 400
15. DONREs: Department of Natural Resources and Environment of SocTrang. (2012). Annual report of Natural Resource and Environment, 10-184 (in Vietnamese).
16. DWRPIS: Division for Water Resources Planning and Investigation for the South of Vietnam. (2009). Research of geological structure and classification of N-Q sediments in Mekong Delta, 24-86 (in Vietnamese)
17. DWRPIS: Division for Water Resources Planning and Investigation for the South of Vietnam. (2012). Report of groundwater use and protection planning until 2020 for SocTrang, 30-98 (in Vietnamese).
18. Eastham, J., Mpelasoka, F., Mainuddin, M., Ticehurst, C., Dyce, P. Hodgson, G., Ali, R., Kirby, M. (2008). Mekong River Basin Water Resources Assessment: Impacts of Climate Change. CSIRO: Water for a Healthy Country National Research Flagship
19. Engel, B., Storm, D., White, M., and Arnold, J. G. (2007). A hydrologic/water quality model application protocol, Journal of American Water Resources Association, (in press), 72-80.
20. Essink, O. (2000). Groundwater modeling. Utrecht University Press, the Netherland. 134 – 138.
21. Eugene, D. M. (1971). Use of groundwater in developing the Mekong Delta, Vietnam, Earth Science Research Corporation, 20-24.
22. Fujihara, Y., Hoshikawa, K., Fujii, H., Kotera, A., Nagano, T., and Yokoyama, S. (2015). Analysis and attribution of trends in wtare levels in the Vietnamese

Mekong Delta, Hydrological processes, Wiley online library, DOI:10.1002/hyp.10642.

23. Ghassemi, F, Brennan, D. (2000). 'Resource profile subproject: Summary Report.' An evaluation of the sustainability of the farming systems in the brackish water region of the Mekong Delta. ACIAR Project, Canberra.
24. Hamker, C. J. et al (1993). Distributed hydrological modeling
25. Hem, J. D. (1985). Study and interpretation of the chemical characteristics of natural water (3d ed.): U.S. Geological Survey, Water Supply Paper, 2254
26. Hix, G. L. (1995). Land subsidence and ground water withdrawal. Water Well J 49 : 37–39
27. IPPC. (2012). Managing the Risks of Extreme Events and Disasters to Advance Climate Change Adaptation. Cambridge, Cambridge University Press.
28. IUCN: International Union for Conservation of Nature. (2011) (accessed 2015.03.14): Groundwater in the Mekong Delta, Discussion paper, (online),<https//cmsdata.iucn.org/downloads/iucn_groundwater_in_mekong_delta_25_may_11_w.pdf>
29. Kakonen M. (2008). Mekong Delta at the Crossroads: More Control or Adaptation? Ambio 2008;37:205-12.
30. Korkmaz, N. (1988). The Estimation of groundwater recharge from water level and precipitation data, Journal of Islamic Academy of Sciences, 1(2), 67-93.
31. Koudstaal, R., Frank, R. R., Hubert, S. (1992). Water and sustainable development. A united nations sustainable development journal. ISSN:1477-8947, 277-290.
32. Lutz, A. (2007). Groundwater resource sustainability in West Africa, ProQuest information and Learning Company, UMI number 3275835.
33. McDonald, M.G., Harbaugh, A.W., Orr, B.R., and Ackerman, D.J. (1992). A method of converting no-flow cells to variable-head cells for the U.S. Geological Survey modular finite-difference ground-water flow model: U.S. Geological Survey Open-File Report 91-536, 99 p.
34. McKinney, D. C., Gates, G. B. and Lin, M. D. (1994): Groundwater Resource Management Models, In: Peters, A. et al. (Eds.), Computational Methods in Water

Resources, Kluwer Academic Publisher, 859-866.

35. MONRE: Ministry of Natural Resources and Environment. (2010): Report of climate change in the Mekong Delta, Vietnam, Vietnam-Netherlands Mekong Delta Master Plan project, 6-13.
36. MONRes: Ministry of Natural Resources and Environment. (2015). Groundwater quality standard of Vietnam (in Vietnamese).
37. MONRes: Ministry of Natural Resources and Environment. (2012). Climate change impacts and adaptation efforts in Vietnam (in Vietnamese).
38. Morita, N., Goto, A., Mizutani, M., Matsui, H. (2014). Modeling of land subsidence caused by excessive groundwater exploitation. Annual JISRDE conference proceeding, 1-2.
39. Minderhoud, P., Stouthamer, E., Erkens, G. (2016). Subsidence in Mekong Delta: Impacts of groundwater abstraction on delta subsidence. International conference proceeding: Rise and Fall, CanTho city, Vietnam, 14-45
40. Minnema, B., P. T. M. Vermeulen, et al. (2013). Utilization of Interactive MODeling (iMOD) to Facilitate Stakeholder Engagement in Model Development Using a Sustainable Approach with Fast, Flexible and Consistent Sub-Domain Modeling Techniques. MODFLOW AND MORE 2013: TRANSLATING SCIENCE INTO PRACTICE. Colorado, The United State of America.
41. Nam, N. D. G., GOTO, A., Trung, N. H. and Duy, T. T. (2013). Groundwater quality and its suitability for domestic and irrigation use in the coastal zone of Mekong Delta, annual CENREs conference proceeding, CanTho University, 67-76 (in Vietnamese).
42. Nakajama, H., Kaneko, H., and Tsuchida, M. (2010). The management of land subsidence and groundwater conservation in Tokyo. Journal of groundwater hydrology. J-STAGE. 2-6 (in Japanese).
43. Nhan D. K., Be, N. V., Trung N. H. (2008). Chapter 4: Water Use and Competition in the Mekong Delta, Vietnam.
44. Phuc, D. D. (2008). General on groundwater resources in Vietnam, ADB-TA-4903 VIE, Hanoi Water Sector Review, Department of Water Resources Management in Hanoi, 51-65.

45. Piani, C., Haerter, J. O., and Coppola, E. (2010). Statistical bias correction for daily precipitation in regional climate models over Europe, Theoretical and Applied Climatology, 99(1), 187-192, doi:10.1007/s00704-009-0134-9.
46. Phien-wej, N., Giao, P. H., and Nutalaya, P. (2006). Land subsidence in Bangkok, Thai Land. Engineering geology. Vol 82, 1-3.
47. Philip, S. J. et al. (2017). Geophysical research abstracts. Vol.19 EGU2017-12032. EGU general Assempby.
48. Povinec, P. P., Aggarwal, A., Aureli, W. C., Burnett, E. A., Kontar, K. M, Kulkarni, W. S, Moore, R., Rajar, M., Taniguchi, J.-F. Comanducci, G., Cusimano, H., Dulaiova, L., Gatto, M., Groening, S., Hausser, I., Levy-Palomo, B., Oregioni, Y. R, Ozorovich, A. M. G., Privitera, M. A., (2006). Characterisation of submarine groundwater discharge offshore south-eastern Sicily. Journal of Environmental Radioactivity 89(1), 81-101
49. Raju, N. J. (2007). Hydrogeochemical parameters for assessment of groundwater quality in the upper Gunjanaeru River basin, Cuddapah District, Andhara Pradesh, South India, Environmental Geology.
50. Rindahl, (1996). Geographic information systems in water resources engineering.
51. Sarath Prasanth S. V., Magesh, N. S., Jitheshlal, K. V., Chandrasekar, N., Gangadhar, K. (2012). Applied Water Science journal, 165–175.
52. Schiavo M. A., Havser, S., Gusimano, G., Gatto, L. (2006). Geochemical characterization of groundwater and submarine discharge in the south-eastern Sicily. Cont Shelf Res 26(7):826–834
53. Sophocleous, M. (2000). From safe yield to sustainable development of water resources - The Kansas experience. Journal of Hydrology, Volume 235, Issues 1-2, August, 27-43.
54. Spitz, K., Moreno, J. (1996). A practical guide to groundwater and solute transport modeling book.
55. Subramani, T., Elango, L., and Damodarasamy, S. R. (2005). Groundwater quality and its suitability for drinking and agricultural use in Chithar River Basin, Tamil Nadu, India. Environmental Geology.
56. Sun, (1994). The handbook of groundwater engineering.

57. Syvitski, J. P. M., Kettner, A. J., et al. (2009). Sinking deltas due to human activities - Progress article, Nature Geoscience, 681-686.
58. Thomas, N. and Harro, S. (2008). Challenges of the Groundwater Management in the CanTho city Vietnam, BGR-Symposium: Sanitation and Groundwater Protection, Conference proceeding , 110-172.
59. Tuan, L. A., Hoanh, C. T., Miller, F. and Sinh, B. T. (2007): Chapter 1: In: Be, T. T. et al. (Eds.), Flood and salinity management in the Mekong Delta, Vietnam, Challenges to sustainable development in the Mekong Delta: Regional and national policy issues and research needs, The Sustainable Mekong Research Network, 6-25.
60. UNICEF. (1996). Water and Sanitation Program YMW604.
61. USGS: United State Geological Survey. (1997). Modelling groundwater flow with MODFLOW and related programs, USGS Fact Sheet FS-121-97.
62. US Salinity Laboratory, Diagnosis and improvement of saline and alkali soils, Agricultural Handbook, USDA, No. 60, pp. 160, 1954
63. Vermeulen, P. T. M. (2006). Model-Reduced Inverse Modeling. Ph.D. thesis, Delft University of Technology - with ref. - with summary in Dutch. ISBN-10: 90-9020536-5. ISBN-13: 978-90-9020536-6.
64. Vermeulen, P. T. M., Linder, W. V. D. and Minnema, B. (2014). iMOD user manual version 2.6.50, Deltares, 3-19.
65. Vermeulen, P. T. M., Quan, N. H., Nam, N. D. G., Hung, P. V., Tung, N. T., Thanh, T. V. and Rien, D. (2013). Groundwater modelling for the Mekong Delta using iMOD, 20th International congress on modelling and simulation, Australia, 2499-2505.
66. Vien, D. V. (2009). Strongly degradation of groundwater in Mekong Delta, VOV online report (in Vietnamese).
67. Wagner, F., Bui T. V., et al. (2012). Chapter 7: Groundwater Resources in the Mekong Delta: Availability, Utilization and Risks. The Mekong Delta System: Interdisciplinary Analyses of a River Delta. F. G. Renaud and C. Kuenzer, Springer: 201 - 220.
68. WCED: The World Commission on Environment and Development (The

Brundtland Commission). (1987). Our Common Future. The United Nations, New York.

69. WHO. (2004). Guidelines for drinking water quality. World Health Organisation, Geneva.
70. WHO. (2008). Guidelines for drinking-water quality: incorporating first and second addenda, Recommendations, 3rd edition, WHO Press, v.1, 668p.
71. Yangxiao, Z., Wenpeng, L. (2011). A review of regional groundwater flow modeling. Geoscience frontiers, Vol 2, 205-214.

APPENDIX A: GROUNDWATER ASSESSMENT AND ITS SUSTAINABILITY IN THE COASTAL OF MEKONG DELTA

GROUNDWATER ASSESSMENT AND ITS SUSTAINABILITY IN THE COASTAL OF MEKONG DELTA

1 Case Study

The study area (Vinh Chau district) is located in the coastal zone of the Soc Trang province with the mean land surface elevation of about 1.0 m above mean sea level and the land use is mainly covered by agricultural production (Fig. A.1). This is a former salinity-controlled area where rice farming systems were dominated. From the year 2000 onwards, farmers protested against the protection of the salinity-controlled measures leading to a diversification of local land use (Kakonen, 2008). At the present, the impacts of salinity intrusion on surface water resource and freshwater shortage are increasingly serious (DONREs, 2012). Therefore, GW has been accessed as the water supply resource for domestic and agricultural productions (DWRPIS, 2012). In addition, the study area belongs to vulnerable zone of climate change impacts and sea level rise can cause increasing of salt intrusion (Nhan et al, 2008). Those issues have been recognized and concerned by local government and people

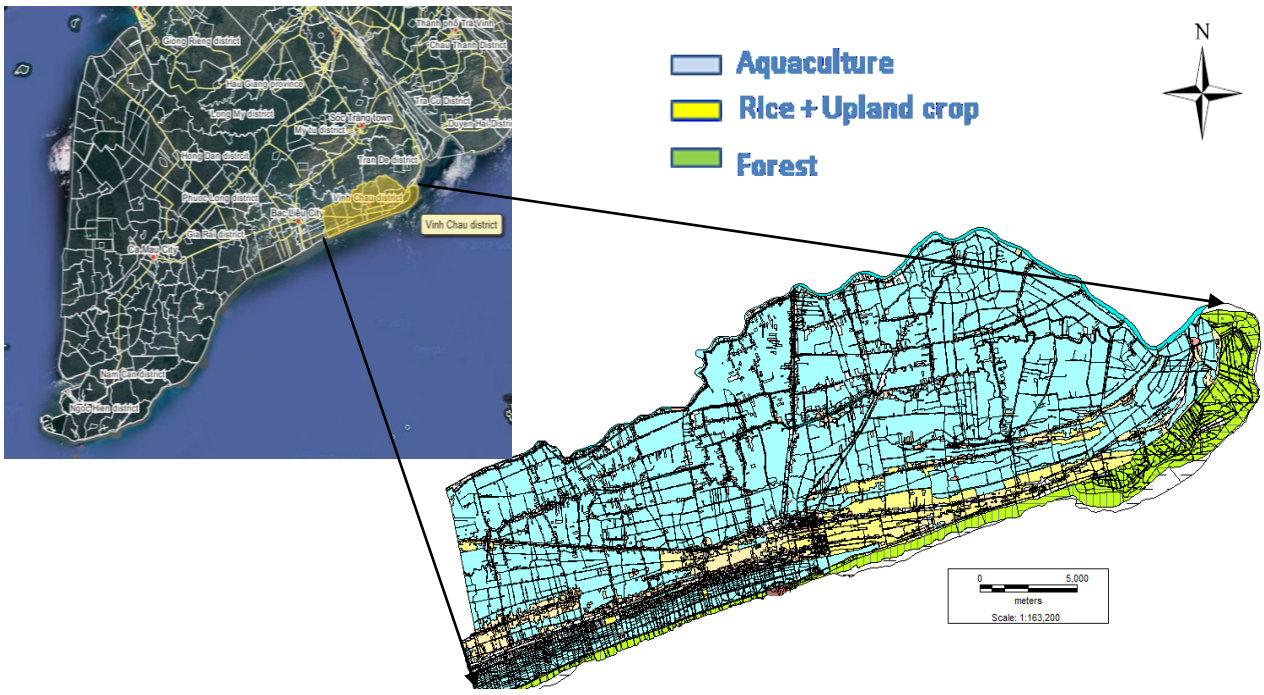

Fig. A-1 The study area at the coastal zone, Vinh Chau, Soc Trang, Vietnam

through environmental education programs (DONREs, 2012). However, due to lack of results of experiment and practical studies on environment in general and GW field in particular, local government has embarrassed to reach strategy plans for natural resources protection and management (DEVC, 2011).

2. Background

The GW has considered as an option of water use for domestic and irrigation in the MD, especially in coastal zone, is most vulnerable area due to water shortage, where the trend of GW use has increased strongly (DONREs, 2012). The quality of GW is equally important to its quantity owing to the suitability of water for various purposes (Schiavo et al, 2006). However, the aquifer is heavily polluted with microbial and inorganic pollutants and considered unfit for drinking water purposes (Danh et al, 2008). In addition, the concentration of natural contaminants and salt water intrusion cause the decline in GW quality and it may not meet for domestic water supply and the effective using for irrigation (IUCN, 2011). The major factors driving a decline in the quality of GW in the MD are a combination of: (i) Poor environmental practices in the delta contributing to surface and aquifer pollution; (ii) Over-exploitation inducing sea water intrusion, mixing and concentration of contaminants and (iii) Poor well construction that creates a direct pathway for inferior quality aquifer water and surface pollutants to mix with otherwise good quality aquifer (IUCN, 2011). GW used for domestic and irrigation purposes can vary greatly in quality depending upon type and quantity of dissolved salts (Sarath et al, 2012). The chemical quality of GW is related to the geological history of the aquifers and it could reveal important information on the suitability use for domestic and agricultural purposes (Povinec, 2006). Therefore, understanding the hydro-chemical characteristics is crucial for GW planning and management.

3. Objectives

This part focuses on:

- To point out the suitability of GW for domestic water supply

- To indentify and classify the irrigation suitability of the GW, six computed water quality parameters have been considered; such as Sodium Adsorption Ratio (SAR), Soluble Sodium Percentage (SSP), Permeability Index (P.I.), Sodium Percent (%Na), Residual Sodium Carbonate (RSC) and Magnesium Adsorption Ratio (MAR).

- To determine the hydro-chemical facies and GW type. It reveals that the GW samples falls under the sodium-potassium-chloride-sulfate category and there is a dominance of sodium type water.

4. Material and Method

4.1 Sample Collection

GW samples were collected from 10 wells for irrigation and 30 wells for domestic use ranging in depth between 90 – 120 m BGL representing the post monsoon season. The location of sampling points is shown in Fig. A.2. High-density polyethylene (HDPE) bottles were used for sample collection. The bottle was completely filled with water taking care that no air bubble was trapped within the water sample and it also was sealed with double plastic caps and precaution was taken to prevent evaporation and avoid sample agitation during transfer to the laboratory. Then, the samples were immediately transferred to the laboratory. During sample collection, standard procedures recommended by the American Public Health Association (APHA) were followed to ensure data quality and consistency.

4.2 Laboratory Measurements

Temperature, electrical conductivity, pH and DO were measured in-situ with the use of appropriate multi-parameter instruments at the same points of water sample collection. The labeled samples were analyzed in the laboratory for the major ionic concentrations (Ca, Mg, Na, K, HCO3, SO4, Cl, F) employing the APHA standard methods (APHA, 1995). Among the analyzed ions, sodium (Na) and potassium (K) were determined by flame photometer. Total hardness (TH) as CaCO3, calcium (Ca2+), magnesium (Mg2+), bicarbonate (HCO3-) and chloride (Cl) were analyzed by

volumetric methods and sulfates (SO42-) were estimated by using the colorimetric method.

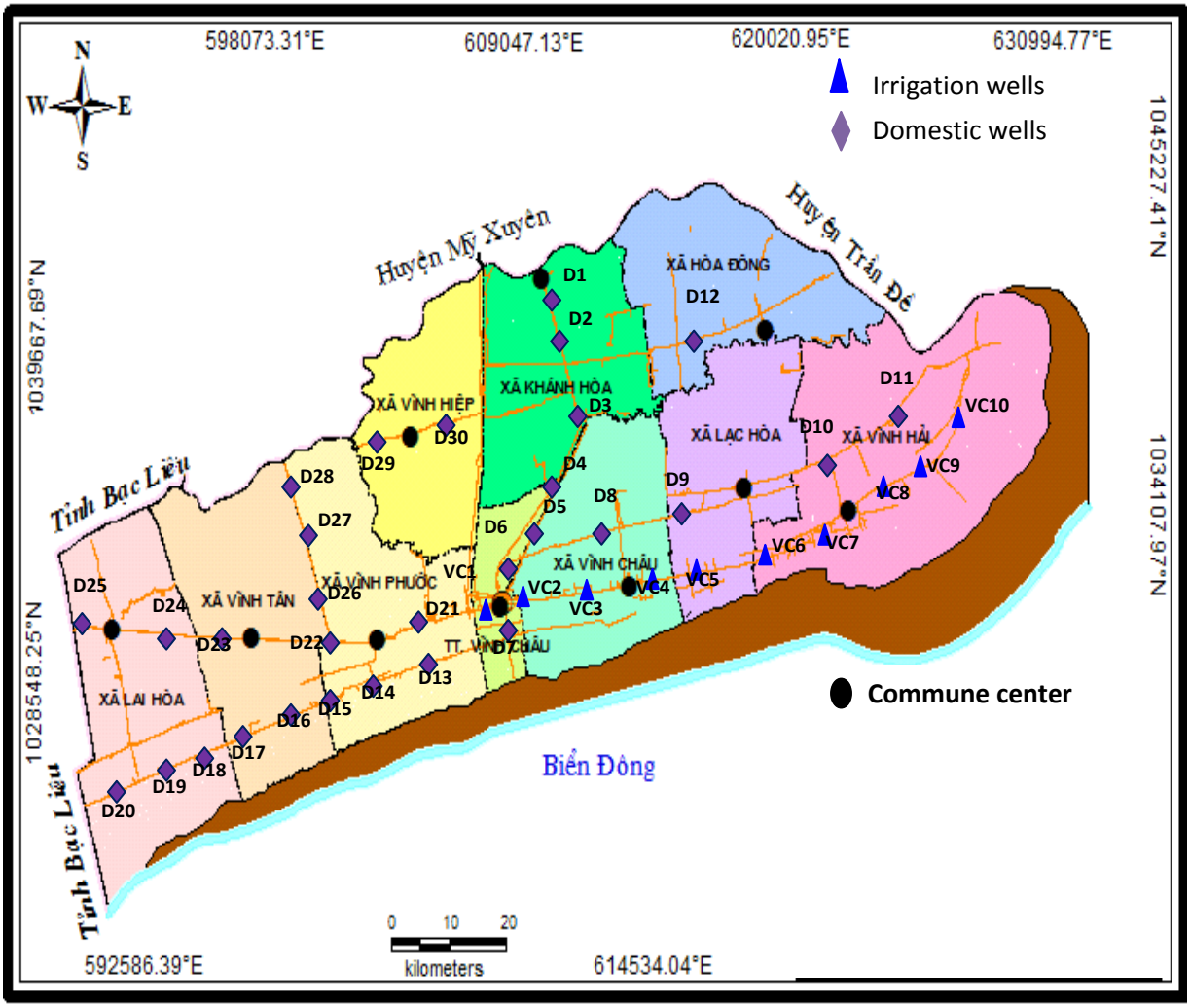

Fig. A-2 Administrative map of study area and sample locations

4.3 Classification Methods

The suitability of GW for agricultural purposes was evaluated by the parameters such as Sodium Adsorption Ratio (SAR), Soluble Sodium Percentage (SSP), Permeability Index (P.I.), Sodium Percent (%Na), Residual Sodium Carbonate (RSC) and Magnesium Adsorption Ratio (MAR). Further the results of the analysis were interpreted using graphical representations from United States Salinity Laboratory (USSL) and Wilcox diagram. To determine the suitability of domestic water supply, the comparing the values of different water quality parameter with those of the World Health Organization (WHO, 2004) and Vietnamese standard (QCVN09) (MONREs,

2015) was mentioned. Further the results of the analyses were represented using Piper diagram for showing the relationships between the different cations and anions to understand the hydrochemistry of GW.

5. Results and Discussion

5.1 Domestic Water Supply

The analytical results have been considered to determine the suitability of GW in the study area for domestic water supply. The chemical analysis results of GW samples have been presented in presented in the Table A1.

pH

pH of a solution is the negative logarithm of the hydrogen ion concentration. Acids have low pH values with anything lower than a 7 and alkaline solutions have high pH with anything above a 7. Value range of pH from 7 to 14 is alkaline, from 0 to 7 is cidic and 7 is neutral. Mainly drinking water pH lies from 4.4 to 8.5 (Devendra et al, 2014). The pH scale commonly ranges from 0 to 14. The pH of water provides vital information in many types of geochemical equilibrium or solubility calculations Hem et al, 1985). The pH values in the study area meet the standard value for drinking water is specified as 6.5–8.5 (WHO) (WHO, 2004) and 5.5-8.5 (QCVN09) (MONREs, 2015) . In the study area, the pH value of less than 7 was given (6.6-6.8) at the four sample points while the pH value of most of the GW samples is larger than 7 (7.1-8.4) (Table. A1), which clearly shows that the GW in the study area is slightly alkaline. Alkalinity of GW may be due to the presence of one or more of a number of ions. These include hydroxides, carbonates and bicarbonates. The phenomenon may be attributed to the salt intrusion which affects pH value. Alkalinity is formed by the salt of strong base and weak acid is dissolved in the water.

Sulfate

Natural water contains sulphate ions and most of these ions are also soluble in water. Sulfate is a combination of sulfur and oxygen and is a part of naturally occurring minerals in some soil and rock formations that contain GW. The mineral dissolves over time and is released into GW. The maximum contaminant level

Table A1 Chemical analysis results for domestic supply evaluation in the study area

Location No.	pH	COD	$SO4^{2-}$	Fe	Cl^-	$NO3^-$	T. Coliforms
	mg/L	mg/L	mg/L	mg/L	mg/L	mg/L	MPN/mL
D1	8.1	14	161.6	10.75	113	0	-
D2	7.1	5	163	2.02	204	0.0	-
D3	6.8	3	180	8.00	158	5.4	-
D4	7.1	13	163	0.71	161	0	-
D5	7.4	7	195	0.29	164	2.5	-
D7	7.6	5	190	0.95	220	1.4	-
D8	7.0	4	190	0.86	136	0	7
D9	7.3	3	183	0.07	132	1.5	-
D10	7.5	4	173	0.17	160	1.8	-
D11	6.7	3	173	1.16	137	0	-
D12	6.8	8	189	2.04	145	1.1	7
D13	8.1	4	163	0.30	124	1.4	-
D14	7.4	2	172	0.09	148	0.8	-
D15	7.3	3	234	0.20	123	0.1	-
D16	7.2	7	54	0.08	124	0.0	-
D17	6.6	4	57	29.60	170	0.0	-
D18	8.4	0	67	0.09	181	0.3	-
D19	7.5	2	78	0.17	338	0.8	4
D20	7.5	2	155	0.26	320	1.1	-
D21	7.7	9	75	0.01	210	0.4	-
D22	8.2	5	121	0.44	149	0.3	-
D23	8.3	5	189	0.34	480	3.2	-
D24	7.0	7	140	2.39	176	2.7	-
D25	7.6	8	110	0.61	210	0.0	-
D26	7.2	3	250	0.29	276	0.0	-
D27	7.6	0	168	0.49	363	0	-
D28	7.5	11	127	0.86	321	0.7	-
D29	8.0	3	75.6	0.01	340	1.7	-
D30	7.9	2	53	0.50	162	0.7	7

is 400 mg/L (WHO) and (QCVN 09) (WHO, 2004) and (MONREs, 2015). The sulfate concentration in the study area ranges between 53 and 250 mg/L (Table. A1), with an average value of 146.5 mg/L indicating that all samples fall within the desirable limit.

Nitrate

Nitrate is present in raw water and mainly it is a form of N2 compound (of its oxidizing state). Level of nitrates in GW in the study area ranges between 0.0 and 5.4 mg/L (Table. A1) implying that all samples are in the safe levels proposed by WHO (50 mg/L) and QCVN09 (15 mg/L) (WHO, 2004) and (MONREs, 2015).

Chloride

Chloride is a negative ion of the element chlorine (Cl) and is widely distributed in the environment. Chloride is found naturally in GW through the weathering and leaching of sedimentary rocks and soils and the dissolution of salt deposits. Chloride concentration in some wells of the study area is slightly high comparing with WHO and QCVN09 (250 mg/L) (WHO, 2004) and (MONREs, 2015) which may be affected by saltwater intrusion (Table. A1). The average chloride concentration was about the 205 mg/L, with a maximum of 480 mg/L and minimum of 113 mg/L.

Iron

Iron (Fe) is the metal that occurs naturally in soils, rocks and minerals. In the aquifer, GW comes in contact with these solid materials dissolving them, releasing their constituents, including Fe, to the water. Some samples at D1, D3 and D17 give the very high values. At concentrations approaching 0.2 mg/L Fe [13], the water use efficiency may become seriously impacted. However, most of sample points give the safety value comparing with WHO and QCVN09 (WHO, 2004) and (MONREs, 2015).

Chemical Oxygen Demand (COD)

COD is a measure of the oxygen required for the chemical oxidation of organic matter with the help of strong chemical oxidant. In the study area, the presence COD of most of GW samples indicates the organic contamination (Table. A1). It is clearly evident that the contamination generated from the surface is affecting the GW quality in the adjacent areas through percolation in the subsoil.

Total Coliform

Normally, the GW does not contain this contamination which is clearly shown by the analysis results in the study area. However, the Coliform was found in wells of D8, D12, D19 and D30 at very low concentrations. The presence of Coliform may indicate recent contamination of the GW by human sewage in the study area.

5.2 Irrigation Suitability

To assess the overall irrigational water quality of the samples collected, water quality parameters have been calculated and considered which are Sodium Adsorption Ratio (SAR), Soluble Sodium Percentage (SSP), Permeability Index (P.I.), Sodium Percent (%Na), Residual Sodium Carbonate (RSC) and Magnesium Adsorption Ratio (MA). In addition, electrical conductivity (EC) is a good measure of salinity hazard to crop and its relationship with water quality parameters also reflects the GW classification. Their corresponding values have been presented in Table A2.

Table A2 Values of calculated water quality parameters

Sample	SAR	SSP	RSC	PI	MA	%Na
VC1	24.41	63.97	-74.10	66.94	47.38	63.97
VC2	20.90	58.94	-85.50	61.74	52.74	58.94
VC3	25.91	59.80	-122.43	62.49	57.49	59.80
VC4	19.26	53.73	-109.85	56.72	50.14	53.73
VC5	22.47	61.98	-68.56	66.00	53.77	61.98
VC6	15.90	55.34	-53.08	61.09	35.07	55.34
VC7	29.67	66.90	-84.12	69.77	41.73	66.90
VC8	31.73	76.57	-35.75	79.25	43.92	76.57
VC9	27.77	62.74	-112.80	65.07	48.81	62.74
VC10	21.94	58.28	-100.71	60.92	51.24	58.28

Sodium Adsorption Ratio (SAR)

Sodium adsorption ratio is a measure of the sodicity of the soil determined through quantitative chemical analysis of water in contact with it. An excess of HCO3- and CO32- ions in water react with Na+ in soil, resulting in a sodium hazard (Subramani, 2005). SAR values are plotted against EC values (in µmhos/cm) over the U.S. Salinity diagram to categorize analyzed water samples according to their irrigational suitability quotient. The sodium adsorption ratio (SAR) was calculated using the following equation:

$$\mathbf{SAR = Na^{+} / ((Ca^{2+} + Mg^{2+})/2)^{0.5}}$$

Where, concentrations of all ions have been expressed in meq/L

In the study area, the SAR values range from 15.90 – 31.73. Based on the SAR values all samples have high sodium hazard and on plotting over the U.S. Salinity diagram (Fig. A.3), the 80% of GW samples fall in the C3-S4 and 20% of the samples fall C4-

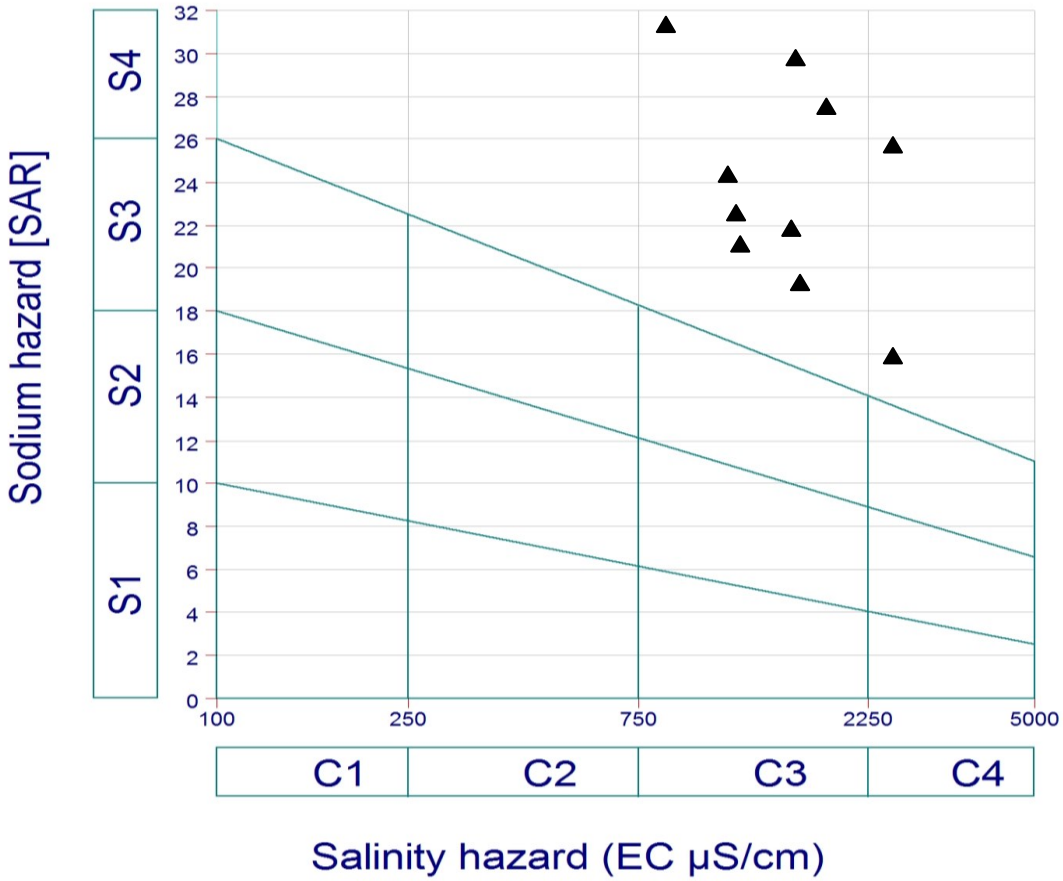

Fig. A-3 U.S.S Salinity Diagram, with respect to salinity hazard and sodium hazard in the study area

S4 category which means that very high sodium content and high salinity in GW. For irrigation purpose, salinity should be controlled and plants with good salt tolerance should be proposed in the study area.

Permeability index (PI)

Based on the permeability index (PI), a water suitability classification for irrigation water was developed (Doneen, 1964). The PI was calculated by the following equation:

$$\mathbf{PI = (Na^{+} + (HCO_3^{-})^{0.5})x\ 100/\ (Na^{+} + Ca^{2+} + Mg^{2+})}$$

where all the ions are expressed in meq/l

The PI values vary from 56.72 to 79.25, with the average value of about 65.00. A classification based on PI was recommended by WHO for assessing suitability of irrigation (WHO, 2008). This reveals that all samples belong to class 2 which PI ranged between 25 and 75%.

Sodium percent (%Na)

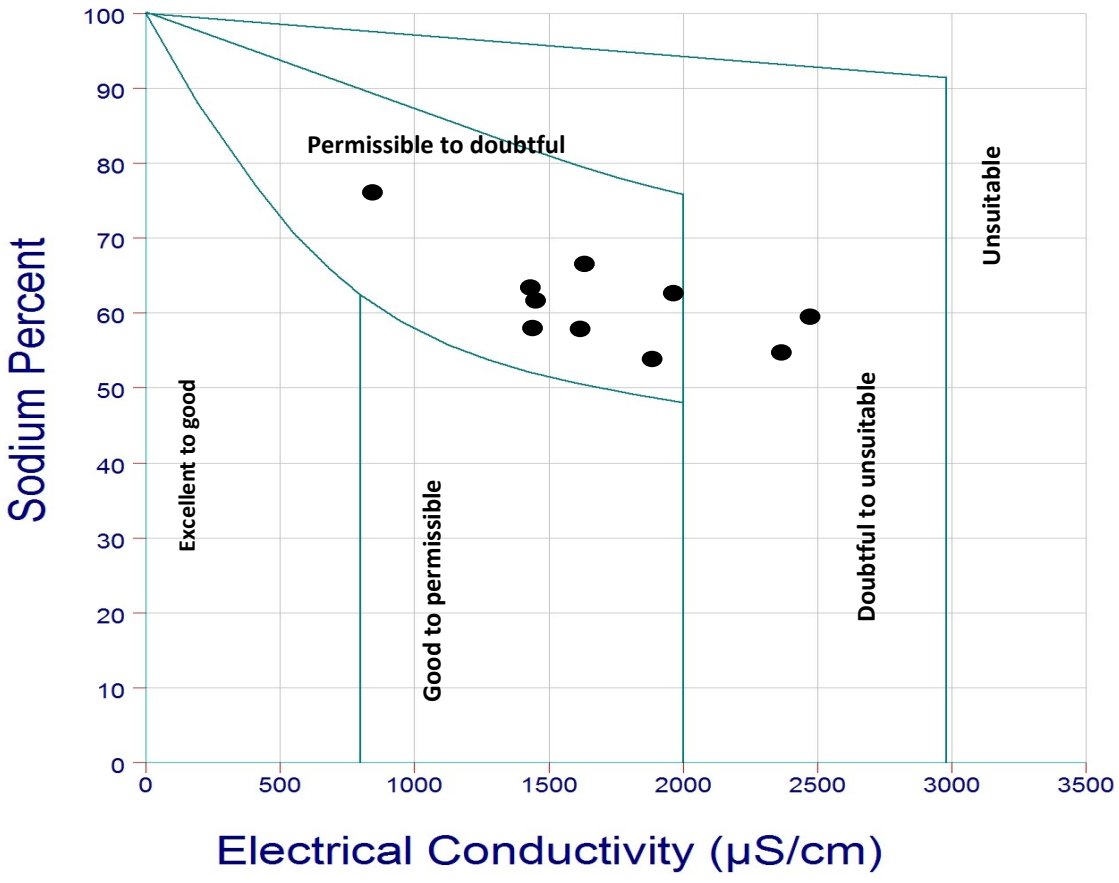

Fig. A-4 Wilcox Diagram for water quality classification

The concentration of sodium in the GW samples collected vary from 53.73 to 76.57 mg/L (Table 7.2). For rating irrigation waters, the Wilcox diagram was used, in which the %Na is plotted against EC (Fig. A.4)

shows the diagram plot which indicates that 80 % of the GW samples fall in the "Permissible to doubtful" and 20% of the samples fall in the "Doubtful to unsuitable". The source of Na+ into the GW has been attributed to the weathering of feldspar and due to over exploitation of GW.

Soluble Sodium Percentage (SSP)

SSP values should be preferably less than 60% to be rendered suitable for irrigational purposes and hence in the present study where SSP values range between 53.73 and 76.57 and 50% of the water samples have SSP < 60 %. However, 50% of water sample exceed the "permissible" level [20] (Table A3).

Table A3 Classification based on SSP value (USSL)

SSP (%)	Class	Percentage of samples
<20	Excellent	0
20-40	Good	0
40-60	Permissible	50
60-80	Doubtful	50
>80	Unsuitable	0

Residual Sodium Carbonate (RSC)

The residual sodium carbonate index of water signifies the alkalinity hazard posed by it and it finds the suitability of water for irrigation in case of clay soils [21]. The RSC values range from -122.43 to – 35.75. Based on the USSL's classification level (USSL, 2015), the Table A.4 indicates that 100 % of water samples are suitable level.

Table A4 Classification based on RSC value (USSL)

RSC	Condition	Percentage of samples
< 1.25	Suitable	100%
1.25-2.5	Marginal	0
>2.5	Not Suitable	0

Magnesium hazard

MAR categorizes water into two broad classes – water having MAR < 50 is considered suitable for irrigation whereas water with MAR > 50 is considered high magnesium hazard value has an adverse affect on the crop yield, based on which it can be revealed that 50% of GW samples is in safe level and a half of samples is unsuitable for irrigation (Table A1).

5.3. Hydro-chemical Facies

The proposed diagram is a modification of Piper diagram with a view to extend its applicability in representing water analysis in the possible simplest way. A Piper diagram is a graphical representation classifying water based on the dominant presence of cations and anions and has widespread use to assess the water type. The

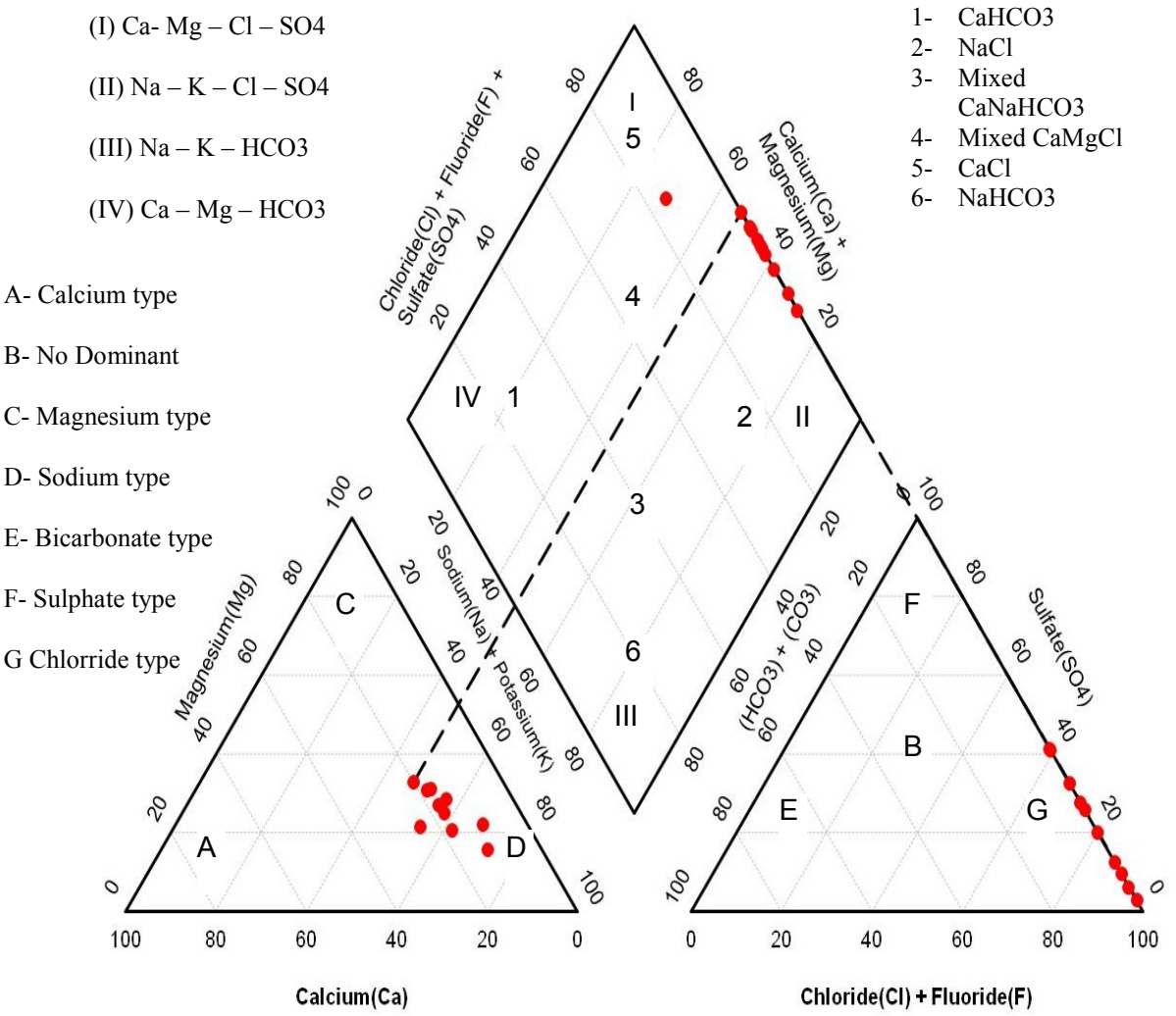

Fig.A5 Piper diagram represents the hydro-chemical facies of groundwater in the study area

results were plotted on the proposed diagram to test its applicability for geochemical classification of GW and hydro-chemical facies. The values obtained the GW type in the study area, and their plot on the Piper's diagrams reveal that the major GW type is Na – K – Cl – SO4 and sodium (Fig. A.5).

6. Conclusions

The study related to GW quality, the results and conclusions can be summarized as:

(1) The suitability GW use for domestic supply and irrigation in term of GW quality was assessed in the coastal zone of Mekong Delta.

(2) The analyzed chemicals results showed that the suitability for domestic supply is rather good to medium and chemical contents were found to be safe and suitable for drinking purposes.

(3) According to six computed GW quality indicators: Sodium Adsorption Ratio (SAR), Soluble Sodium Percentage (SSP), Permeability Index (P.I.), Sodium Percent (%Na), Residual Sodium Carbonate (RSC) and Magnesium Adsorption Ratio (MAR), the GW quality has been found to be suitable to permissible for irrigation. However, it was found in the most of testing locations is unsuitable for irrigation in term of sodium and salinity hazards analyzing.

(4) For finding the hydro-chemical facies of GW, it revealed that the GW samples falls under the sodium-potassium-chloride-sulfate category and there is a dominance of sodium type water

APPENDIX B: COMPUTER PROGRAM OF THE MONITORING DATA INPUT

```
! Last change:  PTM   9 Mar 2013    2:29 pm
PROGRAM OBSWELLS
IMPLICIT NONE
INTEGER :: I,J,K,ID,IM,IY,IL,ILABEL,IOS
INTEGER,DIMENSION(2) :: NLABEL,NDATES
CHARACTER(LEN=256),DIMENSION(:),ALLOCATABLE :: CDATE,LABEL,CLABEL
CHARACTER(LEN=256),DIMENSION(:,:),ALLOCATABLE :: RECORD
CHARACTER(LEN=256),DIMENSION(2) :: FNAME
CHARACTER(LEN=256) :: LINE
CHARACTER(LEN=2000) :: STRINGBIG
REAL,DIMENSION(:,:),ALLOCATABLE :: X
LOGICAL :: LREADLINE
CHARACTER(LEN=10) :: ITOS
CHARACTER(LEN=15) :: RTOS
CHARACTER(LEN=256) :: CAP

WRITE(*,'(1X,A$)') 'Give *.CSV file ?'
READ(*,'(A)') FNAME(1)
!FNAME(1)='Cap_HungTTSX_2011_adj.csv'
WRITE(*,'(1X,A$)') 'Give *.DAT file ?'
READ(*,'(A)') FNAME(2)
!FNAME(2)='Observationwell(test).dat'

OPEN(10,FILE=FNAME(1),STATUS='OLD',IOSTAT=IOS)
IF(IOS.NE.0)THEN
 WRITE(*,'(1X,A)') 'Can not open file for reading:'
 WRITE(*,'(1X,A)') TRIM(FNAME(1))
 STOP
ENDIF
OPEN(11,FILE=FNAME(2),STATUS='OLD',IOSTAT=IOS)
IF(IOS.NE.0)THEN
 WRITE(*,'(1X,A)') 'Can not open file for reading:'
 WRITE(*,'(1X,A)') TRIM(FNAME(2))
 STOP
ENDIF
```

```
!## ----------------------
!## find number of label in the file (columns: first is date m\dd\yyyy)
!## ----------------------
DO K=1,2
 IF(.NOT.LREADLINE(9+K,STRINGBIG))EXIT
 NLABEL(K)=0
 J=1
 DO
  I=INDEX(STRINGBIG(J:),',')
  IF(I.EQ.0)EXIT
  NLABEL(K)=NLABEL(K)+1
  J=J+I+1
 ENDDO
 WRITE(*,*) '('//TRIM(FNAME(K))//') Number of columns=',NLABEL(K)
ENDDO

!## ----------------------
!## find number of dates in the file (rows)
!## ----------------------
DO K=1,2
 NDATES(K)=0
 DO
  IF(.NOT.LREADLINE(9+K,STRINGBIG))EXIT
  NDATES(K)=NDATES(K)+1
 ENDDO
 WRITE(*,*) '('//TRIM(FNAME(K))//') Number of rows=',NDATES(K)
ENDDO

!PAUSE
!## allocate memory
IF(ALLOCATED(CDATE))DEALLOCATE(CDATE); ALLOCATE(CDATE(NDATES(1)))
IF(ALLOCATED(X))DEALLOCATE(X); ALLOCATE(X(NLABEL(1),NDATES(1)))
IF(ALLOCATED(LABEL))DEALLOCATE(LABEL); ALLOCATE(LABEL(NLABEL(1)))
IF(ALLOCATED(CLABEL))DEALLOCATE(CLABEL);
ALLOCATE(CLABEL(NLABEL(2)))
```

```
IF(ALLOCATED(RECORD))DEALLOCATE(RECORD);
ALLOCATE(RECORD(NLABEL(2),NDATES(2)))

!## ----------------------
!## restart reading the file but now put everything into memory
!## ----------------------

REWIND(10)

IF(.NOT.LREADLINE(10,STRINGBIG))STOP 'end of file'
READ(STRINGBIG,*) CDATE(1),(LABEL(J),J=1,NLABEL(1))

!## write labels found:
WRITE(*,'(1X,A)') TRIM(CDATE(1))
DO I=1,NLABEL(1); LINE=TRIM(ITOS(I))//': '//TRIM(LABEL(I)); WRITE(*,'(1X,A)')
TRIM(LINE); END DO

DO I=1,NDATES(1)
 IF(.NOT.LREADLINE(10,STRINGBIG))EXIT
 J=LEN_TRIM(STRINGBIG)

 IF(STRINGBIG(J:J).EQ.',')THEN
  READ(STRINGBIG,*) CDATE(I),(X(J,I),J=1,NLABEL(1)-1)
  X(J,I)=-999.99
 ELSE
  READ(STRINGBIG,*) CDATE(I),(X(J,I),J=1,NLABEL(1))
 ENDIF

 J=INDEX(CDATE(I),'\')-1
 READ(CDATE(I)(:J),*) IM
 K=INDEX(CDATE(I),'\',.TRUE.)+1
 READ(CDATE(I)(K:),*) IY
 READ(CDATE(I)(J+2:K-2),*) ID
 WRITE(CDATE(I),'(I4,2I2.2)') IY,IM,ID
END DO

!WRITE(*,*) (TRIM(LABEL(J)),J=1,NLABEL(1))
```

```
!DO I=1,NDATES(1)
! WRITE(*,*) I,','//TRIM(CDATE(I)),(X(J,I),J=1,NLABEL(1))
!ENDDO

REWIND(11)

IF(.NOT.LREADLINE(11,STRINGBIG))STOP 'end of file'
READ(STRINGBIG,*) (CLABEL(J),J=1,NLABEL(2))

DO I=1,NDATES(2)
 IF(.NOT.LREADLINE(11,STRINGBIG))EXIT
 J=LEN_TRIM(STRINGBIG)
 WRITE(*,*) TRIM(STRINGBIG),J
 IF(STRINGBIG(J:J).EQ.',')THEN
  READ(STRINGBIG,*) (RECORD(J,I),J=1,NLABEL(2)-1)
  RECORD(J,I)=''
 ELSE
  READ(STRINGBIG,*) (RECORD(J,I),J=1,NLABEL(2))
 ENDIF

END DO

!DO I=1,NDATES(2)
! WRITE(*,*) I,(TRIM(RECORD(J,I)),J=1,NLABEL(2))
!ENDDO

CLOSE(10)
CLOSE(11)

!# ================
!## write ipf
!# ================

!## column for label
ILABEL=3

OPEN(10,FILE='obs.ipf',STATUS='UNKNOWN')
```

```
WRITE(10,*) NDATES(2)
WRITE(10,*) 5
WRITE(10,'(A)') 'X'
WRITE(10,'(A)') 'Y'
WRITE(10,'(A)') 'ID'
WRITE(10,'(A)') 'Z1'
WRITE(10,'(A)') 'Z2'
WRITE(10,'(A)') '3,txt'
DO I=1,NDATES(2)
 WRITE(10,'(99A)') (TRIM(RECORD(J,I))//',',J=1,NLABEL(2))
 OPEN(11,FILE=TRIM(RECORD(ILABEL,I))//'.txt',STATUS='UNKNOWN')
 !## find correct label
 DO IL=1,NLABEL(1)
  IF(TRIM(CAP(LABEL(IL),'U')).EQ.TRIM(CAP(RECORD(ILABEL,I),'U')))EXIT
 ENDDO

 IF(IL.LE.NLABEL(1))THEN
  WRITE(*,*) 'Writing label: '//TRIM(LABEL(IL))
  WRITE(11,*) NDATES(1)
  WRITE(11,*) '2,1'
  WRITE(11,*) 'DATES,-999.99'
  WRITE(11,*) 'HEADS,-999.99'
  DO J=1,NDATES(1)
   WRITE(11,'(A,F10.2)') TRIM(CDATE(J))//',',X(IL,J)
  END DO
  CLOSE(11)
 ELSE
  WRITE(*,*) ' Can not find label: '//TRIM(RECORD(ILABEL,I))
 ENDIF
END DO
CLOSE(10)

STOP
END PROGRAM

!###=============================================================
=======
```

```
LOGICAL FUNCTION LREADLINE(IU,STRING)
!###================================================================
=======
IMPLICIT NONE
INTEGER,INTENT(IN) :: IU
CHARACTER(LEN=*),INTENT(OUT) :: STRING
INTEGER :: IOS

LREADLINE=.FALSE.

DO
 READ(IU,'(A)',IOSTAT=IOS) STRING
 IF(IOS.NE.0)RETURN
 !## no comment read, process line
 IF(STRING(1:1).NE.'#')EXIT
ENDDO

LREADLINE=.TRUE.

END FUNCTION LREADLINE

!###================================================================
=======
FUNCTION ITOS(I)
!###================================================================
=======
IMPLICIT NONE
INTEGER,INTENT(IN) :: I
CHARACTER(LEN=10)  :: TXT,ITOS

WRITE(TXT,'(I10)') I
TXT=ADJUSTL(TXT)
ITOS=TXT

END FUNCTION ITOS
```

```
!###=====================================================================
=======
FUNCTION RTOS(X,F,NDEC)
!###=====================================================================
=======
IMPLICIT NONE
INTEGER,INTENT(IN) :: NDEC
REAL,INTENT(IN) :: X
CHARACTER(LEN=1),INTENT(IN) :: F
CHARACTER(LEN=15) :: TXT,FRM,RTOS
INTEGER :: IOS

IF(F.EQ.'*')THEN
 WRITE(TXT,*,IOSTAT=IOS) X
ELSE
 WRITE(FRM,'(2A1,I2.2,A1,I2.2,A1)') '(',F,LEN(RTOS),'.',NDEC,')'
 WRITE(TXT,FRM,IOSTAT=IOS) X
ENDIF
IF(IOS.NE.0)TXT='error'
TXT=ADJUSTL(TXT)
RTOS=TXT

END FUNCTION RTOS

!###=====================================================================
=======
FUNCTION CAP(STR,TXT)
!###=====================================================================
=======
IMPLICIT NONE
CHARACTER(LEN=*),INTENT(IN) :: TXT,STR
INTEGER :: I,J,K,B1,B2
CHARACTER(LEN=256) :: CAP

IF(TXT.EQ.'l'.OR.TXT.EQ.'L')THEN
 B1= 65
 B2= 90
```

```
 K = 32
ELSEIF(TXT.EQ.'u'.OR.TXT.EQ.'U')THEN
 B1= 97
 B2= 122
 K =-32
ENDIF

CAP="
DO I=1,LEN_TRIM(STR)
 J=IACHAR(STR(I:I))
 IF(J.GE.B1.AND.J.LE.B2)J=J+K
 CAP(I:I)=ACHAR(J)
END DO

END FUNCTION CAP
```

APPENDIX C: COMPUTER PROGRAM OF COMBINED WELLS PACKAGES AND BOREHOLE DATA

```
!     Last change:  PTM   11 May 2014    2:32 pm
PROGRAM BOREHOLE2IPF
IMPLICIT NONE
INTEGER :: I,J,NZ,IL,NL,ILAY,IOS
CHARACTER(LEN=256),DIMENSION(2) :: FNAME
CHARACTER(LEN=256) :: LINE
CHARACTER(LEN=2000) :: STRINGBIG
TYPE BOREHOLE
 CHARACTER(LEN=50) :: SYMBOL,LOCATION
 REAL :: XCRD,YCRD,FINALDEPTH
 REAL,POINTER,DIMENSION(:) :: Z
END TYPE BOREHOLE
TYPE(BOREHOLE) :: BORE
LOGICAL :: LREADLINE
CHARACTER(LEN=10) :: ITOS
CHARACTER(LEN=15) :: RTOS
INTEGER,PARAMETER :: IUIN=10,IUOUT=20,IUTXT=30

!## write information to the screen, how to use program
WRITE(*,'(/1X,A/)') 'Borehole2IPF-conversion program'
WRITE(*,'(1X,A)') 'Syntax file:'
WRITE(*,'(1X,A)')  '============'
WRITE(*,'(/1X,A)') 'use # to identify comment'
WRITE(*,'(1X,A)') 'x,y,symbol,location,finaldepth,top1,bot1,...,topn,botn'
WRITE(*,'(/1X,A/)') 'Example:'
WRITE(*,'(1X,A)') '#x,y,symbol,location,finaldepth,top1,bot1,top2,bot2'
WRITE(*,'(1X,A)') '100.0,100.0,"Hq-32","Prov Inda",-132,10.03,4.22,-54.0,-105.2'
WRITE(*,'(1X,A/)') '....'

WRITE(*,'(/1X,A/)') 'Give filename with borehole information'
READ(*,'(A)') FNAME(1)

!## get position in string where the point is, search backwards (.true.)
I=INDEX(FNAME(1),'.',.TRUE.)
J=INDEX(FNAME(1),'\',.TRUE.)+1
!J=MAX(1,J)
!## output name is input with ipf extension
```

```
FNAME(2)=FNAME(1)(J:I)//'ipf'

!## open file for reading
OPEN(IUIN ,FILE=FNAME(1),STATUS='OLD',ACTION='READ',IOSTAT=IOS)
IF(IOS.NE.0)THEN
 WRITE(*,'(1X,A)') 'Can not open file for reading:'
 WRITE(*,'(1X,A)') TRIM(FNAME(1))
 STOP
ENDIF

!## open file for writing
OPEN(IUOUT,FILE=FNAME(2),STATUS='UNKNOWN',ACTION='WRITE',IOSTAT=IO
S)
IF(IOS.NE.0)THEN
 WRITE(*,'(1X,A)') 'Can not open file for writing:'
 WRITE(*,'(1X,A)') TRIM(FNAME(2))
 STOP
ENDIF

!## find number of lines that are no comment
NL=0
DO
 IF(.NOT.LREADLINE(IUIN,STRINGBIG))EXIT
 NL=NL+1
ENDDO

WRITE(*,*) 'Number of Boreholes=',NL

!## write header of ipf-file
STRINGBIG=TRIM(ITOS(NL))
WRITE(IUOUT,*) TRIM(STRINGBIG)
WRITE(IUOUT,*) '5'
WRITE(IUOUT,*) 'X'
WRITE(IUOUT,*) 'Y'
WRITE(IUOUT,*) 'Symbol'
WRITE(IUOUT,*) 'Location'
WRITE(IUOUT,*) 'FinalDepth'
```

```
WRITE(IUOUT,*) '3,txt'

!## rewind file, start reading on first line
REWIND(IUIN)

DO IL=1,NL
 !## find number of label in the file
 IF(.NOT.LREADLINE(IUIN,STRINGBIG))STOP 'error reading file'

 NZ=1
 J =1
 DO
  !## try ',' first
  I=INDEX(STRINGBIG(J:),',')
  IF(I.EQ.0)EXIT
  NZ=NZ+1
  J =J+I+1
 ENDDO
 !## reduce nz for 5 fixed columns
 NZ=NZ-5
 !## associate memory for borehole
 IF(ASSOCIATED(BORE%Z))THEN
  IF(SIZE(BORE%Z).LE.NZ)THEN
   DEALLOCATE(BORE%Z)
   ALLOCATE(BORE%Z(NZ))
  ENDIF
 ELSE
  ALLOCATE(BORE%Z(NZ))
 ENDIF

 LINE='Number of DepthIntervals for borehole '//TRIM(ITOS(IL))//' is '//TRIM(ITOS(NZ))
 WRITE(*,*) TRIM(LINE)

 !## read borehole information from file
 READ(STRINGBIG,*,IOSTAT=IOS)
BORE%XCRD,BORE%YCRD,BORE%SYMBOL,BORE%LOCATION,BORE%FINALDE
PTH,(BORE%Z(I),I=1,NZ)
```

```
 IF(IOS.NE.0)THEN
  WRITE(*,'(1X,A,I10)') 'Error reading line ',IL
  WRITE(*,'(1X,A)') TRIM(STRINGBIG)
  STOP
 ENDIF

 !## write current borehole in ipf-file
 LINE=TRIM(RTOS(BORE%XCRD,'*',0))//','// &
     TRIM(RTOS(BORE%YCRD,'*',0))//','// &
     '"'//TRIM(BORE%SYMBOL)         //'",'// &
     '"'//TRIM(BORE%LOCATION)       //'",'// &
     TRIM(RTOS(BORE%FINALDEPTH,'*',0))

 WRITE(IUOUT,'(A)') TRIM(LINE)

 !## write associated file (*.txt)

OPEN(IUTXT,FILE=TRIM(BORE%SYMBOL)//'.txt',STATUS='UNKNOWN',ACTION='
WRITE')
 LINE=TRIM(ITOS(NZ))
 WRITE(IUTXT,*) TRIM(LINE)
 WRITE(IUTXT,*) '2,2'
 WRITE(IUTXT,*) '"Depth (m+MSL)",-999.99'
 WRITE(IUTXT,*) '"Lithology",-999.99'
 ILAY=0
 DO J=1,NZ
  ILAY=ILAY+MOD(J,2)
  IF(MOD(J,2).EQ.0)LINE=TRIM(RTOS(BORE%Z(J),'*',0))//',AQT'//TRIM(ITOS(ILAY))
  IF(MOD(J,2).NE.0)LINE=TRIM(RTOS(BORE%Z(J),'*',0))//',AQF'//TRIM(ITOS(ILAY))
  WRITE(IUTXT,*) TRIM(LINE)
 END DO
 CLOSE(IUTXT)

END DO

CLOSE(IUIN)
CLOSE(IUOUT)
```

```
STOP
END PROGRAM BOREHOLE2IPF

!###================================================================
=======
LOGICAL FUNCTION LREADLINE(IU,STRING)
!###================================================================
=======
IMPLICIT NONE
INTEGER,INTENT(IN) :: IU
CHARACTER(LEN=*),INTENT(OUT) :: STRING
INTEGER :: IOS

LREADLINE=.FALSE.

DO
 READ(IU,'(A)',IOSTAT=IOS) STRING
 IF(IOS.NE.0)RETURN
 !## no comment read, process line
 IF(STRING(1:1).NE.'#')EXIT
ENDDO

LREADLINE=.TRUE.

END FUNCTION LREADLINE

!###================================================================
=======
FUNCTION ITOS(I)
!###================================================================
=======
IMPLICIT NONE
INTEGER,INTENT(IN) :: I
CHARACTER(LEN=10)  :: TXT,ITOS

WRITE(TXT,'(I10)') I
```

```
TXT=ADJUSTL(TXT)
ITOS=TXT

END FUNCTION ITOS

!###=================================================================
=======
FUNCTION RTOS(X,F,NDEC)
!###=================================================================
=======
IMPLICIT NONE
INTEGER,INTENT(IN) :: NDEC
REAL,INTENT(IN) :: X
CHARACTER(LEN=1),INTENT(IN) :: F
CHARACTER(LEN=15) :: TXT,FRM,RTOS
INTEGER :: IOS

IF(F.EQ.'*')THEN
 WRITE(TXT,*,IOSTAT=IOS) X
ELSE
 WRITE(FRM,'(2A1,I2.2,A1,I2.2,A1)') '(',F,LEN(RTOS),'.',NDEC,')'
 WRITE(TXT,FRM,IOSTAT=IOS) X
ENDIF
IF(IOS.NE.0)TXT='error'
TXT=ADJUSTL(TXT)
RTOS=TXT

END FUNCTION RTOS

!###=================================================================
=====
FUNCTION SUBST(FNAME,SUB1,SUB2)
!###=================================================================
=====
IMPLICIT NONE
CHARACTER(LEN=*),INTENT(IN) :: SUB1,SUB2
CHARACTER(LEN=*),INTENT(IN) :: FNAME
```

```
INTEGER :: I,J
CHARACTER(LEN=256) :: SUBST

SUBST=FNAME

I=INDEX(FNAME,SUB1)
IF(I.EQ.0)RETURN
I=I-1
J=I+LEN_TRIM(SUB1)+1

SUBST=FNAME(:I)//TRIM(SUB2)//FNAME(J:)

END FUNCTION SUBST
```

APPENDIX D: APPLIED COMPUTER PROGRAM FOR LAND SUBSIDENCE MODEL

```
Sub JIBANN()
Dim M As Double Dim lv0 As
Dim k1 As Double  Dim c1 As Double  1
Dim c2 As Double  ,Q
Dim t As Double
Dim f(520) As Double  "“y^³

Dim lv(520) As Double Dim ld(520) As Double  Dim l(520) As Double
Dim n_day As Integer
Dim i As Integer



M = 0#
lv0 = 0#
ld0 = 530

k1 = Cells(1, 6).Value

c1 = Cells(2, 6).Value
c2 = Cells(3, 6).Value
t = Cells(4, 6).Value

n_day = 504

For j = 1 To n_day
 f(j) = Cells(7 + (j - 1), 3).Value
Next j

Sheet1.Activate

For i = 1 To n_day

 If i = 1 Then
   lv(i) = lv0
   ld(i) = ld0
```

```
Else

  lv(i) = lv(i - 1) + t * (k1 * (M - lv(i - 1)) - f(i)) / c1
  ld(i) = ld(i - 1) - t * f(i) / c2
End If

l(i) = lv(i) + ld(i)

 Cells(6 + i, 5).Value = l(i) / 1000#

Next i

End Sub
```